Universidade Federal do Rio Grande do Sul – UFRGS
Escola de Engenharia
Programa de Pós-graduação em Engenharia de Minas, Metalúrgica e de Materiais

Pedro Henrique Alves Campos

SPATIAL MODELING, MINE SCHEDULING AND BLENDING CONSIDERATIONS ABOUT GEOMETALLURGICAL VARIABLES

Porto Alegre - RS
2023

Pedro Henrique Alves Campos

SPATIAL MODELING, MINE SCHEDULING AND BLENDING CONSIDERATIONS ABOUT GEOMETALLURGICAL VARIABLES

CONSIDERAÇÕES SOBRE MODELAGEM ESPACIAL, SEQUENCIAMENTO DE LAVRA E MISTURAS A RESPEITO DAS VARIÁVEIS GEOMETALÚRGICAS

Thesis submitted in partial fulfillment of the requirements for the degree of Doctor of Science in Mining Engineering.
Supervisor: Prof. Dr. João Felipe Coimbra Leite Costa
Co-supervisor: Profa. Dra. Vanessa Cerqueira Koppe

Porto Alegre - RS

2023

ACKNOWLEDGEMENTS

I would first like to thank my supervisor Prof. João Felipe, for the affection, encouragement, and support. Over the last few years, I have developed a deep admiration for the way you teach and treat your students. I have you as a great reference for my career as a university professor, researcher, and geostatistician. Thanks also to Prof. Vanessa, Prof. Marcel, and Prof. Rodrigo Peroni for the excellent teaching, shared knowledge, and fruitful discussions. I was very fortunate to develop my doctorate at UFRGS and LPM.

I am very grateful to Prof. Clayton Deutsch, who warmly welcomed me to CCG and the University of Alberta for eight months. Much of this work was the result of our several weekly meetings, always very valuable for my learning and improvement. Thanks so much for the opportunity to learn from you.

I thank Luciano and Rodrigo for their kindness in providing me with the real database used in this thesis and for the explanations about it.

Thanks to the Conselho Nacional de Desenvolvimento Científico e Tecnológico (CNPq - Brazil) for the financial support, without which it would not have been possible to carry out the part of the research developed in Canada. I will strive to contribute to the education of students in Brazil in the same way that this opportunity contributed to my education.

I thank my friends in Brazil who supported me during the development of this research, especially Kairo for receiving me at his home in Porto Alegre several times, and colleagues from LPM. Thanks to my friends and fellow researchers at CCG, especially Karim Mokdad, Luis, Jinpyo, Di Yang, Caio, Rafael, Paulo, and Fábio. In addition to the rich discussions on geostatistics, you have made my stay in Canada more joyful. Thank you all for the company.

And finally, I would like to thank my family for their unconditional support and love in the face of the difficulties encountered in carrying out this doctorate, most of all to my love Mariana.

ABSTRACT

There is a growing demand for studies related to geometallurgical variables, their spatial prediction in a block model, and their use in mine planning. This thesis aims to clarify important characteristics of these variables and the data obtained from the measurement of geometallurgical properties, which influence the application of spatial estimation methodologies and should also be considered for mine planning. Geometallurgical properties can be classified into intrinsic rock or response properties. Given the complexity of measuring the response properties (e.g., cost, the volume required for testing, equipment accuracy), a geometallurgical database tends to be smaller than a geological exploration database, resulting in sparse data with different support and missing values. In addition to these data-related particularities, geometallurgical variables generally average nonlinearly and exhibit complex multivariate behavior. These specificities require special treatment for spatial estimation. Two methodologies are employed in this thesis: one approach by multivariate geostatistical modeling and the other by machine learning. An analysis is made of their differences and when to use each method. The first is suggested when it is possible to infer all variables' variograms and the joint uncertainty is important; the second is most suitable when the inference of variograms is not possible and when there are high correlations between the variables. The impact of the complexities of geometallurgical variables extends to mine planning. The nonlinear blending averaging is related to the transformation from the estimated value in the mining block to the value of the material that feeds the processing plant. Considering that there is an intrinsic blending during mining and mineral processing, the estimated values in the blocks are not realized when processed, as no block is fed alone but together in a mixture with other blocks. Therefore, the estimated value in a block must consider the values of the other blocks with which it mixes. Mine planning must be scheduled to form the best mixtures concerning the response of the processing plant. A mixture model is necessary so that mine planning can optimize block sequencing. When there is a synergistic blending, the optimal sequencing will be the one that mixes different materials. When there is antagonist blending, it is better to extract similar blocks in sequence. In any case, better mine planning is possible when considering ore blending and nonlinear variables.

Key-words: Geometallurgy. Nonlinear variables. Spatial modeling. Mine schedule optimization. Blending.

CONSIDERAÇÕES SOBRE MODELAGEM ESPACIAL, SEQUENCIAMENTO DE LAVRA E MISTURAS A RESPEITO DAS VARIÁVEIS GEOMETALÚRGICAS

RESUMO

Existe uma demanda crescente por estudos relacionados a variáveis geometalúrgicas, sua previsão espacial em um modelo de blocos e seu uso no planejamento de lavra. Esta tese visa esclarecer características importantes dessas variáveis e os dados obtidos a partir da medição de propriedades geometalúrgicas, que influenciam a aplicação de metodologias de estimativa espacial e também devem ser consideradas para o planejamento de lavra. As propriedades geometalúrgicas podem ser classificadas em propriedades intrínsecas da rocha ou propriedades de resposta. Dada a complexidade de medir as propriedades de resposta (por exemplo, custo, volume necessário para testes, precisão dos equipamentos), um banco de dados geometalúrgico tende a ser menor do que um banco de dados de exploração geológica, resultando em dados esparsos com diferentes suportes e valores faltantes. Além dessas particularidades relacionadas aos dados, as variáveis geometalúrgicas geralmente têm uma média não linear e exibem um comportamento multivariado complexo. Essas especificidades requerem tratamento especial para a estimativa espacial. Duas metodologias são empregadas nesta tese: uma abordagem por modelagem geoestatística multivariada e outra por aprendizado de máquina. É feita uma análise de suas diferenças e quando usar cada método. A primeira é sugerida quando é possível inferir os variogramas de todas as variáveis e a incerteza conjunta é importante; a segunda é mais indicada quando a inferência de variogramas não é possível e quando existem altas correlações entre as variáveis. O impacto das complexidades das variáveis geometalúrgicas se estende ao planejamento da lavra. A média não linear de uma mistura está relacionada à transformação do valor estimado no bloco de lavra para o valor do material que alimenta a usina de beneficiamento. Considerando que há uma mistura durante a lavra e o beneficiamento mineral, os valores estimados nos blocos não se concretizam quando processados, pois nenhum bloco é alimentado sozinho e sim em conjunto com outros blocos em uma mistura. Portanto, o valor estimado em um bloco deve considerar os valores dos outros blocos com os quais ele se mistura. O planejamento da lavra deve ser programado para formar as melhores misturas em relação à resposta da planta de beneficiamento. Um modelo de mistura é necessário para que o planejamento da lavra possa otimizar o sequenciamento de blocos. Quando há uma mistura sinérgica, o sequenciamento ótimo será aquele que mistura materiais diferentes. Quando há mistura antagonista, é melhor extrair blocos semelhantes em sequência. De qualquer forma, um melhor planejamento de lavra é possível quando se considera a mistura de minério e variáveis não lineares.

Palavras-chaves: Geometalurgia. Variáveis não lineares. Modelagem espacial. Otimização do sequenciamento de lavra. Misturas.

LIST OF FIGURES

LIST OF TABLES

LIST OF ABBREVIATIONS AND ACRONYMS

2D	Two Dimensions
3D	Three Dimensions
BEV	Block Economic Value
BWI	Bond Work Index
DDH	Diamond Drill Hole
DT	Decision Trees
EDA	Exploratory Data Analysis
EM	Expectation-Maximization
GC	Grade-Control
GMM	Gaussian Mixture Model
KNN	K-Nearest Neighbors
LR	Linear Regression
LRT	Likelihood Ratio Test
MAF	Min./max. Auto-correlation Factors
MI	Multiple Imputation
NPV	Net Present Value
NS	Normal Score
NW	Northwest
OF	Objective Function
OK	Ordinary Kriging
PCA	Principal Component Analysis
PPMT	Projection Pursuit Multivariate Transform
QA/QC	Quality Assurance/Quality Control

RCP	Ratio CaO/P_2O_5
ReV	Regionalized Variable
RF	Random Forest
ROM	Run-Of-Mine
RSS	Residual Sum of Squares
SCT	Stepwise Conditional Transformation
SE	Southeast
SGS	Sequential Gaussian Simulation
SK	Simple Kriging
SMU	Selective Mining Unit
WI	Work Index

CONTENTS

1 INTRODUCTION

1.1 Problem setting

The computational representation of mineral deposits is currently conceived through the use of a block model (SINCLAIR; BLACKWELL, 2006), a set of three-dimensional blocks, regular or not, on which the process of estimating the geological variables is carried out. Geological properties such as the content of elements (of economic interest or contaminants), density, lithology, and degree of alteration of the rocks are some of the information of interest to estimate. These properties are intrinsic to the rock, also termed primary variables, under the Primary-Response Framework (COWARD et al., 2009). Primary variables are usually additive. Additive properties are those in which the averaged quantity is equal to the average of the quantities (CARRASCO et al., 2008). As they are additive, primary variables can be predicted spatially through linear geostatistical methods without the risk of introducing bias in the estimates.

After estimating primary geological information into the block model, technical aspects of mining, processing, and metallurgy are also considered for the evaluation of mineral reserves, as well as economic, infrastructure, legal, environmental, social, and governmental factors (HUSTRULID et al., 2013). Mine planning engineers develop production schedules, defining the order in which each block will be mined to achieve a certain objective. In long-term planning, the objective is usually related to maximizing the economic value of the project, commonly measured by the Net Present Value (NPV). In the short-term, scheduling also considers the ore characteristics that impact the operational performance of the processing plant. Ore blending is a strategy commonly used in mining, whose purpose is to provide a uniform feed to the processing plant, balancing high-grade and low-grade ore (LIU et al., 2021). Further down the mineral chain, ore processing is responsible for adapting the mined ore, the Run-Of-Mine (ROM), for the subsequent phase. Grain size reduction, classification, and mineral concentration operations are routine. The ore response to mineral processes is represented by a response variable, under the Primary-Response Framework (COWARD et al., 2009). In this sense, metallurgical recovery is the response variable of the ore to the concentration operations to which it is submitted. The metallurgical response of a rock is a function of its mineralogy, grade, texture, and process conditions (DOMINY et al., 2018). Due to this multivariate nature, response variables are mostly nonadditive, unlike primary variables.

While classical geometallurgy emerged as a collaboration between the areas of geology and mineral processing in providing information for a better understanding of the ore deposit and its characteristics, modern geometallurgy, on the other hand, aims to

integrate geological, mineralogical, physical, and chemical properties with metallurgical processes through a single spatial model, called the geometallurgical model (LISHCHUK et al., 2020; COWARD et al., 2009; DOWD et al., 2016; DOMINY et al., 2018). The end product of this model is the creation of integrated-spatial estimates for primary (geological) and response (metallurgical) variables, such as metallurgical recovery and the comminution energy of the ore, like the Work Index (WI), providing a basis for mine and plant optimization (LISHCHUK et al., 2020; DOWD et al., 2016; DUNHAM; VANN, 2007). Environmental, geotechnical, and economic information can also be included, aiming at best sustainable practices and decision-making (DOMINY et al., 2018; WALTERS, 2011).

The successful integration of several geometalurgical pieces of information in one single spatial model demands carefulness. The amount of geometallurgy data has increased in recent years, but the prediction procedures of these variables still cause confusion among practitioners. Bad practices can lead to errors with a high potential impact on the success of a project (DUNHAM; VANN, 2007). Therefore, each geometallurgical variable must be studied and well understood, as each has its own characteristics and may be supported by data from different sources. Issues like additivity/linearity, scale/support, and sampling play an important role in how the data should be measured, treated, and used for spatial modeling, which, in turn, is used for mine planning purposes.

For example, it is not correct to use linear functions, such as kriging, to spatially estimate nonadditive geometallurgical variables. One of the solutions to this problem is to use a modern multivariate geostatistical approach to estimate all the additive variables in the desired location and scale, and then obtain the nonadditive variables through nonlinear regressions, which are methods for predictive modeling in machine learning. Nonlinear geometallurgical variables such as recovery and throughput can be estimated from whatever linear high-correlated variables are available, such as grade (DUNHAM; VANN, 2007; WALTERS, 2011). A similar approach is to use a function to transform the nonadditive variable into one or more linear variables that could be kriged and then back transform to obtain the original variable of interest (ADELI et al., 2021; CARRASCO et al., 2008; PERONI, 2002).

Another solution for predictions in three-dimensional models of nonadditive variables is to work with stochastic approaches, as they allow joint modeling of variables and their uncertainties (BARNETT, 2016; BOISVERT et al., 2013). Modern multivariate simulation may require the imputation of missing values and variable transformations. The importance of knowing the uncertainty to deal with nonadditive variables is evident in cases where the behavior of the variable is controlled by extreme values and not by its mean. Dunham and Vann (2007) present an example: in a talc-sensitive flotation, a smoothed-kriging estimate in a three-dimensional model may indicate material within specifications, when, in fact, there is a small part of it highly contaminated and that

compromises the entire operation efficiency.

Although the nonadditivity aspect of the geometallurgical variables is already recognized, in current practice this particularity is only considered in the spatial prediction workflows (BARNETT, 2016; BOISVERT et al., 2013; DEUTSCH, 2015; ADELI et al., 2021; GARRIDO et al., 2020). In all scale (also known in geostatistics as support) transformations, geometallurgical variables are simplified as being linear, which occurs when upscaling the value from the (point) data scale to the resource block scale. Mine planning and all downstream processes are also affected by this simplification. Scale transformation is inevitable between the resource estimated model and the mineral processing prediction model. Just as a block consists of the mixture of several estimated points, the processing plant receives volumes that consist of the mixture of several blocks. The optimal dimensions of the blocks for a geometallurgical model may correspond to the production volume of one working shift (LISHCHUK, 2016). This volume is called *feed volume* in this thesis. As the geometallurgical variables are usually nonadditive, the average value in the feed volume is different from the average of the blocks that compose it. In this context, transforming the predicted value from one support to the other is challenging. For these transformations to be carried out, it is necessary to understand and model the nonlinear behavior of the variable. Direct experimentation of different mixtures on different scales is necessary for such modeling (DEUTSCH, 2015).

Some studies consider geometallurgical information and their uncertainties in mine planning (BYE, 2011; CASTILLO; DIMITRAKOPOULOS, 2016; MORALES et al., 2019; KUMAR; DIMITRAKOPOULOS, 2019; NAVARRA et al., 2018; SEPÚLVEDA et al., 2018), but they implicitly assume scale linearity. Moreover, the main limitation of these studies is that they assign a value of the geometallurgical variable to each individual block. Assigning a deterministic value of the geometallurgical variable to each block is currently common practice. Two methodologies for estimating the value of metallurgical recovery are more common; in the first, an average and fixed value is assigned to all blocks within a given geological-weathering domain; in the second, the value is estimated from a function of the primary variables of each block. Nevertheless, this practice implicitly assumes that each block is processed individually, neglecting the effect that the blending of the blocks has on the metallurgical response of interest. The volume of material processed in the plant is equal to the volume of several mining blocks. Plant feed typically represents a mixture of ores from various mining faces and locations (WAMBEKE et al., 2018). The mixture of blocks begins to be formed in the blasting/excavation and loading of the material and can increase if the ore is intentionally blended and homogenized in piles. Even when the ore is fed into the plant in batches, the properties of the blended material dictate the process responses more than the properties of any other individual block (DEUTSCH, 2015; ROSSI; DEUTSCH, 2014). The ore mixtures formed are a consequence of the scheduling of the blocks and/or the blending and homogenization process, if any. Each set

of blocks that are mixed and processed together is termed a *blending unit* in this thesis. In cases where the sequencing is done to maximize the NPV, this problem is recursive. The order of sequencing each block depends on its economic value, which is a function of its metallurgical recovery. However, the metallurgical recovery of a block depends on how the blocks will be mixed during the processing. And this mixture depends on the mine scheduling/blending. The use of linear techniques in spatial modeling and support transformation of nonadditive variables may cause, among other reasons, discrepancies between estimated values and those observed in reality.

1.2 Geometallurgy-related studies

Studies from the last fifteen years in the area of geometallurgy are highlighted next.

Dunham and Vann (2007) demonstrated that any grade-recovery regression curve is scale-dependent, that is, is valid only for the scale of the data used for modeling the regression. They also presented an example in which the consideration of metallurgical recovery and throughput in the block model impacts production scheduling. They demonstrated that, with two blocks with the same grade, it may be better to mine the block with the lowest metallurgical recovery but higher throughput first than the other with higher metallurgical recovery but lower throughput, in the case of NPV maximization optimization.

David (2007) discussed how a geometallurgical model should be developed throughout the phases of the industrial plant design so that, when put into operation, the plant works as expected. He also mentioned the importance of defining metallurgical domains, which may or may not be related to geological domains, as well as the identification of rock properties that are predictive of the metallurgical response of interest. He also presented a table with examples of critical properties that affect each type of process circuit. In the case of iron ore, these are the lump/fine ratio and the contaminant contents. In the case of sulfide copper, critical properties are the mineralogy, degree of alteration, and impurities.

Carrasco et al. (2008) presented a work on the characteristics of nonadditive variables and the problems when they are estimated by linear techniques. Through two experiments, they showed that the consideration or not of additivity can impact the results, depending on the scale of interest and the variability of the variable. Finally, they pointed out that, whenever possible, it is better to make spatial estimates with additive variables and then obtain the nonadditive variable through regression, rather than to try to spatially estimate the nonadditive variables. To obtain the nonadditive metallurgical recovery variable, they worked with three additive variables: feed grade, mass recovery, and in situ recovered metal.

Coward et al. (2009) presented a framework for classifying geometallurgical variables

into primary and response, helping to understand the most appropriate methodology for sampling and spatial modeling of each type. They suggested that, whenever possible, response variables should be reduced to additive variables, given their advantages for modeling and scale change. Furthermore, they warned about the care in applying fixed adjustment factors in reconciliation.

Tonder et al. (2010) demonstrated experimentally that blends of platinum ores display nonlinear behaviors when there are large differences in metallurgical properties between the ore types. The study was focused on grinding, flotation grade, and flotation recovery properties. They end up speculating some reasons why such behavior occurs.

Walters (2011) discussed the AMIRA P843 GeMIII, a research project focused on geometallurgy, with the objectives of understanding the intrinsic variables of the rock that impact metallurgical performance, developing tools and methodologies for rapid and low-cost testing of rock characteristics, applying technology and methods with high automation potential, defining metallurgical spatial domains, and understanding the geological controls on process performance behavior. He stated that the prediction of the metallurgical performance of mixtures is a challenge.

Newton and Graham (2011) presented a study in which performance indices such as recovery, throughput, and specific power are estimated directly in the block model through the use of regression models and additive variables. They used this approach to obtain the bias of the alternative methodology, in which the variables are discretized into classes to be spatially estimated by kriging indicators, and subsequently estimated in blocks.

Bye (2011) recognized that any linear support change technique should only be applied to additive variables. According to him, the solution to accommodate the nonlinear relationship between the different scales is the creation of a mixture response model. He also showed case studies with different methods of incorporating geometallurgical attributes into numerical spatial models of the mineral deposit. Finally, he advocated that reserve modifying factors should be replaced by indicated, probable, or proven spatial geometallurgical attributes.

Cornah (2013) used the same approach explained by Carrasco et al. (2008) to quantify the bias resulting from the linear estimation of a nonadditive iron ore attribute. He concluded that the bias was more significant locally than globally, and greater in the estimation of higher-variability areas, which is related to lower-grade ore for iron ore deposits.

Boisvert et al. (2013) spatially modeled six geometallurgical variables from their correlation with 204 more extensively-sampled variables. The methodology consisted of variable reduction, quantile-to-quantile univariate transformation to a Gaussian distribu-

tion, aggregation of variables into four super-secondary variables, multivariate regression, back-transformation, and geostatistical simulation. The predictive model with correlations to the plant performance variables ranged from 0.65 to 0.90. The spatial models of the six variables had the same scale as the samples.

Deutsch (2015) proposed an integrated geostatistical approach for the spatial modeling of nonadditive metallurgical variables to solve the problems of *i*) prediction and modeling of nonlinear behavior and mixing laws of metallurgical variables; *ii*) downscaling metallurgical variables; *iii*) spatial modeling of these variables; *iv*) selection of appropriate multivariate techniques for the uncertainty assessment workflow of such variables.

Dowd et al. (2016) stated that one of the greatest current challenges of strategic mine planning is the integration of geometallurgical variables in spatial block models. This challenge is justified by the nonadditive behavior of the response variables, the limited data available on such variables, and the difficulty in finding primary variables correlated with them. They presented an example of production sequencing based on the integrated optimization of the mining system, considering geometallurgical information.

Lishchuk (2016) developed a two-dimensional system for classifying geometallurgical programs for benchmarking. He also made a framework for planning and creating a geometallurgical model through a synthetic model so that it was possible to assess the economic impact of a geometallurgical model on a mineral project. He believes that the optimal dimensions of the block for a geometallurgical model correspond to the production volume of a shift, which is the equivalent of ten to thirty hours of production. Questions related to the number of samples suitable for geometallurgical modeling, types of appropriate tests, and the importance of mineralogical analysis over chemical analysis were answered.

Barnett (2016) stated that as processing performance is a multivariate problem, multivariate relationships must be properly modeled. Some multivariate complexities are heteroscedasticity, nonlinearity, and constraints. Transformations such as Normal Score (NS), Principal Component Analysis (PCA), and Min./max Auto-correlation Factors (MAF) do not remove these complexities. The solution he proposed is the application of techniques for the multiGaussian variable transformation, such as the Projection Pursuit Multivariate Transform (PPMT) for independent simulation of each uncorrelated variable, with subsequent back-transformation. Finally, he presented a case study, in which four correlated variables were modeled through PPMT and simulation.

Dominy et al. (2018) presented a historical review of the development of geometallurgy up to the year in question and future trends.

Wambeke et al. (2018) developed an algorithm based on real-time plant reconciliation for continuous calibration of the WI variable in the estimated geometallurgical

block model. Each metallurgical response observation in the plant was compared with the estimate of the set of blocks fed, and adjustments were made both in the mined and the neighboring blocks simultaneously. The algorithm is based on Monte Carlo simulation and automatically handles the support issue and measurement errors.

Lishchuk et al. (2020) critically reviews current practices and trends in geometallurgy programs. They also show different definitions of geometallurgy proposed in several publications.

Niquini (2020) developed an algorithm based on neural networks capable of predicting the mass and metallurgical recovery of products and waste of a processing plant from ROM data in a phosphate mine.

Adeli et al. (2021) performed the spatial modeling of the metal mass contained in the concentrate (obtained from laboratory tests) and metal mass contained in the feed (by chemical analysis of drilling), both additive, through cokriging. After the proper modeling and proper support transformation, the metallurgical recovery is obtained by dividing these two variables.

Hoffimann et al. (2022) proposed a new methodology combining Bayesian models with Kriging in Hilbert spaces to quantify the spatial uncertainty of geometallurgical variables. They applied the methodology to a real copper deposit.

1.3 Thesis statement

The evolution of geometallurgical modeling in recent years has been noted, with the focus being on defining the most relevant geometallurgical variables, discovering the best tools for their measurements, defining methodologies for their spatial estimation, or developing mine sequencing that considers the geometallurgical characteristics attributed to the blocks. However, the author of this thesis faced a shortage of studies that identify how to combine estimation and mine planning of nonadditive variables, more specifically, how the upscaling from mining blocks to the processing plant feed volume and, consequently, the mixing of mining blocks, impact the prediction of these variables.

The goal proposed for this thesis is to investigate how nonadditive geometallurgical variables must be estimated in the block model and used in mine planning. The thesis statement is:

A nonlinear geometallurgical variable value of an individual block depends on the set of blocks that are blended with it (blending unit) when processed. It is possible to model the nonlinear blending behavior of a variable and use it to optimize mine scheduling when nonadditive geometallurgical variables are of interest.

The specific objectives are:

1. Understand particularities related to geometallurgical data and variables;
2. Review different spatial modeling approaches for geometallurgical variables;
3. Demonstrate that the current practice of estimating individual and independent values of a geometallurgical variable for each block is conceptually incorrect;
4. Propose a blending model that can be used to effectively estimate process responses for the blending unit volume;
5. Propose a methodology for estimating the geometallurgical variables in each block that takes into account the blending of the blocks;
6. Develop a production schedule that identifies the best combinations of blocks to form each blending unit.

The workflow with the proposed methodology to consider the blending of nonlinear variables in mine scheduling is illustrated in Figure 1. With the data and performing all the required procedures, spatial models for all variables are estimated. There are two main methodologies to spatially estimate geometallurgical variables: the multivariate geostatistical approach and the machine learning approach. They are explained and applied further in this thesis. The spatial model is used together with a blending model as inputs to the algorithm that optimizes block scheduling based on the blending units.

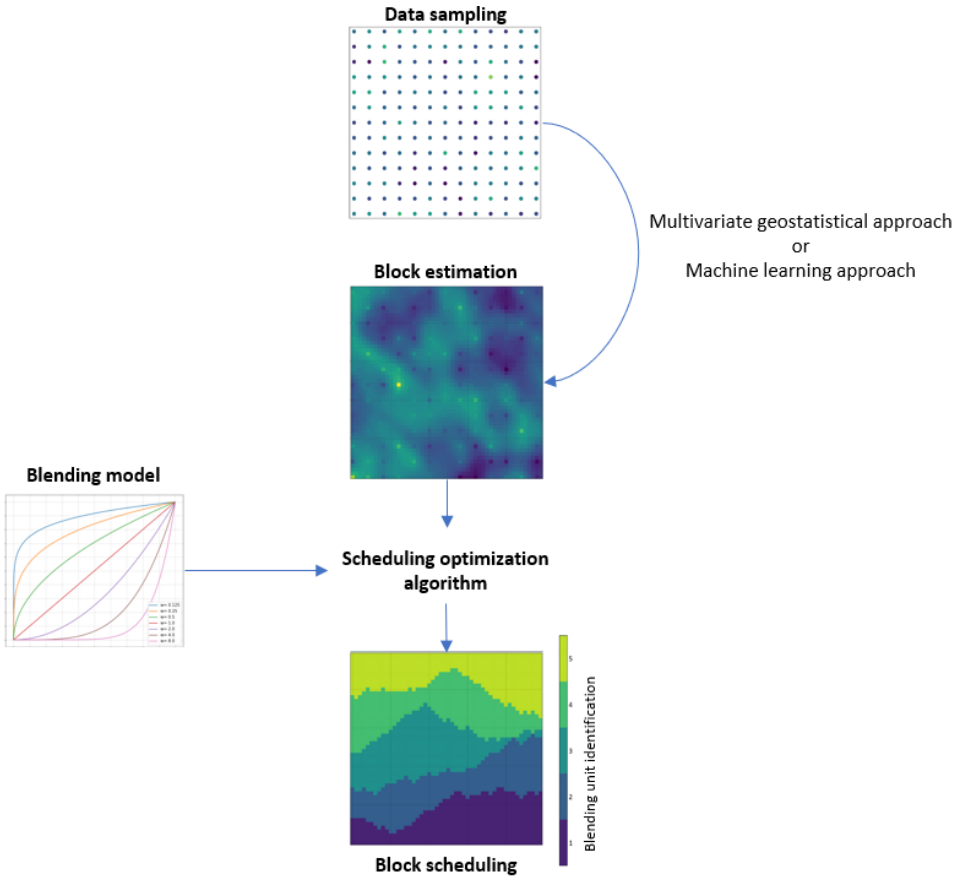

Figure 1 – Illustration of the thesis statement. The proposed methodology is to estimate geometallurgical variables at the block support from the multivariate geostatistical approach or the machine learning approach. An optimization algorithm that considers the blending of nonlinear variables is developed and applied to optimize block scheduling.

1.4 Thesis relevance

The relevance of this thesis is related to providing a methodology that indicates the best approach to spatially model nonadditive geometallurgical variables in the block support and how to use this multivariate model to optimize mine planning, considering that blending is nonlinear.

Geometallurgical models allow the early prediction of production possibilities and their results, contributing to the increase of mineral resources and reserves, the improvement of mining and process operations, mining planning strategies, ore blending, and quality predictions (COWARD et al., 2009; DEUTSCH, 2015; DOMINY et al., 2018; DUNHAM; VANN, 2007).

1.5 Thesis outline

This thesis is outlined as follows: Chapter 2 reviews the methodologies concerning conventional geostatistical modeling, the modern approach for multivariate and probabilistic geostatistics, machine learning modeling, and suggested workflows when dealing with geometallurgical variables. Production scheduling, and ore blending practices are also recalled. Chapter 3 clarifies some aspects regarding geometallurgical data, sampling, and variables. A statistical analysis of a lab bench test database is compared against a plant database of a real mine. Chapter 4 is related to how a variable behaves when there is blending. Neutral blending, synergistic blending, and antagonistic blending are explained. A flexible mathematical blending model is proposed and applied to an example, where a sensitivity analysis is also performed. Chapter 5 presents how ore scheduling can be optimized when dealing with nonadditive variables and blending. A simulated annealing algorithm is developed and applied in a synthetic demonstration study. The developed workflow is written in Python and made available to the reader through a Jupyter Notebook in the following GitHub link: https://github.com/phacampos/PhD-thesis. Chapter 6 shows the application of the whole methodology - data analysis, spatial modeling, and mine scheduling optimization considering a blending model - on real data from an existing mine. Guidelines and suggested workflows when dealing with geometallurgical variables are provided. Conclusions and future work are addressed in Chapter 7.

2 METHODOLOGY OVERVIEW

This chapter overviews the existing methodologies for resource modeling prediction and mine planning. First, conventional geostatistical modeling workflow is reviewed. Variogram calculation, kriging, and simulation are addressed. Then the focus turns to modern geostatistical modeling, a preferred approach when dealing with multivariate and complex relationships, such as those in a geometallurgical database. Machine learning regressors are also an option for geometallurgical variables. The differences between the last two approaches are highlighted, and best practices are presented. At last, the usual procedures for mine scheduling and blending are recalled.

2.1 Conventional geoestatistical modeling

Geostatistics is an approach and toolkit that applies statistical and numerical analysis to the spatial modeling of a regionalized variable (ReV) (DEUTSCH, 2021). A ReV Z is a variable distributed in space, related to natural phenomena, that possesses two apparently contradictory characteristics: i) an erratic local behavior and ii) a structured, general behavior. The solution to represent the spatial variability considering this double aspect of randomness and structure, inherent to ore deposits, is through probabilistic interpretations such that the set of values $z(u_i)$, $i = 1, ..., N$, of a regionalized variable over a domain A are interpreted as particular realizations of the random function $\{Z(u), u \in A\}$ (JOURNEL; HUIJBREGTS, 1978).

This interpretation is only possible because of spatial homogeneity assumptions or *hypothesis of stationarity*. Strict stationarity occurs when a random function's entire probability distribution, consequently its spatial law, is invariant under translation. Second-order stationarity occurs when the stationarity is limited to the first two moments of the random function, that is: i) the mathematical expectation $E\{Z(u)\}$ exist and does not depend on the location u (Equation 2.1):

$$E\{Z(u)\} = m, \quad \forall u \in A \tag{2.1}$$

and ii) the covariance for each pair $Z(u)$ and $Z(u+h)$ exists and depends on the vector h only (Equation 2.2):

$$C(h) = E\{Z(u+h)Z(u)\} - m^2, \quad \forall u \in A \tag{2.2}$$

A weaker assumption of stationarity is the intrinsic hypothesis, also known as the stationarity of the variogram. It occurs when i) the mathematical expectation $E\{Z(u)\}$

exist and does not depend on the location u (Equation 2.1), and *ii*) the increment $[Z(u+h) - Z(u)]$ has a finite variance that does not depend on the location u:

$$Var\{Z(u+h) - Z(u)\} = E\{[Z(u+h) - Z(u)]^2\}, \quad \forall u \in A \tag{2.3}$$

Preferential sampling, common in mining, leads to the inference of unrepresentative probability distributions. Their adjustment is possible through declustering techniques, which consist of assigning different weights to different samples. The closer a sample is to other data, the smaller its weight. One of the existing declustering methods is cell declustering (DEUTSCH, 1989). It works by creating grid cells along the interest region and weighting each data by $\frac{1}{n_d \cdot n_{oc}}$, n_d being the number of data falling in the same cell, and n_{oc} being the number of cells occupied by at least one sample. As the weights depend on the cell size and the grid's origin, cell declustering is an iterative procedure. The optimal cell size is found based on the diagnostic plot and is often associated with the spacing in the sparsely sampled areas (DEUTSCH, 2015).

2.1.1 Variogram

Geostatistics relies on the spatial variability of a regionalized variable. A value at the location u, $z(u)$, is spatially correlated to a value at the location $u+h$, $z(u+h)$, h being a vector that separates the two points (JOURNEL; HUIJBREGTS, 1978). The spatial variability of a regionalized variable is associated with the process which originated the phenomenon. Therefore, in mining, spatial variability is the consequence of the genesis of the deposit and can be modeled considering the correlations between the samples taken at different locations along the deposit.

The variogram function $2\gamma(h)$ measures the variability of a given vector h, with magnitude and direction, by taking the average of the squared differences between all the available data that are separated between this vector h apart (Equation 2.4). The exact locations of these points do not matter because the intrinsic hypothesis is assumed, which means that the variability between two points separated by the vector h is constant and depends only on the separation h.

$$2\gamma(h) = \frac{1}{N(h)} \sum_{i=1}^{N} [z(u_i) - z(u_i + h)]^2 \tag{2.4}$$

Intuitively, two points close to each other are more likely to be similar than two points far from each other in space. Therefore, the correlation between $Z(u)$ and $Z(u+h)$ generally decreases with the increase of the magnitude of h. Conversely, the variability, or the variogram value, increases with the increase in h. Under the assumption of second-order stationarity, the variogram and covariance are related by the variance σ^2 (Equation 2.5). In practice, after a large distance, the correlation between samples disappears, and their

variogram value stabilizes. This distance is known as *range*, and the plateau reached is called the *sill*. Different directions of the vector h analyzed may have different ranges or sills; in that cases, the phenomenon is anisotropic.

$$\gamma(h) = \sigma^2 - C(h) \tag{2.5}$$

Fitting the experimental variogram points with a function is necessary for estimation and simulation since they require a variogram/covariance value for all possible directions and distances. Because the covariance values must lead to a positive definite kriging matrix, a few parametric functions are usually used to fit the experimental values: the spherical, the exponential, the gaussian, and power-law models. A positive definite function ensures the kriging equations have a unique solution and that the kriging variance is positive.

2.1.2 Kriging

Kriging is a family of best linear unbiased estimators. It is linear because it is a linear combination of each data value $z(u_i)$ times their weight ω_i, $i = 1, ..., N$ (Equation 2.6), it is unbiased because the expectation of the error (the difference between the real value Z and the estimated value Z^*) is zero (Equation 2.7), and is considered to be best because provides the minimum estimation variance (Equation 2.8).

$$z^*(u) = \sum_{i=1}^{N} \omega_i \cdot z(u_i) \tag{2.6}$$

$$E\{Z - Z^*\} = 0 \tag{2.7}$$

$$Min \;\; E\{[Z - Z^*]^2\} \tag{2.8}$$

Ordinary Kriging (OK) requires the assumption of the intrinsic hypothesis, where no prior inference about the mean is made, and variograms with or without sills can be used. Conversely, Simple Kriging (SK) requires the hypothesis of the second-order stationarity, where the mean is known, and only variograms with sills are accepted, since the covariance for each pair $Z(u)$ and $Z(u+h)$ exists. It follows from the definition of kriging and the stationarity hypothesis that the weights for OK can be obtained by Equation 2.9.

$$\begin{cases} \sum_{i=1}^{N} \omega_i \cdot C(u_i, u_j) - \mu = C(u_i, u_0) \;\; \forall i = 1, ..., N \\ \sum_{i=1}^{N} \omega_i = 1 \end{cases} \tag{2.9}$$

where $C(u_i, u_j)$ is the covariance between data i and j, $C(u_i, u_0)$ is the covariance between data i and the estimated location, and μ is the Lagrange parameter added so that there is only one possible solution to the system.

Kriging on larger support than the data support is generically called block kriging. In this case, the estimate is given by Equation 2.10:

$$z_V^*(u) = \sum_{i=1}^{N} \omega_{i,V} \cdot z(u_i) \tag{2.10}$$

where $z_V^*(u)$ is the estimated value at the block V, and $\omega_{i,V}$ is the weight for each datum i. The equations for block kriging are similar to those in Equation 2.9 but with the replacement of $C(u_i, u_0)$ for the average covariance between data and points within the block $C(u_i, V_0)$.

In practice, given that the estimation process is linear, the average value of a block $z_V^*(u)$ is approximately equal to the average of the estimated values at the N points within the block (Equation 2.11) (GOOVAERTS, 1997).

$$z_V^*(u) \approx \frac{1}{N} \sum_{j=1}^{N} z(u_j^*) \tag{2.11}$$

By minimizing the estimation variance, kriging smoothes the true dispersion of the variable. Limitations of linear geostatistical techniques are, among others: the prediction of only a single value for each unsampled location, extreme values strongly impact them, kriged model does not reproduce the spatial continuity of the data, and they are inadequate for estimating nonlinear variables.

Nonlinear geostatistical techniques are an alternative for predicting a variable. They provide the expected value but also the conditional distribution. Doing so provides reliable measures of uncertainty, as opposed to the kriging variance. These estimates are indicated when the variable presents high asymmetry caused by extreme values that impact the analysis of the spatial variability, when the sample spacing is large in relation to the size of the block to be estimated, and when the variable is not sufficiently represented only by the mathematical expectation. However, these nonlinear methods are more complex and are based on more restrictive assumptions. Yet, these estimators are still aimed at variables that average linearly (DEUTSCH, 2015).

2.1.3 Simulation

Simulation consists of generating several equiprobable realizations of the ReV so that all of them reproduce the spatial variability of the data and their probability distribution, and meet the experimental values at the actual data locations. The realizations are called

conditional simulations since they are conditioned by the experimental data. Conditional simulations are spatially consistent Monte Carlo simulations (CHILES; DELFINER, 2009). The objective of the simulation is not to provide an estimation as close as possible to the true value but to provide an accurate and precise dispersion of the predicted variable.

The great advantage of simulation over nonlinear estimates is that, in addition to understanding the uncertainty of a location, it evaluates the uncertainty between multiple locations, enabling the transfer of uncertainty of the estimated resources for the risk analysis in later stages, as in the mine design, mine planning, and its economic evaluation, through the application of transfer functions in conditional simulation models (ROSSI; DEUTSCH, 2014).

The resolution of the simulations must be fine grids, compatible with the support of the data. Simulation makes no averaging assumption. The only averaging occurs when upscaling the model to the desired block size, which is why it should be deferred to the last moment possible.

There are several methods for conditional simulation. The Sequential Gaussian Simulation (SGS) relies on a multiGaussian random function model assumption. It is one of the most frequently used methods in mining applications given its convenient properties, easy implementation, and reasonable representation of spatial distributions (ROSSI; DEUTSCH, 2014). The workflow to perform SGS follows (ROSSI; DEUTSCH, 2014):

i. Complete an Exploratory Data Analysis (EDA) of the original data, including variogram and domain definition;

ii. Analyse if the data needs to be de-trended, and simulation run on the residuals;

iii. Transform the variable to be Gaussian;

iv. Obtain the Gaussian variogram models;

v. Define a random path of nodes on the grid to be simulated;

vi. Estimate the conditional distribution for each node to be simulated in the Gaussian space. The mean and its variance are given by the SK mean and variance. If simulating on the residuals, the mean of the conditional distribution is zero;

vii. Draw a simulated value randomly from the previously obtained conditional distribution;

viii. Incorporate the simulated value drawn as conditioning data for nodes simulated later. This process ensures variogram reproduction;

ix. Repeat step 6 to 8 for all nodes;

x. Check histogram and variogram reproduction is Gaussian space;

xi. Back-transform the Gaussian simulated values to original variables space;

xii. Add back trend if the simulation was performed on the residuals;

xiii. Check histogram and variogram reproduction in original data space;

xiv. Verify that the model presents a reasonable spatial distribution.

2.2 Modern multivariate geostatistical modeling

Conventional geostatistics faces obstacles when dealing with large multivariate data. Cokriging workflows require the covariance of each variable and their cross-covariance, that is, K^2 functions considering K variables [1]. The inference becomes demanding in terms of data, and modeling the linear model of corregionalization is very troublesome and tedious.

The modern approach for multivariate prediction is to apply transformations to the variables in order to decorrelate and turn them into multiGaussian factors that can be independently kriged/simulated. After the spatial modeling of each factor, back-transformations are applied to return the variables to their original space and reestablish their original correlations.

A method that simultaneously decorrelates and achieves multiGaussianity is the PPMT. This factorization algorithm requires the data to be Gaussian and sampled at all locations. The former is accomplished by NS transformation, and Multiple Imputation (MI) solves the latter requirement.

2.2.1 Normal Score (NS) transformation

NS is a transformation of a univariate distribution to standard Gaussian units, with a mean equal to zero and a variance of one. The probability density function of a Gaussian distribution is fully parametrized by its mean (m) and standard deviation (σ), given by Equation 2.12:

$$g(z) = \frac{1}{\sigma\sqrt{2\pi}} \exp\left[\frac{-1}{2}\left(\frac{z-m}{\sigma}\right)^2\right] \tag{2.12}$$

The NS is a direct quantile-to-quantile transformation from the original distribution $F(z)$ to the Gaussian distribution $G(y)$, such that the correspondent value of a z value is the y value (Figure 2).

[1] considering that $C_{XY}(h) \neq C_{YX}(h)$

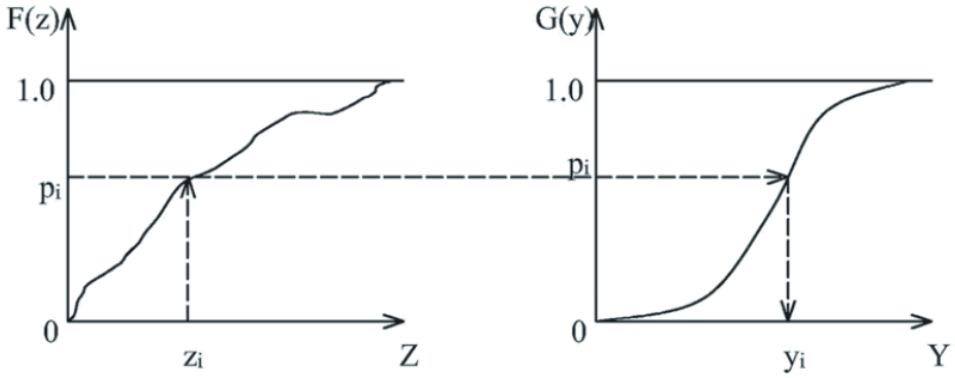

Figure 2 – Illustration of the Normal Score transformation. The z_i value in the original distribution $F(z)$ is transformed to a y_i value in the Gaussian $G(y)$ distribution. Source: Rossi and Deutsch (2014).

The NS is a rank-preserving and reversible transformation. Spikes of constant values are troublesome to the transformation; therefore, if they exist, the ties must be broken through despiking. Despiking can be made *i*) at random, *ii*) using a neighborhood averaging, or *iii*) using a combination of both (ROSSI; DEUTSCH, 2014; DEUTSCH; JOURNEL, 1997).

2.2.2 Multiple Imputation (MI)

The transformations applied to the multivariate modeling require that all variables are sampled at all data locations. Unfortunately, in mining, it is uncommon to have such a situation. The removal of incomplete observations (to keep a homotopic subset of data) leads to a loss of information. It can introduce bias depending on the cause of the missing values (RUBIN, 1976; ZACCHÉ, 2018). An alternative is MI, a framework that imputes (simulates) missing values of regionalized variables, reproducing multivariate and spatial features of the data (BARNETT; DEUTSCH, 2013).

The basic idea of MI is to create multiple realizations of the data, where sampled values are constant and imputed values are variable. The imputed values are drawn with Monte Carlo simulation from the conditional distributions of the variable. The conditional distributions must integrate spatial correlation between samples and the correlation between variables at the same locations, such that the spatial continuity and the multivariate distributions of the data realizations reproduce that of the sampled values.

Silva and Deutsch (2015) proposed a methodology that uses Bayesian Updating to derive the required non-parametric conditional distribution. The likelihood is calculated from a Gaussian Mixture Model (GMM) fitted to the multivariate data set. The use of GMM improves the algorithm's speed and reproduces the existing multivariate complexities well.

The steps for the imputation using GMM are (SILVA; DEUTSCH, 2015):

i. Transformation of each variable to be Gaussian;

ii. Fit the GMM with n components to the transformed data, defining the estimated multivariate density function;

iii. Definition of the Prior distribution;

iv. Definition of the Likelihood distribution;

v. Combining the Prior and the Likelihood distribution into an Updated Distribution through Bayesian Updating;

vi. Sample the Updated Distribution through Monte Carlo simulation, generating the data realizations.

2.2.3 PPMT

Conventional cosimulation techniques require the data to be multivariate Gaussian (multiGaussian). In practice, this is rarely the case for geological variables. The common approach to overcoming the problem is to apply transformations like NS, PCA, and MAF to obtain univariate Gaussian distributions and assume multiGaussianity. However, this assumption is risky for complex data that present nonlinearity, heteroscedasticity, and constraint features. Barnett (2016) showed a case where the cosimulation of two univariate-Gaussian-distributed variables did not reproduce their bivariate correlation nor the complex features (Figure 3).

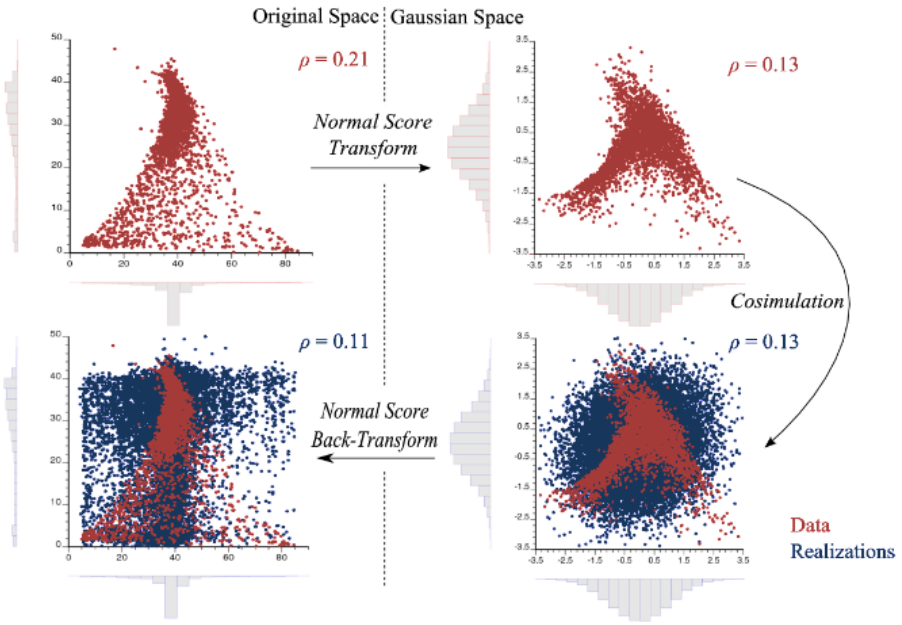

Figure 3 – Cosimulation with complex multivariate data. On the top left, a cross-plot between two variables in the original space (red). After the Normal Score transformation, the variables become univariate Gaussian, but not multiGaussian (top right). Cosimulation generates multiGaussian realizations (blue) that match the correlation of the data, but not the distribution (bottom right). The original data distribution is not reproduced after the back transformation (bottom left). Source: Barnett (2016).

A solution to this problem is to ensure that the variables are multiGaussian through transformations like the Stepwise Conditional Transformation (SCT) (LEUANGTHONG; DEUTSCH, 2003), or the PPMT (BARNETT et al., 2014). According to Barnett (2016), PPMT is the current standard for transforming complex data to a multiGaussian distribution because it is more applicable to data with more variables and/or fewer observations.

The PPMT algorithm applies two preprocessing transformations to all variables, aiming to simplify and improve the results of the PPMT itself:

- NS: standardize each variable to be Gaussian;
- Data sphering: a linear rotation that yields uncorrelated variables of unit variance.

With the preprocessed data, PPMT finds the most non-Gaussian projection of this data and transforms it to be Gaussian. Some iterations of this procedure in other projections ensure the data is multiGaussian (Figure 4). The transformed variables are called PPMT factors.

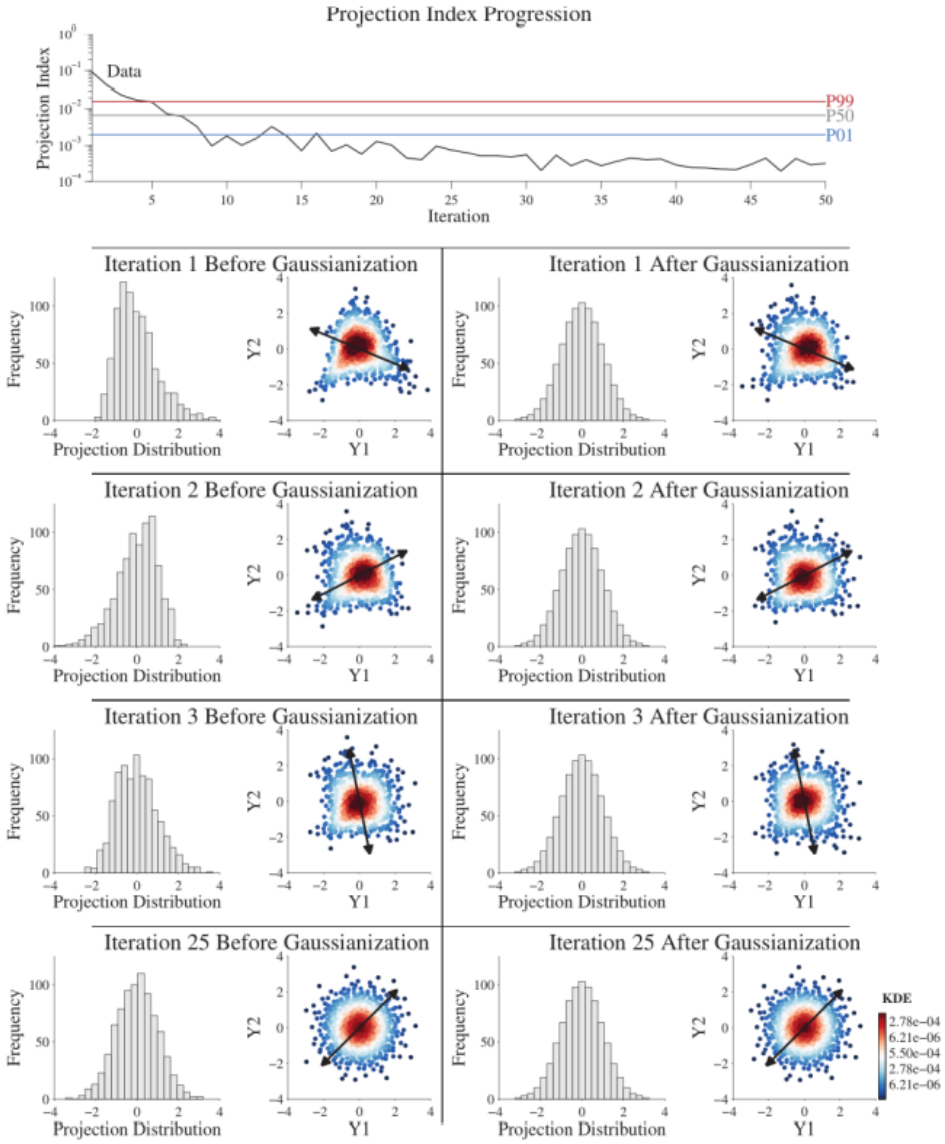

Figure 4 – Illustration of the PPMT process. The data become more multiGaussian after each iteration. Source: Barnett (2016).

MultiGaussian-distributed data means that all the variables are uncorrelated and independent, allowing each variable to be simulated independently. Semivariograms of the PPMT factors are required, but not the cross-variograms. After simulating the PPMT factor in the nodes of a grid, variables in the original space are obtained by applying a back transformation, that is, the inverse of the forward transformation realized.

The reproducibility of the univariate distribution, correlations, and semivariograms should be checked. Figure 5 shows that the complex relationships between variables are reproduced through this workflow.

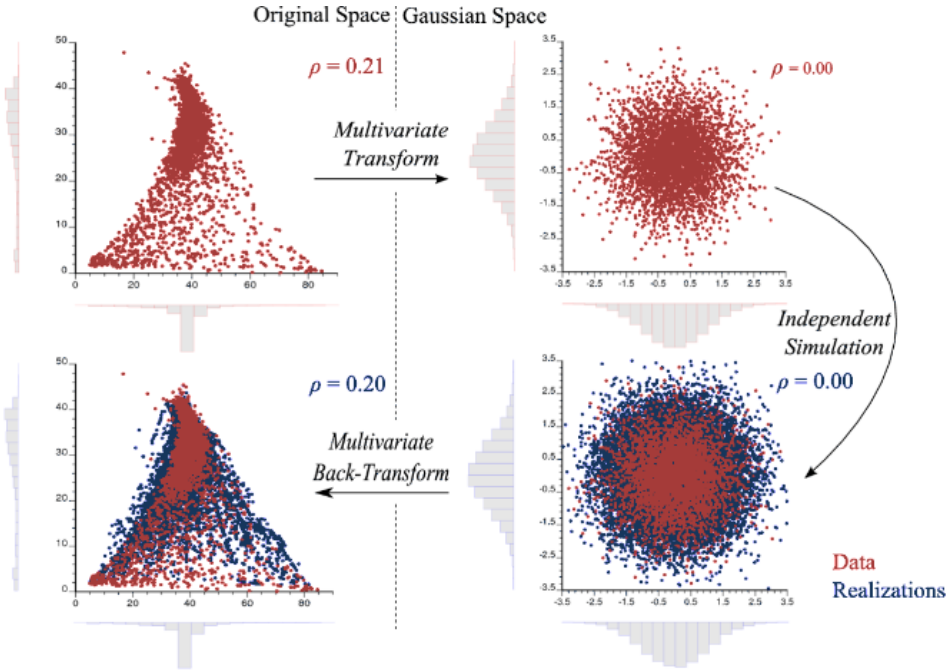

Figure 5 – Simulation of PPMT factors with complex multivariate data. On the top left, a cross-plot between two variables in the original space (red). After the PPMT transformation, the variables become bivariate Gaussian and uncorrelated (top right). Independent simulations generate realizations (blue) that match the correlation and the transformed data distribution (bottom right). Back transformation of the realizations reintroduces the original complexity and correlation (bottom left). Source: Barnett (2016).

2.3 Machine learning modeling

Machine learning algorithms have been increasingly used in the analysis of spatial data for the past few years, whether in *i*) predicting a label to a categorical data, *ii*) predicting a numerical value to continuous data, and *iii*) predicting a probability density function for a stochastic process (IACO et al., 2022). In this thesis, Linear Regression (LR), K-Nearest Neighbors (KNN), Decision Trees (DT), and Random Forest (RF) were the machine learning regressors used to estimate nonlinear variables through their relationships with linear variables. Some of the usual steps required for machine learning modeling are reviewed next.

2.3.1 Data preprocessing

Data preprocessing is an important step before the modeling. It consists of extracting the features in a dataset, cleaning it of inconsistencies, selecting the best features, and transforming them into a space suitable for prediction.

Feature extraction is the process of deriving meaningful features from multiple data sources, according to the objective of the modeling. It is often performed parallel

with data cleaning (AGGARWAL, 2015).

Data cleaning is the phase where the extracted features are integrated into one single unified database. Missing values are estimated, and erroneous entries are corrected. Some data may be removed.

Feature selection is the process of reducing the number of features or input variables used for a prediction. This procedure reduces the computational cost of modeling and, sometimes, improves the model's performance. Selecting a feature is based on its relationship with the target variable and the assessment of its importance in predicting the target. A variable may be removed if it is irrelevant to the target variable, or redundant with other features. Some machine learning algorithms (e.g., RF) contain built-in feature selection, meaning that the model will only include predictors that help maximize accuracy (KUHN et al., 2013).

Data transformation is sometimes required to adjust the features to a new space that is adequate for analysis. Some regression algorithms require scaling and normalization of the features so that the weighting is not affected by the different scales of each variable.

2.3.2 Regression

Regression modeling predicts a numerical value of the target variable from one or more input variables. Multiple output regressors can predict more than one variable simultaneously. The regressors used in this thesis, LR, KNN, DT, and RF are multiple output regressors.

2.3.2.1 Linear Regression (LR)

The LR model finds the best linear fit to the data. It assumes that the target variable $f(X)$ is linearly estimated by Equation 2.13, where β_0 is the intercept, also known as the *bias* in machine learning, and β_1 is the slope - the average increase in $f(X)$ associated with a one-unit increase in X. β_0 and β_1 are model coefficients that minimize the Residual Sum of Squares (RSS) (JAMES et al., 2013). The RSS is given in Equation 2.14, where y_i are the observed values of the data $i = 1, ..., N$ and $f(x_i)$ are their predicted values.

$$f(X) = \beta_0 + \beta_1 X \tag{2.13}$$

$$RSS = \sum_{i=1}^{N} (y_i - f(x_i))^2 \tag{2.14}$$

Linear regression is an example of a parametric approach. Parametric approaches are easy to fit, the coefficients have simple interpretations, and tests of statistical significance

can be easily performed. However, it is a strong assumption that the form of $f(X)$ is linear. The prediction accuracy can be very inferior if the relationships between predictors and target variables are far from linear (JAMES et al., 2013).

The equations and demonstrations for the multiple linear regression case can be found in Hastie et al. (2009).

2.3.2.2 K-Nearest Neighbors (KNN)

KNN is a non-parametric regression that averages the responses y_i of the K closest input observations x_i in the neighborhood $N_k(x)$ to predict the target $f(X)$ (Equation 2.15). Closest implies a metric of distance, which usually is the Euclidian distance.

$$f(X) = \frac{1}{k} \sum_{x_i \in N_k(x)} y_i \tag{2.15}$$

KNN does not rely on any assumption about the form of the data and is very flexible in any situation. In general, the choice of K depends on the bias-variance trade-off. The smaller the K, the lower the bias and the greater the variance. In contrast, larger values of K provide a smooth and less variable fit while creating bias by masking some of the structure of $f(X)$ (HASTIE et al., 2009; JAMES et al., 2013).

2.3.2.3 Decision Trees (DT)

DT are a non-parametric regressor and classifier algorithm that uses a set of splitting rules to segment the predictor space into several simple regions. The algorithm finds the best splitting variables and points given the number of branches in the tree. A tree can be seen as a piecewise constant approximation. The corresponding regression model predicts $f(X)$ with a constant value c_m for each partition of feature space $R_m, m = 1, ..., M$ (JAMES et al., 2013):

$$f(X) = \sum_{m=1}^{M} c_m \cdot 1_{(X \in R_m)} \tag{2.16}$$

The decision of the size of the tree is not simple, as a large tree may overfit the data, while a small tree may not accurately model the structure.

Some of the advantages and disadvantages of decision trees include, among others (SCIKITLEARN, 2022a): Decision trees are easy to interpret and understand, as their regression results can be visualized. They can work with numerical and categorical data, and no normalization is required. They can handle multi-output problems. As disadvantages, they are prone to overfitting, not good at extrapolation, and very unstable to small variations in the data. This problem can be overcome by using an ensemble of trees.

2.3.2.4 Random Forest (RF)

RF is an ensemble of decorrelated trees, where the prediction of the ensemble is given as the averaged prediction of the individual trees. The principle of RF is that tree splits are chosen randomly from m candidate predictors out of the full set of p predictors. The purpose of this randomness is to reduce the variance of the forest estimator by averaging many noisy but approximately unbiased models (JAMES et al., 2013; HASTIE et al., 2009; SCIKITLEARN, 2022b).

2.3.3 Model evaluation

The answer to which model is better depends on the problem. LR will likely work well when the relationships between features and target variables are approximately linear. When the relationships do not show any specific form that a parametric function can approximate, then non-parametric methods are better.

The relative performances of each model can be evaluated and are important for deciding what model to use. The best approach for selecting and assessing a model is to divide the dataset into three parts: a training set, a validation set, and a testing set. The training set is used to fit the candidate model; the validation set is used to estimate the error of one candidate model and compare it against the other candidate's errors; the test set is used to assess the error of the final chosen model (HASTIE et al., 2009). This procedure helps avoiding data leakage and, consequently, overfitting.

A typical split might be 50% for training, 25% for validation, and 25% for testing-set (HASTIE et al., 2009). However, depending on the size of the database, splitting it considerably reduces the number of samples used for learning the model, and the results can depend on a particular random choice for the pair of (train, validation) sets. A solution to this problem is to apply cross-validation techniques.

One approach of cross-validation is the k-fold. In k-fold, the dataset is split into train and test databases, not requiring a validation set. The train set is then split into k smaller sets, where the model is trained with $k-1$ folds, and the model is validated with the remaining fold of the data. This procedure is repeated for each of the k folds. The performance is measured by averaging the results in the loop. The test set is used as usual.

2.4 Geometallurgical workflows

The increasing recognition of the importance of geometallurgy in understanding the behavior of ores and predicting their responses when subjected to the mineral process led to the need for spatial modeling of geometallurgical variables. WI, throughput, recovery, and reagent consumption are often the response variables of interest to be predicted. The

study of the characteristics related to geometallurgical data and variables is extremely valuable and guides the methodologies used for geometallurgical modeling.

Spatial estimation through kriging is not advisable for geometallurgical variables, as these variables average nonlinearly and result in biased kriged estimates. Nonlinear geostatistical estimators such as indicator kriging also require an assumption that the variable averages linearly. Other not common multivariate complexities such as heteroscedasticity and constraint features may also exist. Moreover, geometallurgical data may often present particularities. They are often undersampled relative to exploratory geological data, and their measurements are often performed over different volume support than other properties.

There are two main approaches to geometallurgical spatial modeling. The first is through modern multivariate geostatistical modeling, where all the variables, regardless of their nature, are spatially simulated with geostatistics. The second is through machine learning, where a regression model is fitted between geological (primary) and metallurgical (response) variables. Geostatistics is used to spatially model geological variables, but the metallurgical ones are spatially predicted through the regression model.

2.4.1 Geometallurgical modeling through modern geostatistics

Deutsch (2013) reviews all the concerns related to geometallurgical spatial modeling. He advocates for the use of simulation rather than estimation for several reasons: *i*) simulation is the only practical way to avoid bias in nonlinear-variable estimates, *ii*) it is the way that realistically represents short-scale variability, and *iii*) it is the way to transfer local uncertainty to uncertainty in volumes relevant to decision-making.

Simulated realizations of a nonlinear variable are not biased. Kriging used in simulation does not introduce a bias; it is for deriving conditional distributions or for conditioning unconditional realizations (DEUTSCH, 2013).

The general workflow of spatial geometallurgical modeling starts with defining the objective. The second step is to screen and assemble the variables to be spatially modeled. The third and last step consists of the joint modeling of the variables and post-processing to meet the purpose of the study.

There is no fixed workflow for geometallurgical spatial modeling, as the objective and the characteristics of the geometallurgical data may vary. Deutsch (2013) presents some existing techniques that may be useful. The modeler needs to understand from the problem posed which methods are required to solve and apply them in a hierarchical workflow. For the problem shown in chapter 6, the workflow includes data imputation, variable transformation and decorrelation through NS and PPMT, multivariate simulations, and back transformations.

The geostatistical modeling of geometallurgical variables may be preferred in cases where there is abundant geometallurgical data and a poorly defined regression model between geological and metallurgical variables.

2.4.2 Geometallurgical modeling through machine learning

In this approach, multivariate simulations are performed only for the geological variables. Therefore, the previous process is partially executed. The difference is that the metallurgical variables are predicted last, using the predicted geological values at the required locations as inputs to a regression model previously established between geological and metallurgical variables from the geometallurgical data.

High correlations between target (metallurgical) variables and predictor (geological) variables are required. Poorly correlated variables ($|\rho| < 0.2$) may be removed or combined to improve the prediction power. If data quantity is a concern, it is reasonable to pull data together from subsets larger than the geostatistical domains (DEUTSCH, 2013).

This approach may be preferred in cases where there is a shortage of metallurgical information on the geometallurgical dataset, such that variogram inference may be complicated, and when the regression model between geological and metallurgical variables is well established.

2.5 Mine scheduling and ore blending

Production planning is based on scheduling the mining blocks or Selective Mining Units (SMU). The SMUs have dimensions compatible with mining operations, generally different than the blocks used for calculating mineral resources, in which the dimensions are related to the spacing of the sampling (VANN; GUIBAL, 1998). The dimensions of the estimated blocks are generally reduced by incorporating additional pre-production and grade-control drillings.

In mine planning, engineers classify mine blocks into different categories of ore or waste, commonly by the grade of one or more valuable minerals. However, in more complex situations, other attributes affect the quality of the processed material and must be considered. Contaminant grades and mineralogical/geometallurgical properties are increasingly becoming essential and useful in the understanding and prediction of ore behavior when subject to processing.

Scheduling may have different objectives. In long-term planning, scheduling aims to maximize the project's NPV. To obtain the NPV, it is necessary to calculate the block economic value (BEV) (Equation 2.17). The BEV is based on geological estimates of ore grade (g) and ore mass (M), process estimates such as metallurgical recovery (R_m), and

economic estimates of ore price (P), mining costs (C_m) and processing costs (C_p) per unit of mass, according to whether the block is classified as ore or waste.

$$BEV = \begin{cases} [P \cdot g \cdot R_m - (C_m + C_p)] \cdot M, & \text{if block is ore} \\ -C_m \cdot M, & \text{if block is waste} \end{cases} \tag{2.17}$$

As the NPV is a financial value discounted over time, the intention is to mine the blocks with the highest BEV before those with the lowest value (HUSTRULID et al., 2013). The optimization algorithms applied to long-term mine planning define the order of extracting each block to maximize the NPV, subject to the geotechnical and a few operational constraints. Block precedence restrictions, and minimum mining width are some examples.

The scheduling that provides the best NPV is not necessarily the best for the processing plant, as the fluctuation in the feed properties impairs its performance. Therefore, short-term mine planners are interested in sequencing blocks so that the material sent to the plant is within the specific characteristics of the operation, with as little variability as possible. Blending and homogenizing strategies are widely used to achieve this objective. Other aspects considered in the short-term planning are the movement of equipment and other performance indicators. Therefore, algorithms applied to short-term mine planning have additional constraints to be met, such as mining and processing capacities, the existence of multiple ore destinations, equipment displacement, and ore quality restrictions, among others.

Mathematical formulations for solving the production planning problem through linear, mixed integer, integer, and dynamic programming are available in Osanloo et al. (2008). Due to the complexities involving the high number of combinations of constraints, associated with the large number of blocks needed to represent the mineral deposit, mathematical programming-based methods may have difficulty generating solutions in adequate computational time. Metaheuristic algorithms are alternatives that can provide almost optimal solutions. They consist of iterative processes that manipulate a solution at each iteration. Some examples of metaheuristics include Tabu search, Ant systems, Greedy Randomized Adaptive Search, Variable Neighborhood Search, Genetic Algorithms, Scatter Search, Neural Networks, and Simulated Annealing.

Within the scope of short-term mine planning, heuristic algorithms aim at solving problems of selection of mining faces, equipment allocation, truck dispatch systems, and consistent and homogeneous material feeding in the plant, among others. Optimization objectives include: minimization of operating costs, displacement of equipment, deviations between produced and expected quality, deviation from the long-term plan, maximization of revenues, and equipment utilization (BLOM et al., 2019). The set of important constraints

and objectives varies according to the operation of each mine. Modeling a short-term planning optimization problem is very case-specific.

The reader is referred to Lambert et al. (2014), Newman et al. (2010), Osanloo et al. (2008) if interested in the long-term mine planning optimization problems and to Blom et al. (2019) if a review of short-term optimization is desired.

3 DATA AND VARIABLE CONCERNS

In the process of studying geometallurgical properties, data are obtained from different sources, with different sampling devices and procedures of quality control, in different time periods, with different objectives, and with the supervision of distinct personnel. As a consequence, a geometallurgical database may be very heterogeneous regarding sample spacing, support, and data reliability. Along with that, several variables may be of interest in a geometallurgical study; each one of them has its own characteristics and complexities. Understanding the variables and the data is vital for any decision-making in data treatment and preprocessing, data analysis, spatial modeling, and mine planning. In this chapter, general concepts about data and variables are reviewed. Some concerns about specificities found in geometallurgical sampling, data, and variables when compared to exploratory-geological sampling are raised and discussed. Finally, a lab bench test database and a plant database from a phosphate mine are compared through EDA.

3.1 General concepts about data and variables

3.1.1 Data types

In geostatistics, data types are related to the reliability of the data. Hard data are considered to have high accuracy and precision, while soft data present a lower accuracy and precision. Usually, in mining, this classification is related to the methods of sampling and analysis of the data, as well as compliance with good practices established by Quality Assurance/Quality Control procedures (QA/QC). Data from direct sampling and measurement of the rock properties, such as density or grade obtained from Diamond Drill Hole cores (DDH), are examples considered to be hard data. Data from indirect measurements of the variable of interest, such as those obtained by sensors, or inferred through their relationship with other variables, are examples of soft data. Different data types may refer to the same variable of interest, but should not be merged. Grade, when measured in DDH core, is hard data; when measured in drilling powder is soft data. The identification of the data type is very relevant and determines the methodology of their use in spatial modeling.

3.1.2 Data scale

Data scale or support refers to the size (volume/mass/length) of the material in which the data is sampled and/or measured. A measurement of an element grade taken in a DDH core sample has its scale associated with the core's volume. In petroleum, it

is not unusual to have seismic data with some meters of resolution scale. Likewise, the measurement of metal recovery in a pilot plant has a scale equal to the bulk-sample volume fed into the plant. The differences in scale between data must be considered when integrating all the data and building spatial models. One well-known approach to considering data with different scales is to do compositing. Compositing is a homogenizing-support procedure, where the minor-scale data values are averaged into greater support so a constant support for all data is obtained. Greater-scale data have lower variability than small-scale data as demonstrated by the volume-variance relationship (ISAAKS; SRIVASTAVA, 1989; JOURNEL; HUIJBREGTS, 1978). All transformation involving a change of support, whether data or estimate, is known as scaling (up/down).

3.1.3 Data sampling

Data sampling is related to the frequency, spacing, or location of the samples. Heterotopic sampling occurs when two or more types of data are unequally sampled in the region of study, that is, are not sampled at the same locations. Completely heterotopic sampling occurs when different data do not share any location, whereas partial heterotopic occurs when some locations are shared, but not all. When different data are sampled at the same locations, sampling is called completely equally data sampling (or homotopic sampling). The most common situation in mining is heterotopic sampling, where data is obtained through several different sources: DDH drilling, reverse circulation drilling, blast hole drilling, and chip and channel samples, among others. In such cases, the covariance between the data is accounted for in cokriging/cosimulation workflows.

3.1.4 Variable types

In statistics, variables are classified as quantitative or qualitative. Quantitative variables are those that can be measured numerically, in which numbers have a meaning of intensity. Quantitative variables can be classified into discrete or continuous variables. Discrete variables are those that can assume a finite number of values, previously established. Usually, they are used to represent quantities in integer values. Examples in mining are the quantity of samples or the number of geological domains. Continuous variables are those represented by a range of infinite values, where any rational value within that range can be assigned to the variable. Examples are ore grade, ore tonnage, density, or metal recovery. Conversely, qualitative variables are those that can be classified into categories not quantified by numbers. Categories may be defined by an order relationship, in which case the variable is called ordinal variable; or may not have any relational order, in which case the variable is called nominal variable. Examples of the first are the weathering intensity of a rock or the classifications of resources into measured, indicated, and inferred. Examples of the latter are mineralogy classification and rock lithology. It is important to

mention that category labels can be represented by a number, although the number itself does not have any meaning of intensity.

Another classification of variables is given under the Primary-Response Framework (COWARD et al., 2009), where a geometallurgical variable is classified into 'Primary' if it is related to an intrinsic property of the rock, or 'Response' if it is related to a response to energy or process applied to the rock. Primary variables may be measured directly, but most have to be measured indirectly. Cornah (2013) gives iron ore grade as one example: grades are generally measured through X-ray fluorescence, which is itself a response to a process, but the measurement is interpreted to represent a concentration per unit mass of the rock sample. Other examples of primary variables are density, lithology, weathering, and mineralogy. Most of the primary variables are geological variables, while most of the response variables are metallurgical variables. Response variable examples are throughput, metal recovery, and Bond Work Index (BWI). Cornah (2013) gives as one example the lump-to-fine ratio. While strongly influenced by the inherent properties of the rock, the product yields derive from the blasting, mining, and processing energies applied to the rock. Primary variables are generally additive, while response variables are not.

3.1.5 Linearity and additivity

In mathematics, a linear function $f(x)$ is a function that satisfies two properties: additivity and homogeneity. Additivity is the property that ensures the additive operation is preserved, such that $f(a+b) = f(a) + f(b)$. Homogeneity ensures that a function undergoing a transformation in its variables results in a function that is proportional to the original, that is, $f(xb) = xf(b)$ (HOGBEN, 2013). A linear function preserves the linear combination between the components, such that $f(xa + yb) = xf(a) + yf(b)$. All variables that respect these two properties average linearly; they are referred to as linear variables. In geometallurgical-related publications, linearity and additivity are employed with the same meaning. Carrasco et al. (2008) explained the additivity concept as the averaged quantity of a variable being the same as the average of the quantities.

Let us give some numerical examples to illustrate the concept:

- The property *mass* is additive because when we add 1 t of material A with 1 t of material B, then we have 2 t of a mixture of materials AB.
- The property *grade* is a ratio between *mass* properties. When we add 1 t of material A at 1.0 g/t of gold with 1 t of material B at 2.0 g/t of gold, then we have a mixture AB with 2 t in mass and 3.0 g of gold. The grade of the mixture is 1.5 g/t, which is the same as the linear average of components A and B; therefore, grade is linear.
- The property *volume*, however, may be additive or not. Consider that 1 cm^3 of

material A is added to 1 cm^3 of material B. If A and B are the same substance (e.g., water), the resulting volume is 2 cm^3. Nevertheless, in case they are not the same substance and they react molecularly with each other, the resulting volume can be different. This is what occurs when water and ethanol are mixed; the resulting volume is less than the sum of the individual volumes.

- The property *density* is a ratio between *mass* and *volume*. If *volume* is considered to be nonadditive, then *density* is also nonadditive. In solid mixtures, the possibility of molecular reaction between different substances when mixed is reduced since molecules in this physical state have less movement. Therefore, it is reasonable to consider *volume* and *density* of solid materials as being additive. In that sense, one cubic centimeter of solid material A with density of 1.0 g/cm^3, when mixed, without any chemical reaction, with a cubic centimeter of solid material B with density of 2.0 g/cm^3, results in a mixture with an average density of 1.5 g/cm^3, which is exactly the linear average of the densities.

The identification of the (non)linearity of a geometallurgical variable is important because linearity is often assumed in change of support (e.g., compositing), in spatial interpolation (e.g., kriging), and in the conventional calculation of the average property of a mixture.

3.1.6 Multivariate complexities

In mining, it is often required the modeling of multiple variables simultaneously. Relationships between variables can be very complex. One complexity occurs when the relationship between variables must respect a defined constraint. The composition constraint in chemical assays is an example, where the summation of all the chemical elements in a sample must be equal to one. Another complexity is the heteroscedasticity of a variable about another, that is, the variance of one variable is conditioned to the value of a second variable. A nonlinear relationship between variables is also a complexity. These multivariate features are usually present in geometallurgical variables and they prevent the use of cosimulation techniques that requires the data to be multivariate Gaussian (multiGaussian). To address this issue, some techniques may be considered for transforming variables to be multiGaussian (BARNETT; DEUTSCH, 2015). After multiGaussianity is achieved, the variables can be decorrelated and simulated independently in a modern geostatistics multivariate workflow.

3.2 Differences between geological and geometallurgical sampling, data, and variables

There are significant differences between geological and geometallurgical sampling, data, and variables. The first source of direct-measured geological data usually comes from exploration sampling, where sampling is widely spaced through the region of interest by drill cutting or cores. This sampling aims to intersect the deposit and is mostly interested in determining the in-situ grades, thickness, density, and lithology. The procedures for analyzing the variables are very well-established and controlled. The second source of direct-measured geological data occurs with the grade control sampling in the exploitation phase. Sampling is much more intense, although procedures are not so well-controlled. The objectives consist of better defining the mineralization contours and classifying the material between ore types (oxides, sulfides) or between ore and waste. The vast majority of the geological variables are additive, which allows linear compositing [2] and interpolation to be done without the risk of introducing bias in the process.

Geometallurgical sampling is aimed at understanding the characteristics of the ore at the processing plant. Geometallurgical data are obtained through geometallurgical tests, in which ore processing properties (response variables), are measured and correlated to intrinsic rock properties (primary variables) (LISHCHUK et al., 2020; COWARD et al., 2009). Geometallurgical sample selection, test work, and predictive modeling are guided by a geometallurgical program. Lishchuk et al. (2020) presents in detail all the stages of a geometallurgical program and how it can be planned and developed. The execution starts with the geological variability study, aiming at defining domains. A minimum number of samples for each domain is required and characterization of the metallurgical responses is performed under metallurgical tests. Test work consists of *i*) laboratory-scale metallurgical tests using composited samples; *ii*) variability tests using a large number of samples; *iii*) pilot plant tests; and *iv*) plant observations (LISHCHUK et al., 2020).

For geometallurgical purposes, where test work is carried out to understand only the influence of the primary variables on the response variables, it is ideal to fix the operational settings of the bench-scale testing, such that a default setting is established (e.g., the same amount of collector dosage, or the same period of time for grinding each sample). Other objectives of test work are to preview plant processing results on a smaller scale and/or to test different settings for its operation. If they are carried out in a controlled environment, following standardized and consolidated practices, and meeting all the required QA/QC protocols, bench tests can be considered to provide accurate and reliable data. The input of

[2] it is usual to composite drill holes by a constant length. For the variable *grade*, which is based on *mass*, this procedure implicitly assumes that the *density* of each composite is the same. If this is not the case, compositing should consider the density as a weighting factor to correct the unbalanced mass of each composite.

the tests may be either a composited sample from several drill holes, a composited sample formed from samples with minimum spatial separation, or an individual sample collected at a specific location (also called variability sample) (DOMINY et al., 2019). Composited samples are useful to understand the behavior of blends in the mill. However, variability samples are preferred for spatial 3D modeling of the variables of interest and for assessing the variability. One of the main issues of geometallurgical sampling is its low availability and the requirement for large sample volumes (DOMINY et al., 2019; DEUTSCH, 2015). While resource estimation collects more than 5000 samples, only 25 to 50 samples are usually collected for geometallurgical testing (DOMINY et al., 2018). The characterization of the ore allows the linking of the process responses to the primary properties of the samples. Carefulness should be taken because the regression of the variables is valid only for the scale of the measurements. Application of this regression in different scales may lead to bias (COWARD et al., 2009; DUNHAM; VANN, 2007).

Another sampling occurs in the plant, often conducted with regular extractions taken at small fractions of material, usually in a conveyor belt or in a pile before feeding the plant and after the processing stages, in the concentrates and tailings. The objectives are to evaluate the plant performance, confirm geological and metallurgical test work, and investigate scale-up and metallurgical responses (DOMINY et al., 2019). The relationship between laboratory-scale test work and plant-scale metallurgical performance is unclear (CORNAH, 2013). Because of the complexities that happen in a big-scale processing operation such as material recirculation, real-time adjustments of operational settings, blending of material, and so on, reconciliation with the bench-scale data may be challenging. In section 3.3, a comparison between real bench test and plant dataset is presented.

In summary, metallurgical responses can be spatially predicted through regressions with the spatial estimates of the primary variables as predictors, but the scale of the spatial estimates should approximate the scale of the test work measurements. Most metallurgical variables are found to average nonlinearly. Some examples are metallurgical recovery and BWI. When mixing a ton of material A with a BWI of 10.0 kWh/t with one ton of material B with a BWI of 12.0 kWh/t, the linear average of 11.0 kWh/t does not represent the average value of the mixture. The same reasoning applies to metallurgical recovery. If two similar blocks have recoveries $R1$ and $R2$, respectively, and are combined into a superblock, the value of recovery of this superblock may not match the linear average of $R1$ and $R2$ (CARRASCO et al., 2008).

3.3 Bench test and plant dataset consistency

A bench test database and a plant database from a phosphate mine were compared. EDA was conducted on both of them individually and they were compared in terms of

univariate and bivariate statistics.

3.3.1 Bench test dataset

The geometallurgical bench test database consists of 16,095 samples. Most of the samples have sample identification and geological, assay, and metallurgical information (Table 1). The term metallurgical recovery is used to refer to P_2O_5 recovery. Mass recovery and metallurgical recovery are calculated variables. Measurements of other variables were also available, but omitted since they were not relevant to this study. The location of the 16,095 samples is shown in Figure 6.

Table 1 – Bench test database - Summary

Type of information	**Variable**
Sample information	BHID
	Origin/Type
	Local
	X
	Y
	Z
	Length
Geological information	Lithology
	Weathering
Assay information (ROM)	P_2O_5
	P_2O_{5AP} (apatite)
	Fe_2O_3
	Al_2O_3
	MgO
	SiO_2
	CaO
	BaO
	Nb_2O_5
	TiO_2
	RCP (Ratio: CaO/P_2O_5)
Metallurgical information	Quantity of collector (g/t of ROM)
	Metallurgical recovery
	Mass recovery

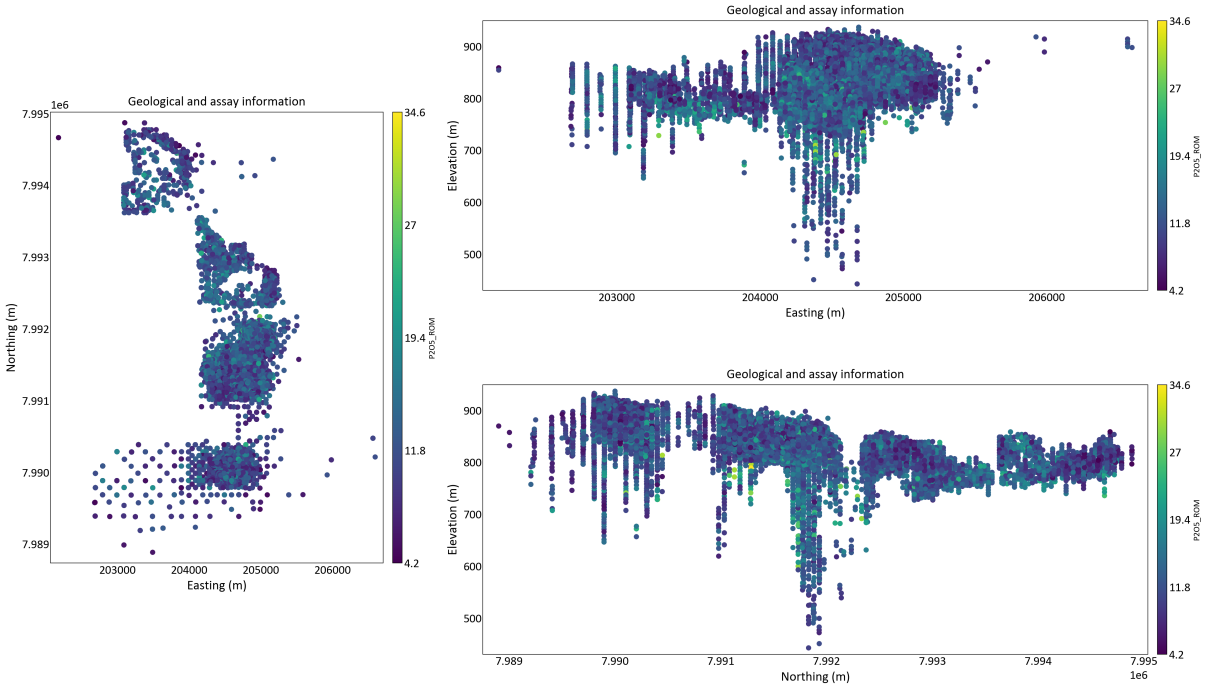

Figure 6 – Bench test database - Sample locations. Colorbar refers to P_2O_5 grade. XZ and YZ planes present vertical exxageration.

In the EDA phase, the first variable analyzed in the dataset is the sample support. Figure 7 shows the samples length distribution. It can be seen that the length ranges from one to 15 m, but most of the data are 5 meters long (78%). Five meters is enough to provide material for the metallurgical tests without the need for compositing samples.

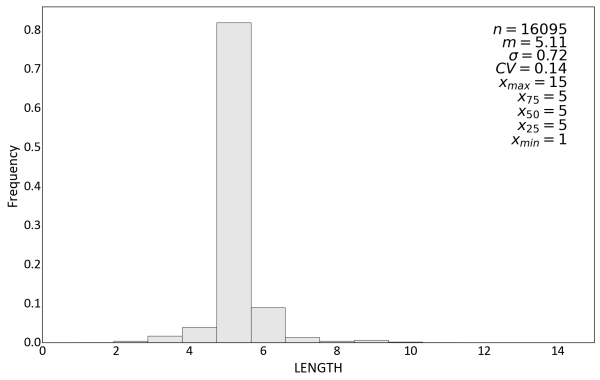

Figure 7 – Bench test database - Sample length distribution.

Another variable related to data consistency is the origin/type of data. In the overall dataset, data are almost divided 51% - 49% - 0% from DDH, drilling powder, or trenches/channels samples, respectively (Figure 8).

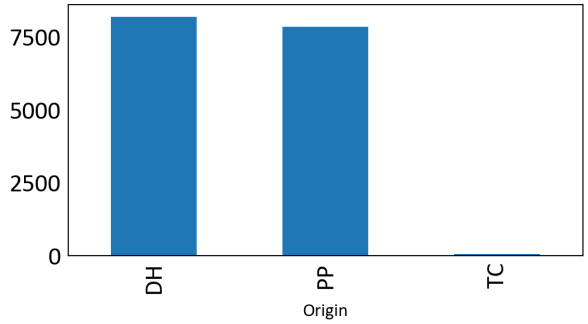

Figure 8 – Bench test database - Sample type quantity. DH refers to diamond drilling. PP refers to drilling powder samples. TC refers to trench and channel samples.

Regarding the categorical variables, there is information about the lithology, weathering, and region/location of the samples. The samples of the database are restricted to the isalterite weathering profile, which is the profile considered to be ore, given the leaching of calcium, magnesium, and high concentration of apatite. ISAOX is the oxidized isalterite, and ISAMC is the micaceous isalterite. The lithology refers to the mineral composition of the samples, mostly carbonatite (CBN), phoscorite (FCR), and bebedorites (BEB). The local variable brings information about the region in the deposit where the samples are from. Note that many samples do not have a registry for lithology and/or weathering, being assigned with the symbol ' - ' (Figure 9). This is mostly related to operational problems during the identification.

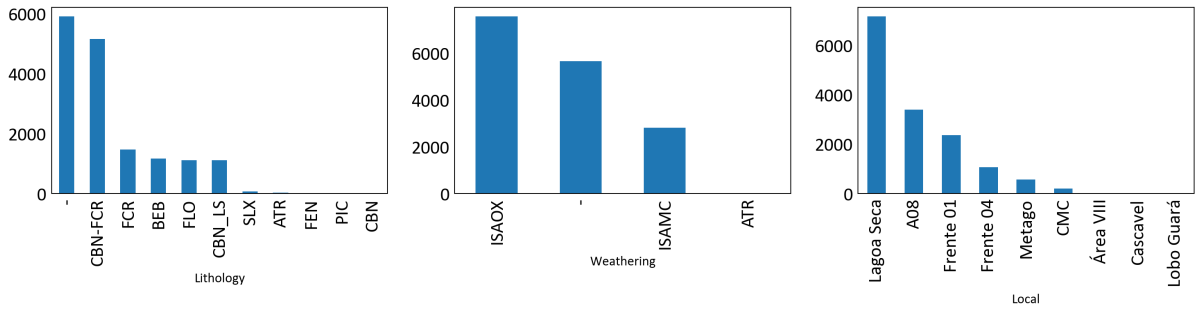

Figure 9 – Bench test database - Categorical variables. In lithology, most data are classified into carbonatite (CBN), phoscorite (FCR), bebedorite (BEB), or phlogopitite (FLO). In weathering, most data are from isalterite profiles, ISAOX and ISAMC.

Before the assay information is analyzed, some data filtering is performed. A decision to keep only the DDH samples was made, as they are considered to be more accurate than the other data types. In addition, only DDH data with a 5-meter core length are used, as they provide enough material mass for the metallurgical test work, avoiding the need to composite samples. These procedures remove bias and increase the precision of the database. Regarding the categories, no relevant statistical differences in assay and metallurgical information were found to justify the separation of the data in the different

lithology/weathering domains. Probably, this occurred because of the operational problems in the classification, which resulted in the assignment of the ' - ' symbol for many samples. Moreover, dividing the data into the various possibilities of lithology or local classification would result in few data for each domain analysis, which is not desirable. After applying the filter, 4,862 data samples were kept. Assay information of the ROM can be visualized in the histograms of Figure 10. Note that some variables are under-sampled in relation to others. The least sampled variable is TiO_2, almost 15% less.

The variable P_2O_{5AP} is a calculated variable from $P_2O_5\_ROM$ and CaO_ROM, depending on the RCP value. RCP is used to determine the percentage of P_2O_5 associated with apatite, such that if $RCP \geq 1.35$, $P_2O_{5AP} = P_2O_5$; if $RCP < 1.35$, $P_2O_{5AP} = CaO/1.35$. As P_2O_{5AP} is not a measured variable, and to reduce the number of variables analyzed, P_2O_{5AP} is excluded from the analysis from now on. If necessary, it can be calculated in any model from $P_2O_5\_ROM$ and CaO_ROM estimated values.

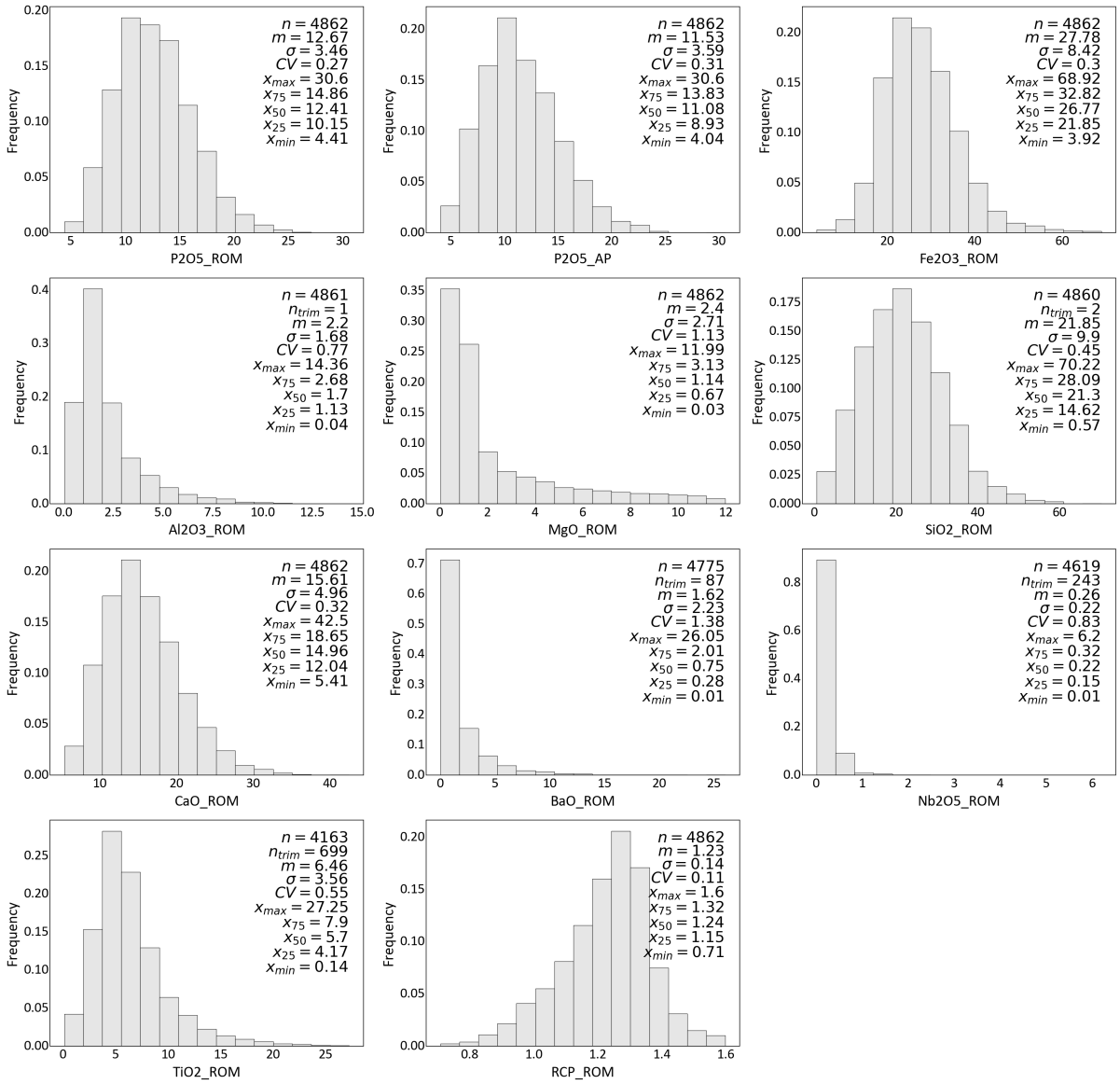

Figure 10 – Bench test database - Histograms for oxides and RCP.

After analyzing the geological data and how they were treated, it is important to understand how the metallurgical test work was performed and its outputs. Bench tests are designed to reproduce what happens to the ore inside the processing plant. Each ROM sample provides approximately five kilograms (5 kg) of material, which is first grounded in a mill. According to what would happen in the plant, the material is forwarded to magnetic separation, except for fines, which go to tailings. The non-magnetic material is quartered until sample aliquots of five hundred grams (500 g) of mass each are reached. The number of aliquots ranges between one to three for each sample of non-magnetic material. These procedures are preparation stages for the flotation tests. One flotation test is performed with each aliquot, varying the collector dosage. Therefore, for each ROM sample input, different dosages of collector are applied and results of metallurgical and mass recovery are obtained. This procedure allowed the increase of the database. Also,

it allowed the understanding of the importance of the variable collector dosage to the results, as discussed later. However, there were still problems with missing values for some variables. To understand the relationship between primary and response variables fairly, it was decided to use just the homotopic sampling, that is, only the data containing information on all the variables. 5,188 samples comply with this decision.

The recoveries refer to the whole process. Metallurgical recovery is calculated by multiplying the recovery of the preparation stage by the recovery of the flotation (Equation 3.1). The metallurgical recovery of each stage is calculated through Equation 3.2.

$$Met.recovery = Met.recovery_{(prep.)} \cdot Met.recovery_{(flot.)} \tag{3.1}$$

$$Met.recovery_{(stage)} = \frac{c \cdot C}{f \cdot F} \tag{3.2}$$

where c is the P_2O_{5AP} concentrate grade of the stage, C is the concentrate mass of the stage, f is the P_2O_{5AP} feed grade of the stage, and F is the mass feed of the stage. The mass recovery is calculated through Equation 3.3.

$$Mass\,recovery = Met.recovery \cdot \frac{f}{c} \tag{3.3}$$

where c is the P_2O_{5AP} concentrate grade of the whole process, and f is the P_2O_{5AP} feed grade of the whole process.

Metallurgical and mass recovery histograms are shown in Figure 11. The histogram for the collector quantity in grams per ton of ROM is shown in Figure 12.

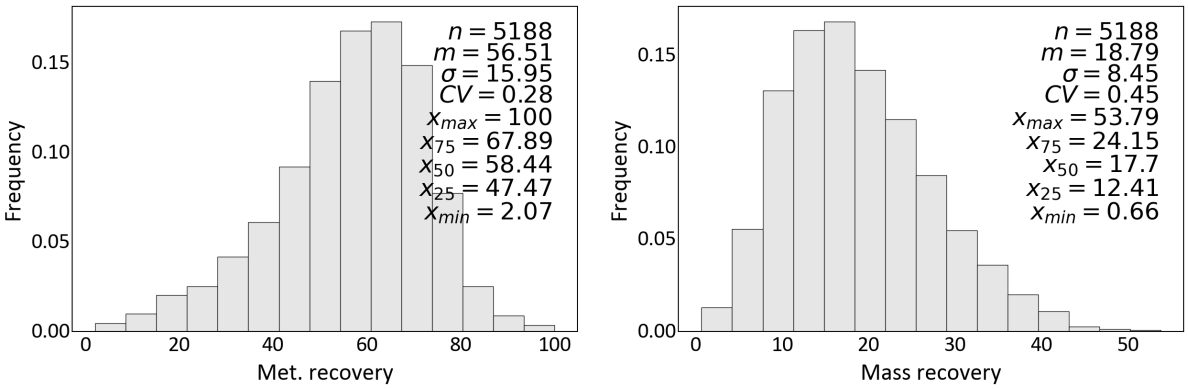

Figure 11 – Bench test database - Metallurgical and mass recovery histograms.

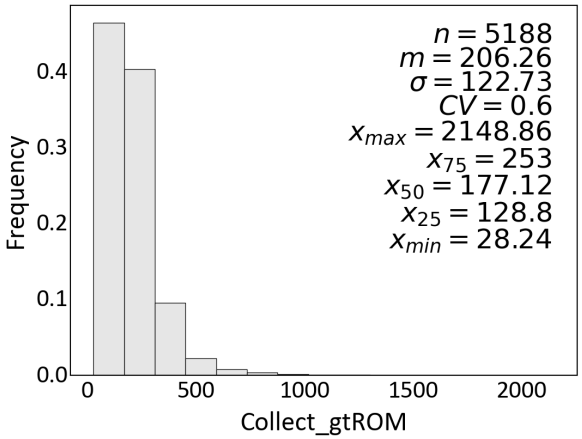

Figure 12 – Bench test database - Collector dosage histogram.

The location plot of the homotopic sampling is shown in Figure 13. Note that homotopic sampling is more representative of the center and south regions.

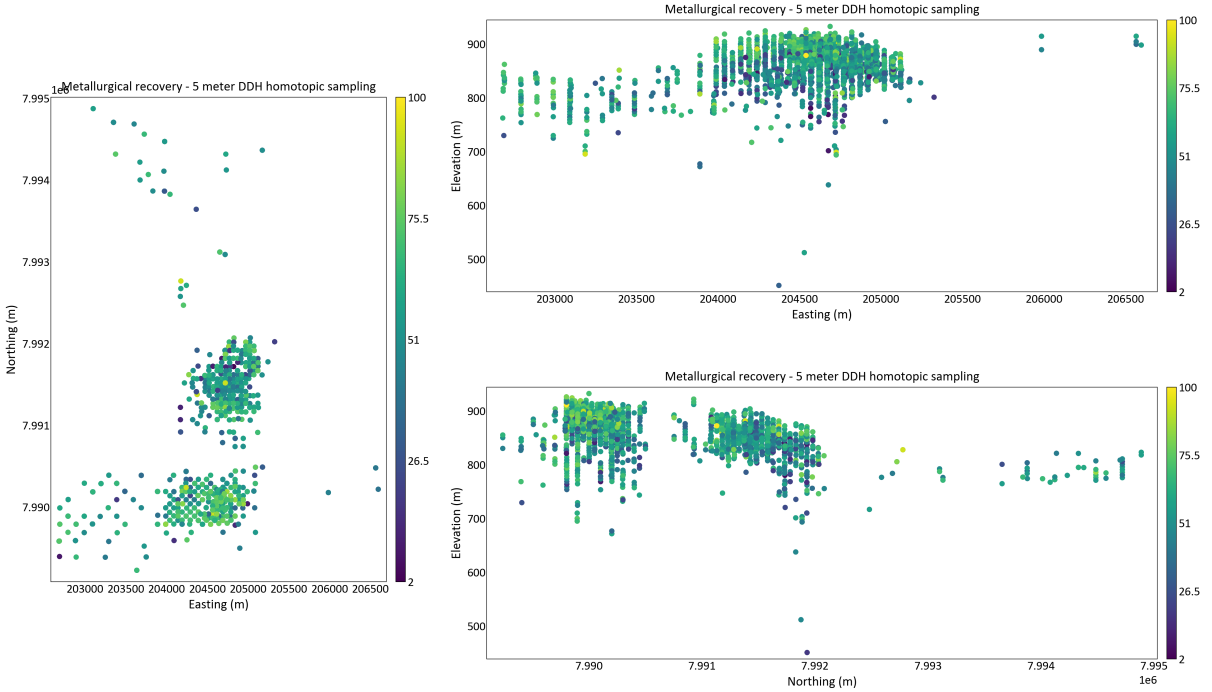

Figure 13 – Bench test database - Location plot of the homotopic sampling. Colorbar refers to metallurgical recovery (%). XZ and YZ planes present vertical exxageration.

Bivariate relationships are shown through the correlation (ρ) matrix in Figure 14. In the bivariate analysis, bench test data results show that mass recovery has a high (0.7 or greater) correlation with P_2O_5 (0.73) and CaO (0.72); and an intermediate correlation with collector dosage (0.69) and SiO_2 (-0.47). Conversely, metallurgical recovery is not well correlated with any ROM variable, only intermediately with the collector dosage (0.46).

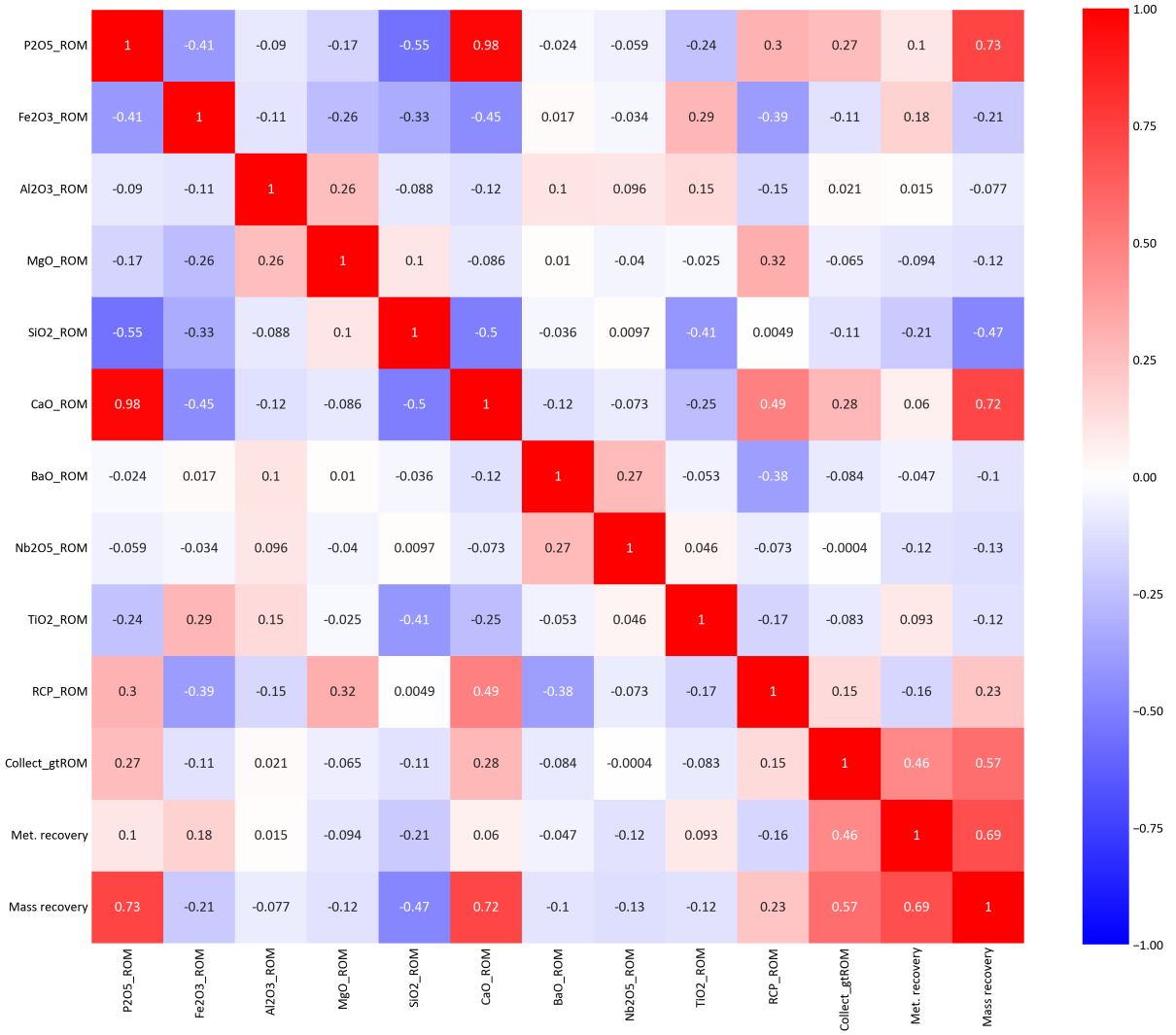

Figure 14 – Bench test database - Coefficient correlation matrix.

Another way to analyze a database and the relationship between its variables is through regression. A random forest regressor was developed and applied to the database, with the aim to predict the two metallurgical variables - metallurgical recovery and mass recovery - given the other measured variables P_2O_5, Fe_2O_3, Al_2O_3, MgO, SiO_2, CaO, BaO, Nb_2O_5, TiO_2, RCP, and collector dosage. The 5,188 geometallurgical samples were randomly split into a current dataset (80% of the samples) and a future set (20% of the samples). The current dataset was used to train and test the random forest regressor and to allow the better tuning of its hyperparameters. The training and testing datasets were generated through the ten-fold splitting of the current dataset, where nine folds were used to fit the regressor and one fold was used to test it. To avoid bias, this procedure is iterative, such that each fold has the opportunity to test the fitting of the regressor trained by the other nine folds. The future set mimicked new data and was used to evaluate the regressor. The correlation coefficient of the predicted vs. the true values in the future set reached up to 0.77% for metallurgical recovery and 0.90% for mass recovery (Figure 15).

In addition, the Random Forest regressor provided a ranking with the most important predictors, which is shown in Table 2.

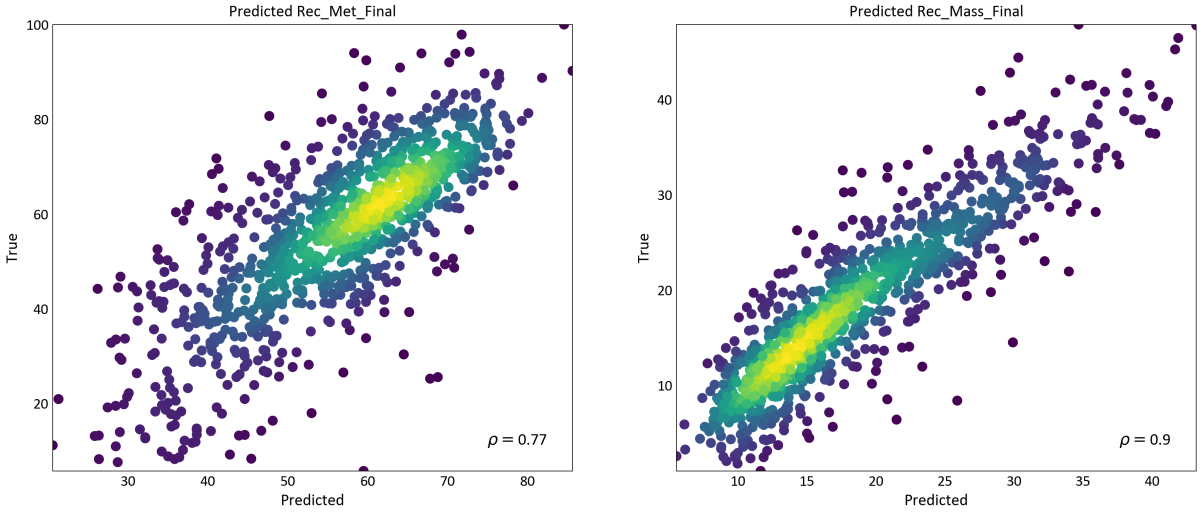

Figure 15 – Bench test database - Scatter-plot of predicted vs. true values in the future set. Left: Metallurgical recovery. Right: Mass recovery.

Table 2 – Bench test database - Ranking of the most important predictors

Predictor variable	**Importance (%)**
Collector dosage g/t	0.38
P_2O_5	0.12
RCP	0.10
CaO	0.05
Fe_2O_3	0.05
Al_2O_3	0.05
MgO	0.05
SiO_2	0.05
BaO	0.05
TiO_2	0.05
Nb_2O_5	0.05

Aiming to have a model that could be compared against the model using the plant dataset, another model was developed without the variable collector dosage (Figure 16), as the collector dosage information is unavailable in the plant database. Note the drop in the prediction of both variables.

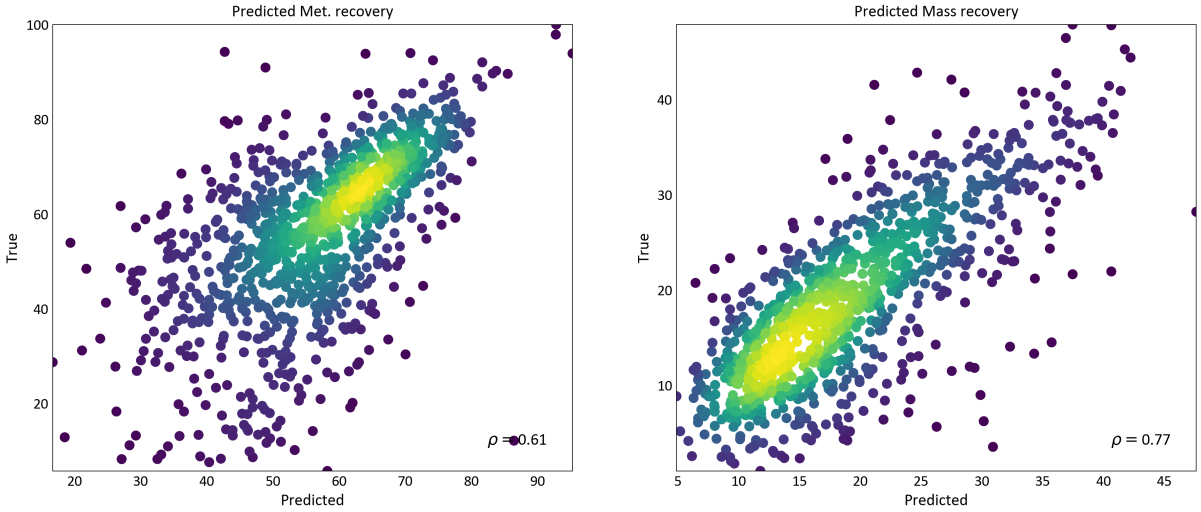

Figure 16 – Bench test database - Scatter-plot of predicted vs. true values in the future set without considering the variable collector. Left: Metallurgical recovery. Right: Mass recovery.

3.3.2 Plant dataset

The plant dataset consists of almost regular daily records of chemical assay of the material feeding the plant (ROM) and their associated metallurgical and mass recoveries. Categorical variables like lithology, weathering, and local are not available, as this information is lost when the material goes to a homogenization pile, where the material is mixed and then reclaimed. There are 1,018 measured data over three years (2019-2021). No data preprocessing were performed. Table 3 shows all the measured variables at the plant. Note that two assay variable measured at the plant are not measured in the bench test, SrO and F. Another difference between bench test data and plant data is the absence of measurement of the collector in the plant. The histograms of the variables are seen in Figure 17 and the results of metallurgical and mass recoveries are in Figure 18. Similarly to the bench test database, the variable P_2O_{5AP} is considered redundant and is excluded from further analysis.

Table 3 – Plant database - Summary

Type of information	**Variable**
Assay information (ROM)	P_2O_5
	P_2O_{5AP}
	Fe_2O_3
	Al_2O_3
	MgO
	SiO_2
	CaO
	BaO
	Nb_2O_5
	TiO_2
	RCP (Ratio: CaO/P_2O_5)
	SrO
	F
Metallurgical information	Metallurgical recovery
	Mass recovery

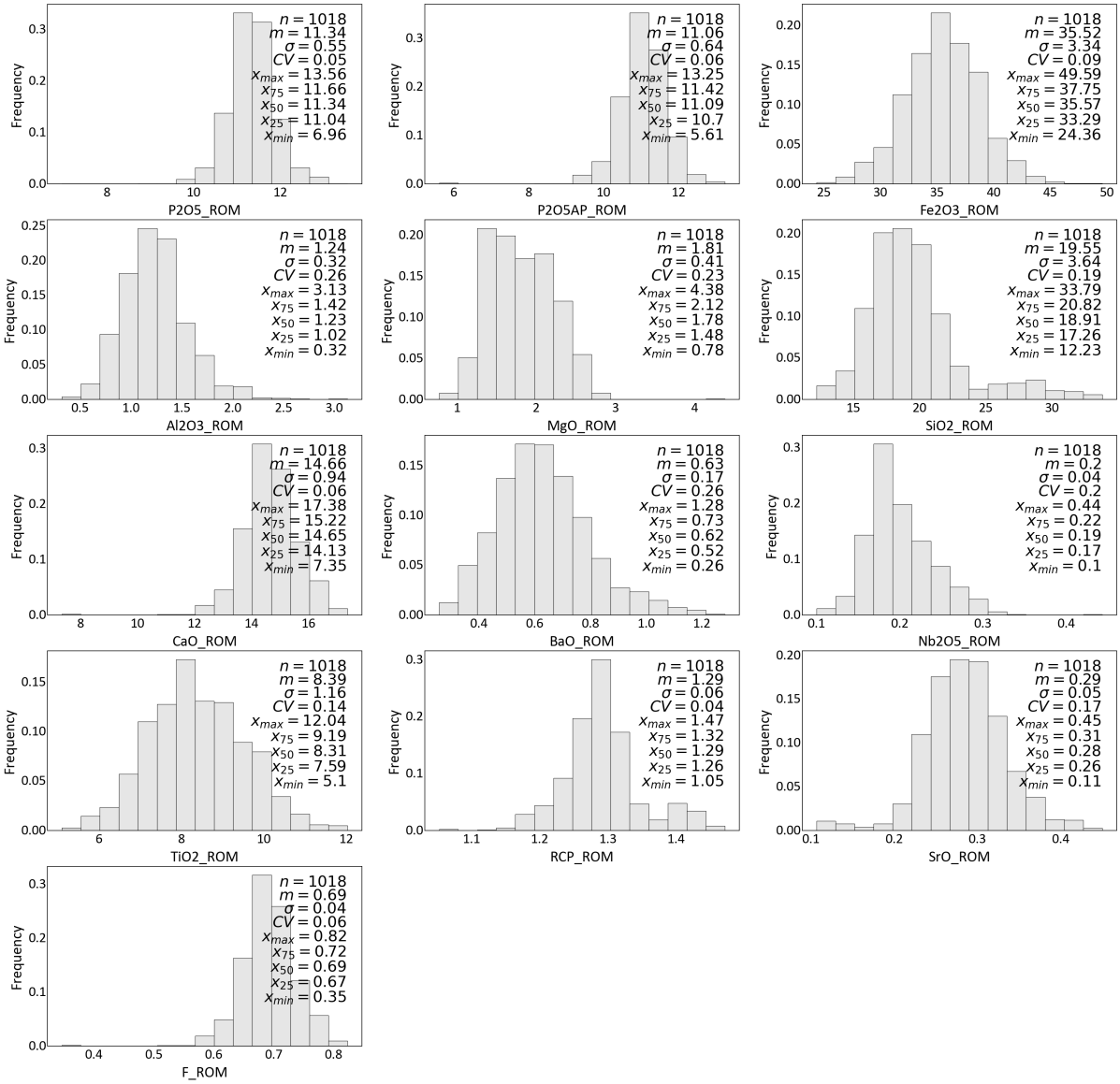

Figure 17 – Plant database - Histograms for the chemical elements.

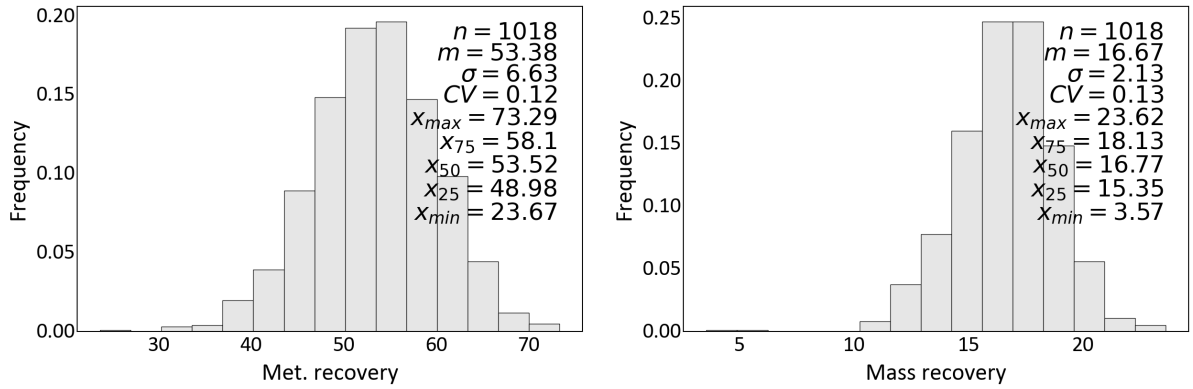

Figure 18 – Plant database - Metallurgical and mass recovery histograms.

Bivariate relationships are shown through the correlation matrix in Figure 19. Plant data do not show high correlations between ROM variables and mass or metallurgical

recovery. The higher correlation for mass recovery is with CaO, F, and RCP (0.4, 0.4, and 0.38, respectively) and for metallurgical recovery is with SiO_2 and Fe_2O_3 (-0.29 and 0.27, respectively). No information about the collector dosage is available in the plant database; hence, no correlation is obtained.

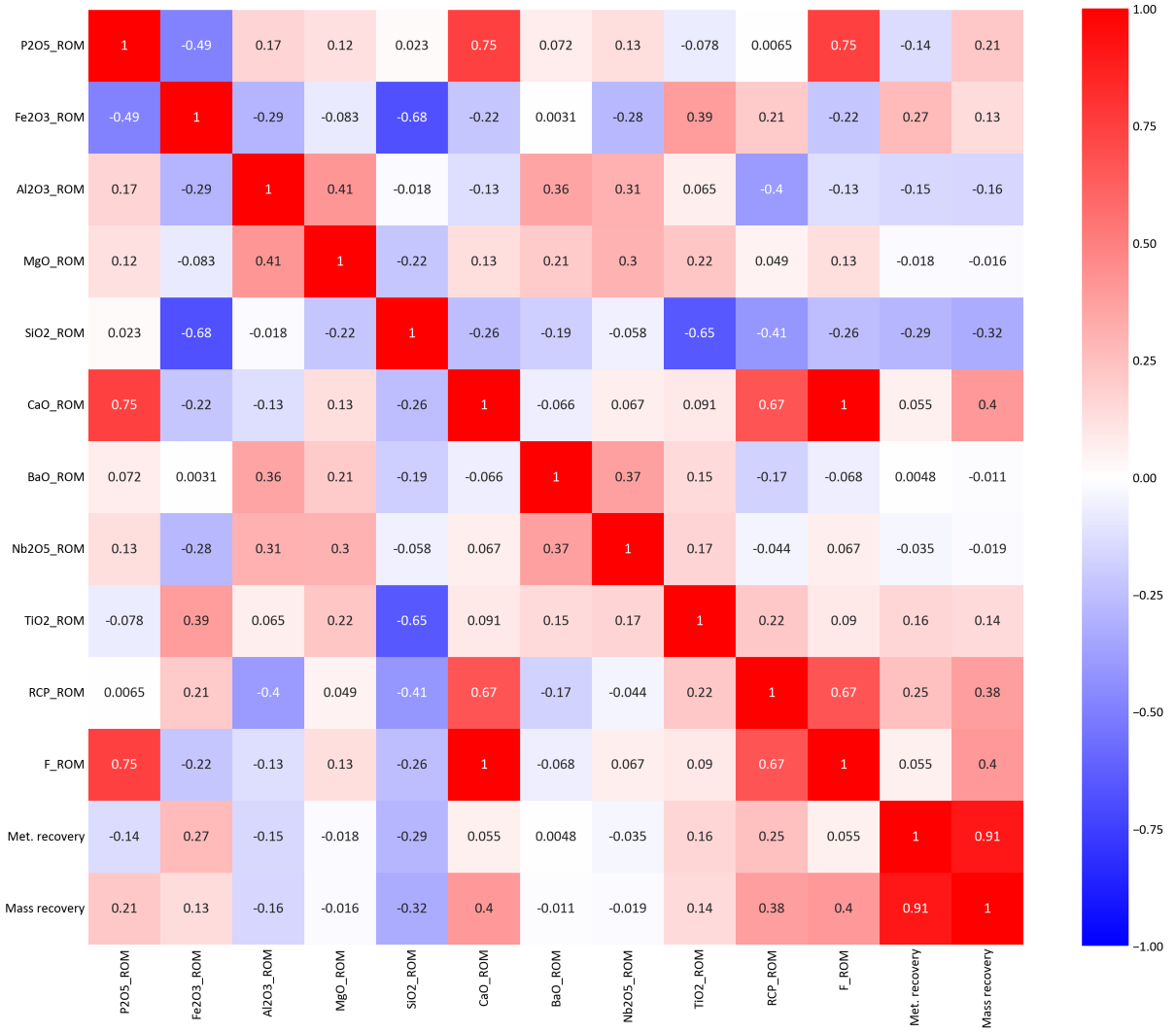

Figure 19 – Plant database - Coefficient correlation matrix.

The same RF regression procedure was applied to the plant database. Predictor variables were P_2O_5, Fe_2O_3, Al_2O_3, MgO, SiO_2, CaO, BaO, Nb_2O_5, TiO_2, RCP, SrO, F. The correlation coefficient of the predicted vs. the true values reached up to 0.44% for metallurgical recovery and 0.45% for mass recovery (Figure 20). The drop in prediction power when applying the machine learning model in the plant database, compared to the application on the bench test database, even when the collector dosage was ignored (Figure 16), is one indication of the plant data complexity. More explanatory variables, related to operational settings, is probably required to increase the prediction power. The ranking with the most important predictors is shown in Table 4.

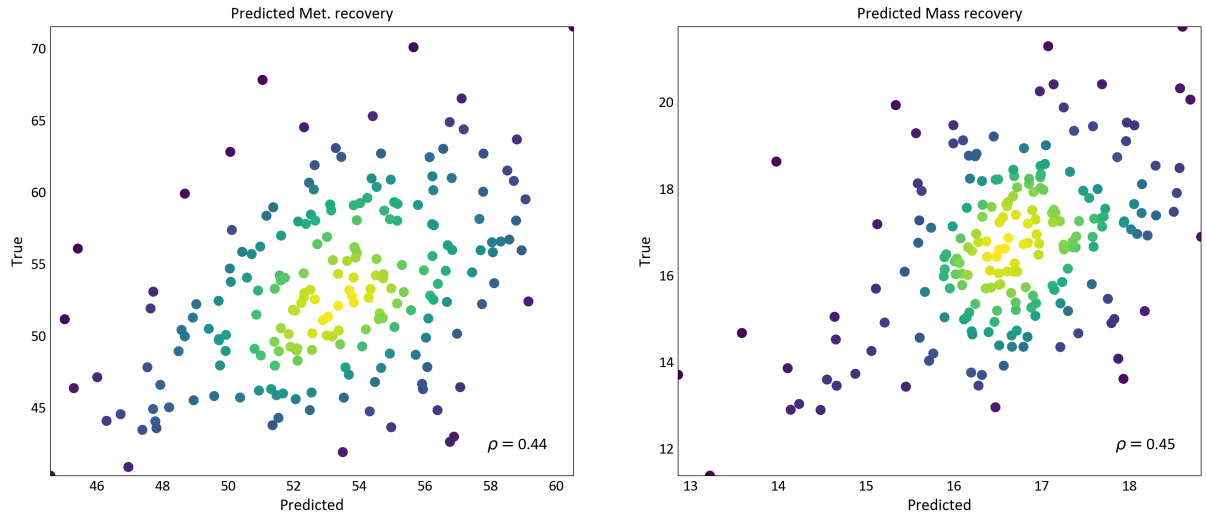

Figure 20 – Plant database - Scatter-plot of predicted vs. true values in the future set. Left: Metallurgical recovery. Right: Mass recovery.

Table 4 – Plant database - Ranking of the most important predictors

Predictor variable	**Importance (%)**
SiO_2	0.13
RCP	0.12
Fe_2O_3	0.11
SrO	0.11
P_2O_5	0.09
MgO	0.08
BaO	0.08
TiO_2	0.07
Al_2O_3	0.07
Nb_2O_5	0.06
CaO	0.05
F	0.03

3.3.3 Bench test - plant data comparison

Checking consistency between the databases consists in comparing univariate and bivariate relationships in both databases. The box-plots for bench test and plant datasets are plotted one below the other, for each variable, in Figure 21. In general, variables in the plant database have fewer outliers and lower variability than the variables in the bench test database. There are also differences in the median and mean (represented by the black x) between both databases for some variables.

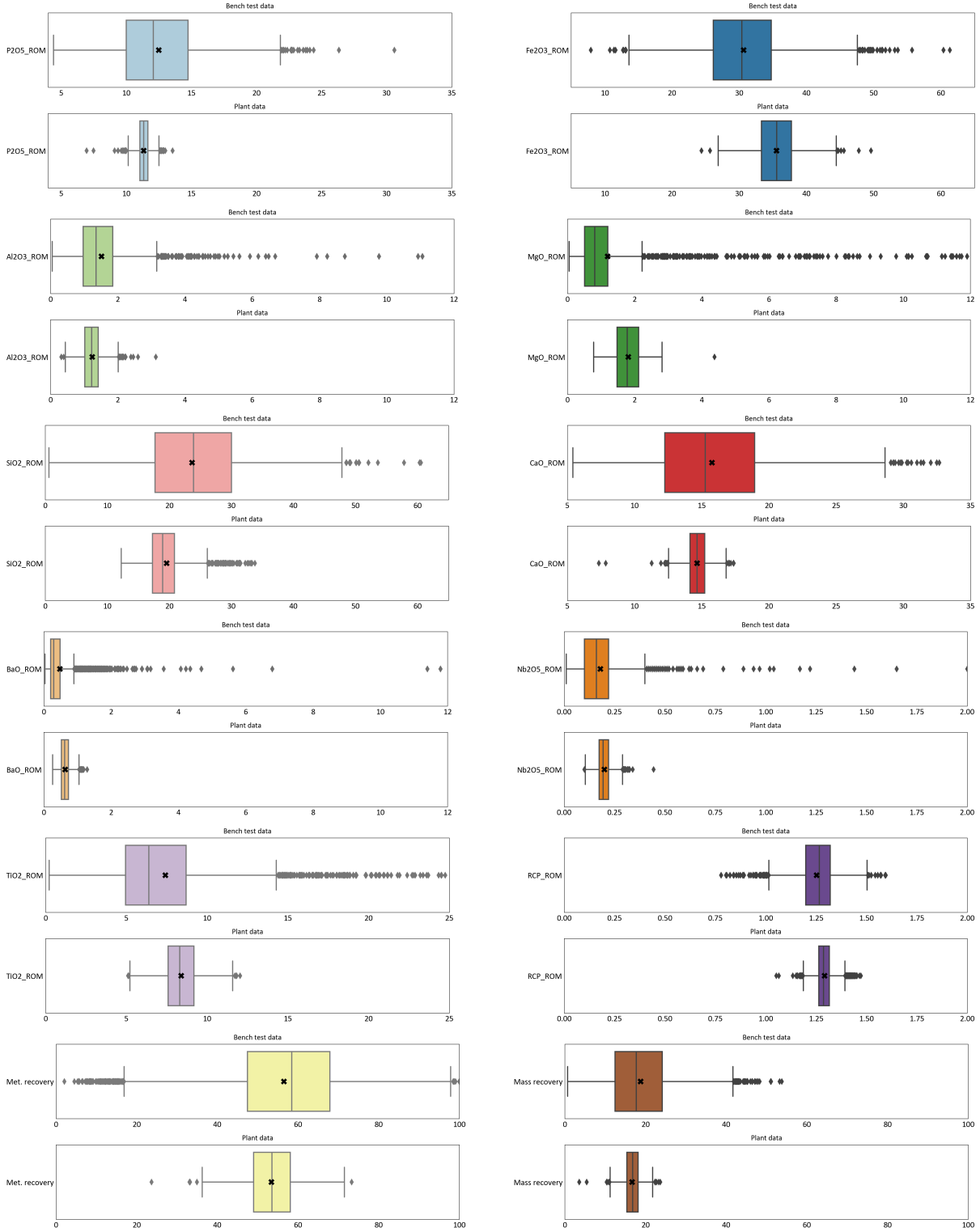

Figure 21 – Box-plots of each variable for each database. Each variable is plotted in a color. The top box-plot refers to the bench test database, while the bottom refers to the plant database. From left to right:P_2O_5 in light blue; Fe_2O_3 in dark blue; Al_2O_3 in light green; MgO in dark green; SiO_2 in light red; CaO in dark red; BaO in light orange; Nb_2O_5 in dark orange; TiO_2 in light purple; RCP in dark purple; metallurgical recovery in yellow; mass recovery in brown.

The difference in quantity and intensity of high correlations between the databases

becomes more clear with Figure 22, where a scatterplot of the correlation matrices of both datasets is plotted. For obvious reasons, only those variables available in both datasets are used.

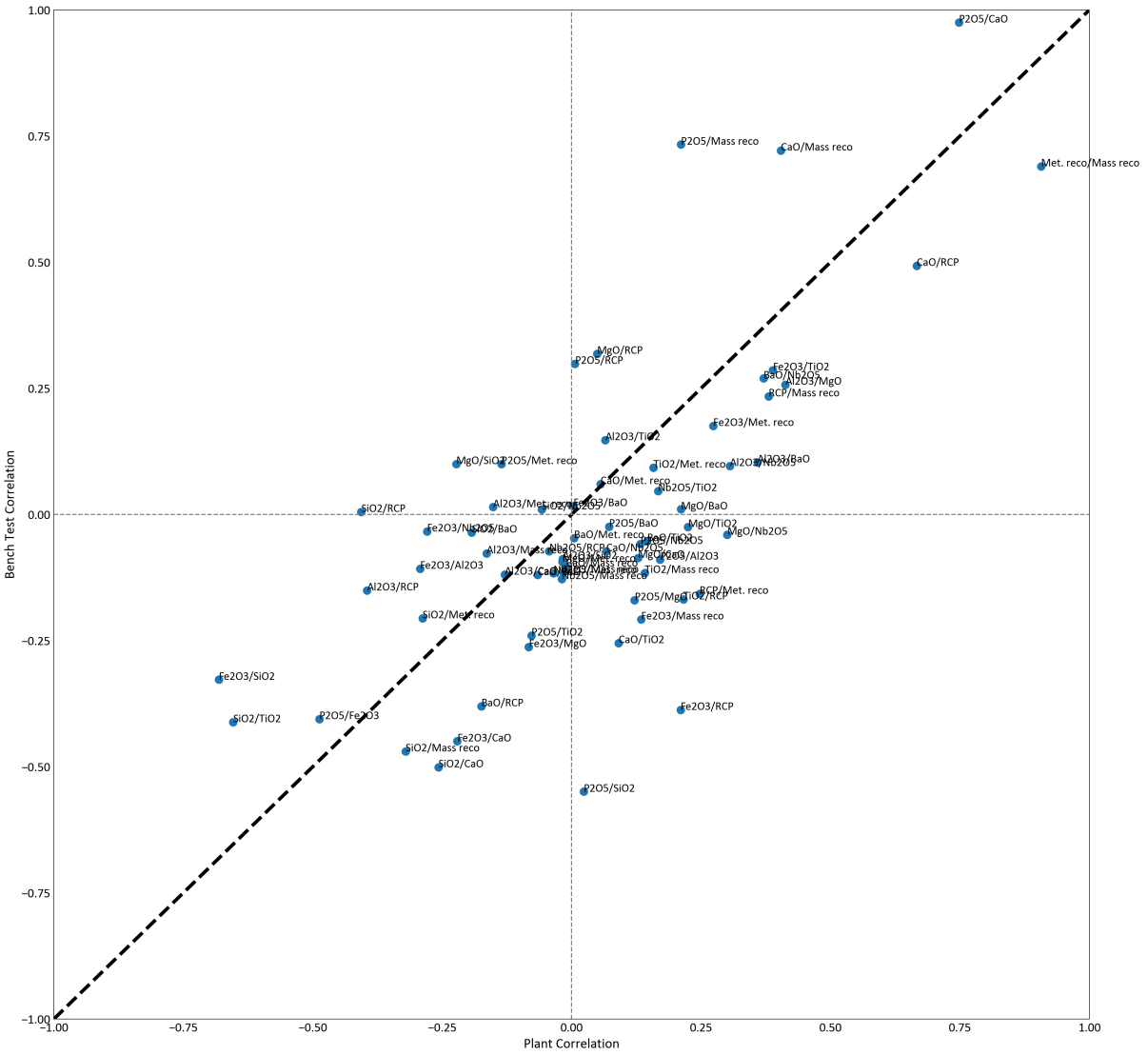

Figure 22 – Scatter-plot of bivariate correlations between plant (X-axis) and bench test (Y-axis) databases.

3.4 Discussion

The bench test database (5,188 samples) can be considered large in comparison to what other mines usually have for metallurgical test work. The existing differences in the data type, the data scale, and the availability of the measurement of the variables indicate that more than one sampling and testing in different time periods were performed during the mine life. These differences justify data filtering, aiming at improving accuracy and precision. From the location plot in Figure 13, one can see that this data is more representative of the center-south region. Considering that this database comes from

controlled test work, the data is very reliable.

The plant database is small compared to the bench test. Each one of the 1,018 samples represents the material fed and processed daily by the plant. There is no (x,y,z) spatial location for each sample, as they were formed by blending material in a homogenization pile; but it is possible to track the origin of the material fed to the plant. Each datum has the assay information and the metallurgical response. While the assay information comes from the plant feed, the metallurgical responses are calculated after concentration. As concentration stages take some time after the feeding of the material into the plant, there is difficulty in exactly matching the output results of the process with the right input in the feed plant (processing time delay). Another issue with the plant dataset is the absence of the variable collector dosage. As indicated by the bench test data, the collector is the most correlated variable to metallurgical recovery.

Comparing the univariate statistics of both databases, there are fewer outliers and lower variability in all variables in the plant database. This is expected because of: *i*) the greater data support of the material sampled, and *ii*) the existence of homogenization piles. Both reasons contribute to the blending of the material, where extreme values are diluted. When comparing the centres of the distributions, the median of both databases are close for some variables (P_2O_5, Al_2O_3, CaO, Nb_2O_5, RCP, Met.recovery and Mass recovery) but they are not for others (Fe_2O_3, MgO, SiO_2, BaO, TiO_2).

Comparing the bivariate statistics of both databases, we observe some high good conformity between bivariate relationships, but some discrepancies in Figure 22. Bench test correlations between the variables are more intense than plant data correlations, as there are four high correlations in the bench test database (P_2O_5/CaO, $P_2O_5/Massrec.$, $CaO/Massrec.$ and $Met.rec/Massrec.$), but three in the plant dataset (CaO/RCP, P_2O_5/CaO and $Met.rec/Massrec.$). A strange behavior occurs in the relationships $P_2O_5/Massrec.$ and $CaO/Massrec.$, which are highly positively correlated in the bench test dataset (0.73 and 0.72, respectively) but are low-intermediately correlated in the plant database (0.21 and 0.4, respectively). Most of the correlations reasonably follow the 45-degree line, meaning that the bivariate relationship is approximately the same in both databases. Attention must be given to the correlations that change signs between the databases, highlighting the P_2O_5/SiO_2 relationship, with no correlation in the plant data, but with an intermediate negative correlation in the bench test database (-0.55) and Fe_2O_3/RCP correlation (-0.39 in bench test, and 0.21 in plant database).

When comparing the regression based on each dataset, it is clear that the metallurgical responses are more accurately predicted using the bench test dataset. The most important variable for predicting them is the collector dosage, which is missing information on the plant dataset. However, even if we disconsider the collector dosage as a variable, the prediction using the bench test dataset is still better than using the plant test.

The reasoning for the discrepancies in both uni- and bivariate relationships could be related to material representativeness: the material fed into the plant is not the same as the material analyzed in the bench test. The consideration of only the bench samples that are on the same time horizon as the plant data, that is, the samples that were within the period from 2019 to 2021 or at least close to that, is a fairer comparison and could improve the adherence between the databases. Other explanations are related to sampling bias in the plant, given the existing complexities in this environment, and/or related to upscaling, as the particle dynamics in an industrial plant are very different from the existing dynamics in a bench test/pilot plant. These differences corroborate the difficulty in doing reconciliation. Just as an illustration, when the Random Forest regressor was used to learn from the bench database and was used to predict the plant database, the correlation coefficient of the predicted vs. the true values was only 0.11% for metallurgical recovery and 0.25% for mass recovery.

Although theoretically the plant database should be used to obtain the correlations between geological and metallurgical variables, as it is consistent with the plant scale, it presents complexities that mask the true impacts of the geological variables over the metallurgical ones. Therefore, for a better understanding of their relationships, the bench database is more suitable.

3.5 Summary

Geometallurgy studies should benefit from the existence of the various sources of data available. However, it must be recognized that data may differ in terms of support, accuracy and precision, scale, availability, and representativeness. These factors can impact the variables obtained in each sampling process, resulting in different characteristics depending on the type of data. This study shows these differences with real data, highlighting the existing complexities when it comes to geometallurgy and the integration of data in decision-making at the mine and at the plant. If the objective of the geometallurgical study is to differentiate the ore and its intrinsic properties when subject to a metallurgical process, it is a good idea to fix the required sampling procedure and support, as well as the operational settings of the bench test. The establishment of a default setting helps avoid bias and precision problems. Variability samples allow the identification in the 3D space of high and low areas concerning the metallurgical response of interest. Composited samples have a place when the objective is to understand the behavior of blends in the mill. Spatial interpolation of the response variable is possible, but with caution, since they probably average nonlinearly (see chapter 4). The complexity of reconciling plant data with pre-production data is evident, whether because they are affected by the complex processes existing in the mine and the mineral plant, because of the difficulty in sampling, or because of material traceability problems.

4 PREDICTING GEOMETALLURGICAL RESPONSE OF ORE BLENDING

Blending is the mixing of different ores. Depending on its benefit, it can be planned or deliberately avoided, if deemed (in-)appropriate. Intentional blending is the direct operation of blending the ore through homogenization piles. However, ores may also mix naturally during mining and mineral process operations. One type of natural blending is when waste is mixed with ore, usually referred to as dilution. Ore dilution occurs indirectly in the blasting of the ore, in its loading into the trucks, in its dumping into a pile or a crusher, and in all stages of a processing plant. Estimating the blended ore properties is usually a straightforward task where the weighted average of the attribute is considered. However, this approach is not correct if the attribute of interest averages nonlinearly. Nonlinearity also affects scaling. Depending on the property mixing and scaling behaviors, the blended property over a material volume V can be higher or lower than the linear average of its N components, each one with volume $\frac{V}{N}$. This difference can be significant enough to modify decisions in mine planning and mine/process operations. This chapter deals with averaging behaviors. Terms such as blending neutral, blending synergistic, and blending antagonistic are explained. A flexible nonlinear mathematical function is proposed to model the blending and scaling of variables. At last, the proposed model is applied to an example case, and a sensitivity analysis is performed.

4.1 Blending in mining

The representation of the orebody through a block model is convenient for ore modeling, spatial estimation, and mine planning. The mining blocks have dimensions according to the selectivity of the mining operations. However, this representation is an approximation, as shovels do not extract cubes or prismoids (ROSSI; DEUTSCH, 2014; DOWD et al., 2016). In all mining and ore processing operations, there is some natural mixing of the material handled. This type of blending is most known as operational dilution, and its intensity degree can be higher or smaller depending on the geological body features, the mining method, the mining operational procedures and equipment, and the plant flow system.

Operational dilution starts to occur in the blasting and excavation operations, is present during the material handling, and goes on until the material is processed in a plant. A simulation study by Deutsch (2015) demonstrated that even when the ore is fed in batches, a large amount of mixing occurs within the mill.

The other type of blending is intentional blending, where homogenization piles are used. The main objectives are *i*) feed material with uniform and low-variability properties to the plant, allowing an optimum and steady operation, and *ii*) blend small quantities of poor-quality ore into high-quality ore, maximizing ore reserves.

Understanding and modeling the blending behavior of mixtures are central for optimum decisions in mine planning. There is a need to spatially model and use geometallurgical variables in mine planning, as well as understand how their averaging is related to blending and change of scale, given their importance and impacts on the downstream process and the project's economical value.

4.2 Averaging behavior

When blending occurs, it is often assumed that the blended material's average property, termed as *effective property*, is the mass or volume-weighted average of each component property. This is correct when dealing with variables that average linearly, such as grades. Equation 4.1 shows the formula to calculate the effective grade g_{eff}, which is the linear average grade $\overline{g}$ from N materials that are mixed, where m_i and g_i are the mass and grade, respectively, of each component $i = 1, ..., N$ in the mixture.

$$g_{\text{eff}} = \overline{g} = \frac{\sum_{i=1}^{N} m_i \cdot g_i}{\sum_{i=1}^{N} m_i} \tag{4.1}$$

Some rock properties, however, average nonlinearly; hence, the denomination *nonlinear variables*. The averaging behavior of nonlinear variables may be very different from the usual-assumed weighted linear average model. The nonlinearity may be explained by one material's greater influence over the other. For example, a 50/50 mixture of two materials with different BWI values does not result in a mixed material with the mean BWI. Its effective BWI is closer to the material with higher BWI, as there is often an accumulation of the hardest component in the mill (TAVARES; KALLEMBACK, 2013; YAN; EATON, 1994; CAMPOS et al., 2019). In special circumstances, it is even possible that the effective property value is beyond the value range established by mixing the two materials. Another nonlinear averaging behavior is seen in the percolation of fluids through porous materials, where a threshold value divides two very different behaviors of the effective property (DEUTSCH, 2020). The three nonlinear behaviors commented above are classified here as Type I, Type II, and Type III, respectively, and are illustrated, as well as a linear behavior, through a binary mixture of white rock and black rock in Figure 23. The X-axis represents the percentage of black rock in the mixture, starting from 0% black rock, that is, 100% white rock on the left end, and ending with 100% black rock, that is, 0% white rock, on the right end. The Y-axis represents the effective property of the mixture, where the lower end represents the effective property of a pure-white rock,

and the upper end represents the effective property of a pure-black rock. Any mixture of black and white rock has an effective property, which is an average, not necessarily linear, of the properties of each individual rock.

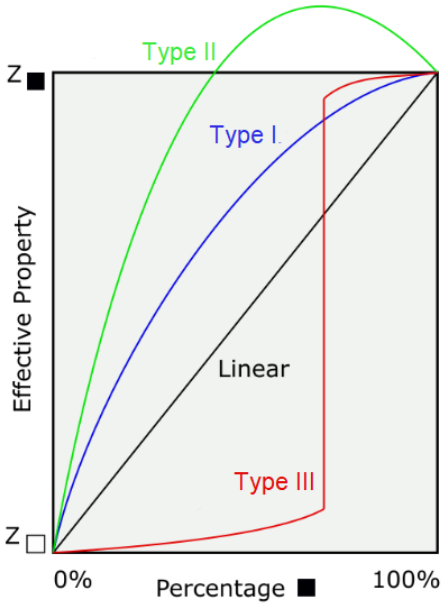

Figure 23 – Different nonlinear behaviors. On the X-axis, the proportion of black rock in a black-and-white rock mixture. On the Y-axis, the effective property, where the lower value corresponds to the property of a pure-white rock, and the higher value corresponds to the property of a pure-black rock. Source: Modified from Deutsch (2020).

The nonlinear behavior may be a function of the blending of different proportions of rock mixtures, as shown in Figure 24, where the effective BWI is estimated, and in Figure 25, where the effective flotation grade is estimated; or be a function of other primary variables. A common nonlinear averaging is found when metallurgical recovery is estimated as a function of the ore head grade, which is displayed by the grade-recovery regression. Figure 26 shows examples where copper and gold recovery depend on the copper and gold head grades and the processing facility.

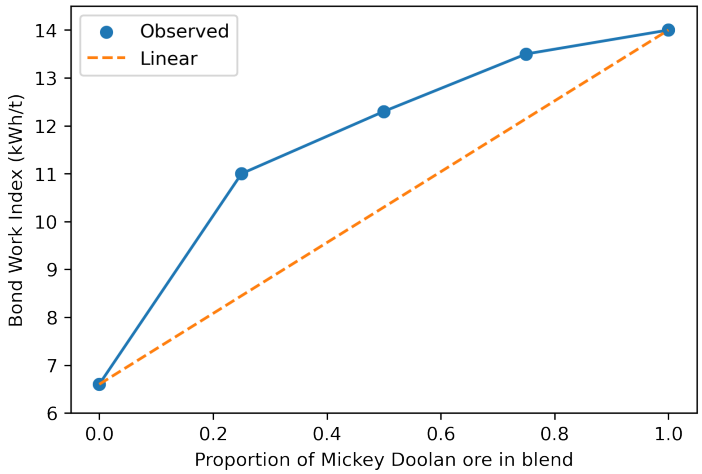

Figure 24 – Bond mill work index for a binary blend. Source: Modified from Yan and Eaton (1994).

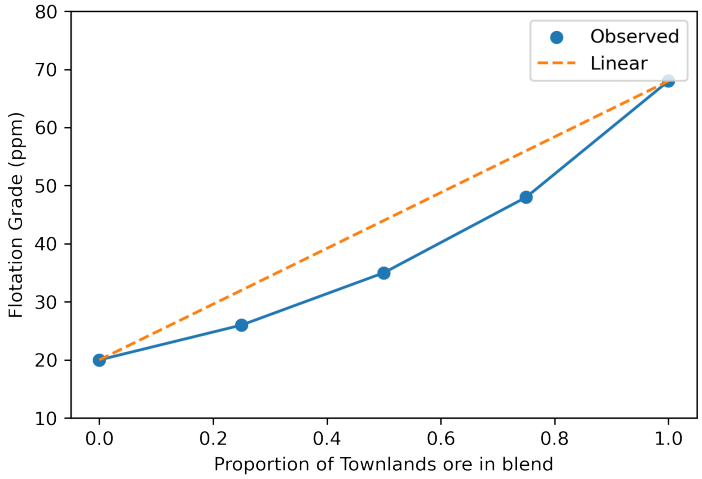

Figure 25 – Flotation grade for a binary blend. Source: Modified from Tonder et al. (2010).

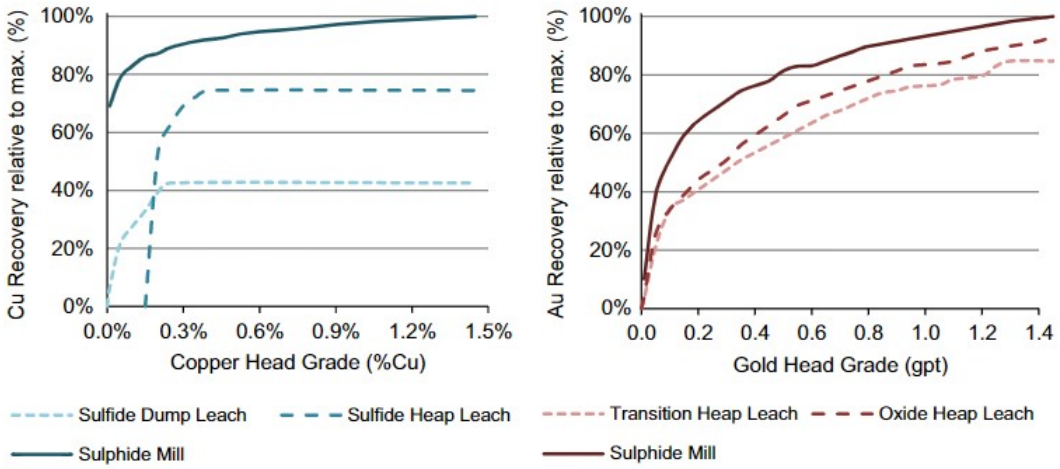

Figure 26 – Grade-recovery regression plot. On the left: Copper recovery as a function of copper head grade. On the right: Gold recovery as a function of gold head grade. Source: Castillo and Dimitrakopoulos (2016).

Similar to blending, scaling may average nonlinearly. Several change-of-scale operations are performed during the process of resource modeling, mine planning, mineral processing production modeling, and reconciliation. Just as a mining block consists of a mixture of several estimated point values, the processing plant receives volumes consisting of several blocks. In practice, all scale regularization procedures implicitly assume linearity, which may not be correct. Newton and Graham (2011) showed an example of the nonlinear behavior of the Zn Recovery, measured at the plant, in relation to the same variable measured at the laboratory scale (Figure 27). This nonlinearity prevents using a single-scale factor for changing the scale from a bench test or a pilot plant to an industrial plant, a common procedure in the industry for reconciliation purposes. A metallurgical recovery in the plant of 85% corresponds to almost 75% obtained in the laboratory. The ratio between them is the scale factor, which in this case is 1.13. However, this scale factor is not suitable if the metallurgical recovery of zinc measured in the laboratory is, for example, 70% or 80%, where the most suitable scaling factors would be 1.16 and 1.08 respectively. As the slope of the behavior curve of the metallurgical recovery varies with each recovery, the scale factor also varies.

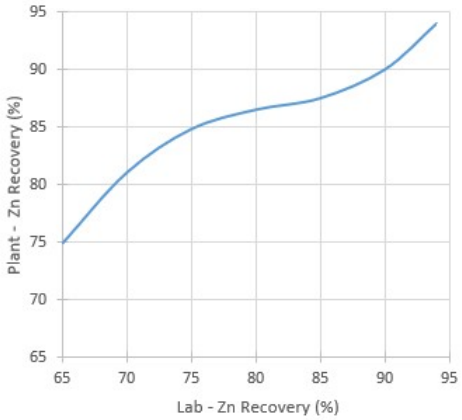

Figure 27 – Nonlinear behavior in upscaling. Modified from Newton and Graham (2011).

No theoretical mixing and scaling laws exist for geometallurgical variables, given the complex physical and chemical interactions between geological/mineralogical properties and processing parameters. Ideally, to accurately model the effective geometallurgical property of a blended mixture, one needs to understand the phenomenon that occurs when ore mixtures are processed. For example, in a flotation test, mixing finer material together with coarser material generates slime coating in the ore particles, reducing the flotation performance. Therefore, it is essential that each mine site do its own experimental tests for each variable of interest, with different combinations of quantity and component proportions in a mixture. These experimental tests must be done according to the best QA/QC protocols in order to minimize the errors associated with them. Campos et al. (2019) used triplicates for BWI blend testing. Tonder et al. (2010) stated that these blending studies should be conducted using statistical mixtures designs, intended to rigorously test the hypothesis that the blend performance is an additive combination of the individual component performances or not.

4.3 Nonlinear blending and scaling impacts

Campos et al. (2022) demonstrated how blending and scaling nonlinearity affect the prediction of metallurgical recovery. They used a regression curve to predict the metallurgical recovery of the material processed at the industrial plant, which is a blended material of several blocks (the feed volume). In their case, data were representative of the plant operation. We replicate this demonstration here.

In a mine, eight ore blocks are free to be mined in the short-term mine plan. Each of these blocks has a copper grade value estimated by geostatistical techniques. For the sake of simplification, let us assume that each block has the same mass. Metallurgical studies for this ore identified that the metallurgical recovery at the plant can be accurately estimated from the copper grade of the feed (Figure 28).

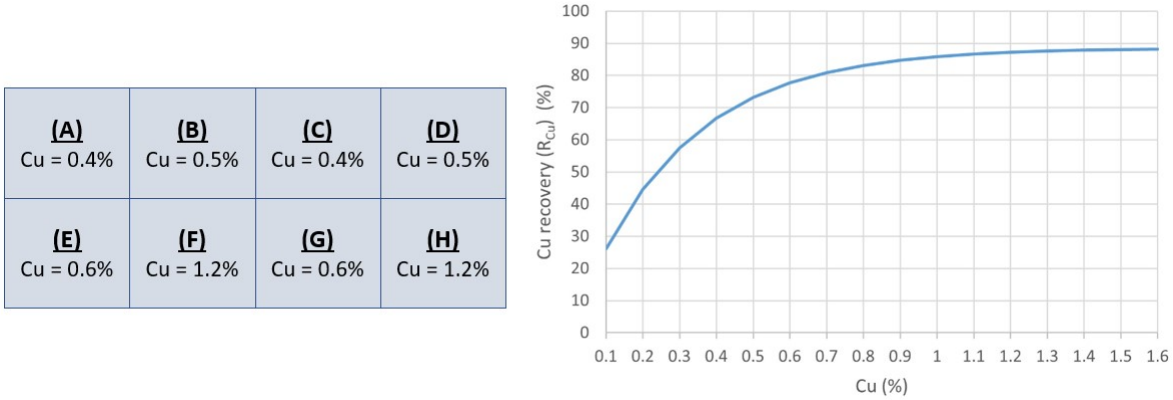

Figure 28 – Blocks with estimated copper grade and copper-recovery regression curve. Source: Modified from Campos et al. (2022)

A common practice would be to assign a copper recovery value for each block through the application of the regression curve. In this situation, the average recovery after processing all blocks is 79.42%. However, the regression curve is only representative of the support of the samples used for its determination, which in this case is the feeding volume. Thus, it must be applied to the grade of each feed volume. If we consider that four blocks compose the feed volume, then different sequences of the blocks form different feed volume mixtures. A schedule that mines the highest grades first, similar to an NPV optimization scheduling results in one mixture with 0.9% and another with 0.45% copper grade. The global recovery, in this case, is 79.86%. However, contrary to what would be expected at first, alternative scheduling, which forms two mixtures of grades of 0.67%, would result in an overall recovery of 80.16%, better than the previous one (Figure 29).

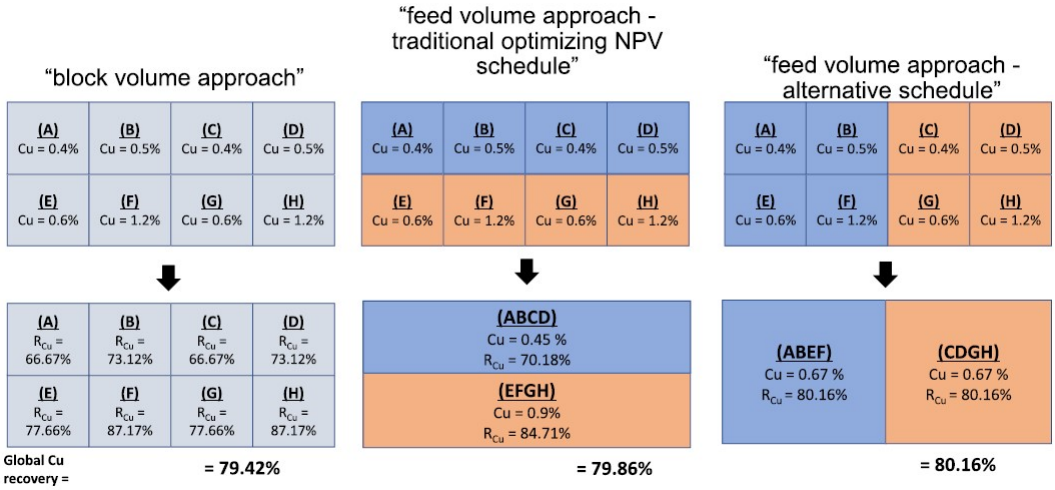

Figure 29 – Blending and scaling effect on the estimation of the copper recovery. Source: Campos et al. (2022).

Nonlinear scaling behavior results in biased predictions if the difference in scale (support) is ignored. When there is nonlinear averaging in blending, the bias can be even

greater. Understanding the scaling behavior helps us to predict accurately. Understanding the blending behavior helps us to build optimal mining plans.

4.4 Blending behaviors

From the perspective of blending, the effective property models can be summarized by three possible behaviors: blending neutral, blending synergistic, and blending antagonistic. In the blending neutral case, the decision to blend does not affect the average value, that is, it occurs when the effective property (p_{eff}) of a blended material is the same as the weighted linear average of its components ($\overline{p}$). By definition, all linear variables have a blending neutral behavior. Grade, as shown in Equation 4.1, is an example.

Attention should be given to how to calculate the linear average of the variable. For example, metal recovery linear average is not calculated through Equation 4.1, with recovery replacing the grade, but weighted by mass m_i and grade g_i of each component $i = 1, ..., N$. Therefore, the metallurgical recovery is blended neutral when the effective metallurgical recovery (r_{eff}) is equal to the linear average ($\overline{r}$), as shown in Equation 4.2.

$$r_{\text{eff}} = \overline{r} = \frac{\sum_{i=1}^{N} m_i \cdot g_i \cdot r_i}{\sum_{i=1}^{N} m_i \cdot g_i} \tag{4.2}$$

Blending synergistic behavior occurs when the blended material has an effective property value greater than the weighted linear average of its components. In such cases, the higher-value component has more influence on the mixture property than the lower-value component. The opposite happens for the antagonistic behavior, when the low-value component has more impact on the effective property value, bringing it down to be smaller than the weighted linear average. Figure 30 illustrates this concept, where there are N=6 material components, each one having a different property value p. Their weighted linear average is 0.77. When the components are blended, the effective property value depends on the blending behavior. When the effective property is assigned to a blended mixture with a scale greater than its individual components, as the case in Figure 30, the scaling averaging is already implicitly considered.

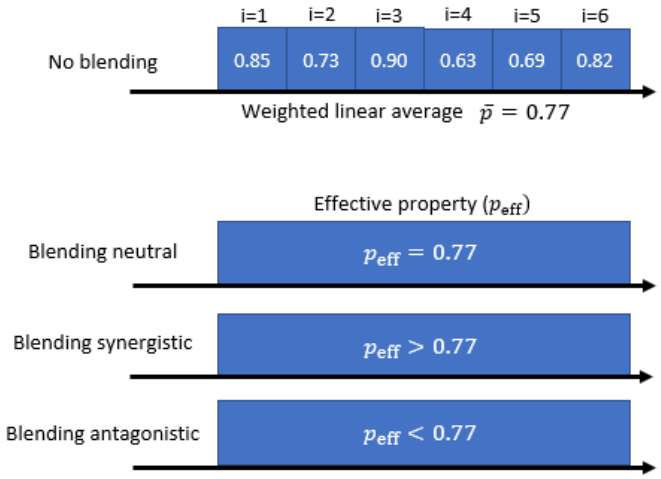

Figure 30 – Illustration of blending cases.

The lack of a theoretical mixing/scaling model should not prevent us from assuming any type of nonlinear behavior. Supported by the nonlinear averaging shown in several studies (DUNHAM; VANN, 2007; NEWTON; GRAHAM, 2011; CASTILLO; DIMITRAKOPOULOS, 2016; XU, 2013; SPLAINE et al., 1982; TAVARES; KALLEMBACK, 2013), it is clear that the averaging of BWI and metallurgical recovery follows more closely the Type I curve, where the effective property value is within the maximum and minimum component values and does not change abruptly according to a threshold. The convexity of the curve can be up or down, depending on whether the low- or high-value component is the most influential on the behavior of the mixture.

4.5 Blending model proposal

Given the difficulty and complexity of modeling the experimental blending and scaling behavior of ores, we propose a flexible and easy-to-use model which allows the setting of all possibilities of blending behavior - neutral, synergistic, or antagonistic - and complies with the Type-I-nonlinear-behavior property of estimating the effective property value within the minimum and maximum values of the components. The scale of the effective property estimation corresponds to the feed volume scale, that is, the scale of the prediction is not based on block support, but on the volume of blocks that are blended/processed together.

Modeling a blending neutral case is straightforward, as it is calculated as the linear weighted average. The complexity arises when modeling the intensity of the increase/decrease in value for synergistic/antagonistic cases. The large range of possibilities in defining how much influence one component of the mixture may have over the other justifies the use of power-law functions. Power laws describe relationships between two variables such that a relative change in one (x) results in a proportional relative change in the other

($f(x)$). Power functions have already been used for the inference of effective permeability (KOZHEVNIKOV et al., 2021; DEUTSCH et al., 2002). The general mathematical formula of a power-law function is given by Equation 4.3.

$$f(x) = a \cdot x^w \tag{4.3}$$

where w is the power-law exponent and a is a constant and refers to the conversion factor between x^w and $f(x)$. Constraint by the interval $0 \leq x \leq 1$, the power law is equal to a linear function when $w = 1$. When $0 < w < 1$ the function steep is the greatest at the minimum x, and it decreases as x becomes higher. The smaller the value of w, the more accentuated this behavior is. When $w > 1$ the opposite happens, as the steep begins small and it increases as x becomes higher. The greater the value of w, the more accentuated this behavior is (Figure 31).

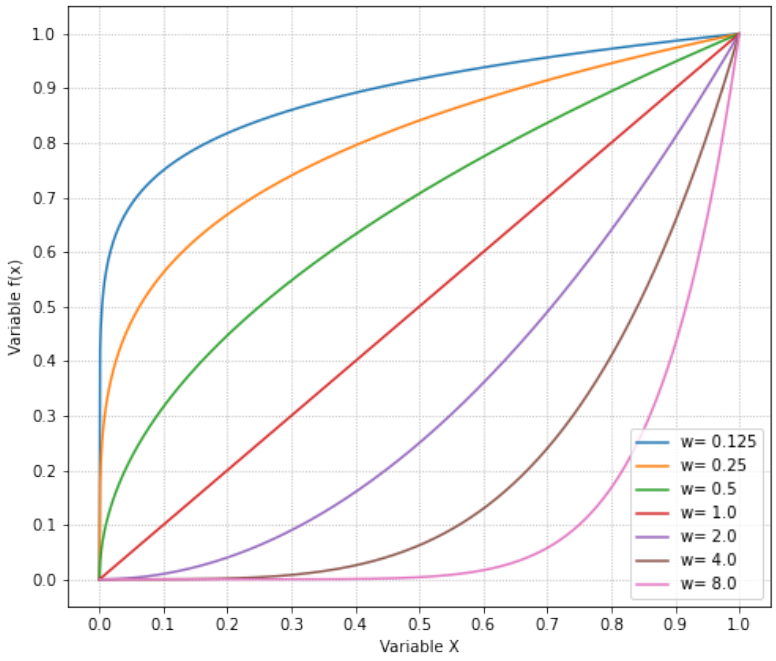

Figure 31 – Illustration of power-law functions constrained by $0 \leq x \leq 1$. Each curve is a power-law function with different exponential.

Using the general power-law function (Equation 4.3) as a base model, a blending model can be developed with some adjustments, such that the shape of the power-law is maintained, but it is bounded by the minimum and maximum component values in each mixture. Besides the minimum and maximum, it is reasonable to consider the influence of the other component values in the effective property by the linear average.

The proposed blending model takes these three values - minimum, maximum, and linear average - as parameters of the mixture. As a parameter of the blending behavior, the power w is required. Equation 4.4 shows the mathematical function for calculating the effective recovery (r_{eff}) given the minimum (r_{min}) and maximum (r_{max}) recovery of the components and their linear weighted average ($\overline{r}$). Synergistic blending is modeled by using $0 < w < 1$. The smaller the w, the greater the influence of the component with the highest property value. Antagonistic blending is modeled with $w > 1$. The greater the w, the greater the influence of the component with the smallest property value. Blending neutral is achieved by $w = 1$. In a particular case where all components have the same property value, there is no reason to believe that the effective property would be different.

$$r_{\text{eff}} = \begin{cases} r, \text{ if } r_i = r \ \forall\, i = 1, ..., N \\ r_{min} + (r_{max} - r_{min}) \cdot \left[\dfrac{\overline{r} - r_{min}}{r_{max} - r_{min}} \right]^w, \ otherwise \end{cases} \tag{4.4}$$

4.6 Implementation and sensitivity analysis

As an example, consider the variable given in Figure 30 is metal recovery. Blocks with individual values of 0.63, 0.69, 0.73, 0.82, 0.85, and 0.90 are fed to a plant. Figure 32 shows the application of Equation 4.4 using different powers w to predict the effective metallurgical recovery of this feed volume. In the X-axis, just the minimum, maximum, and linear average of the values are plotted.

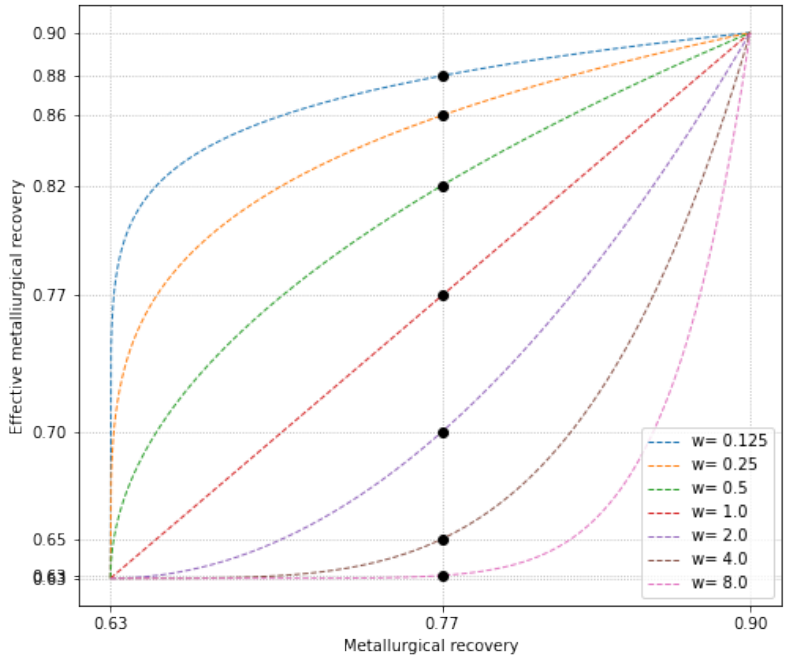

Figure 32 – Effective metallurgical recovery values in function of the w value.

For a blending neutral model, w equals 1 and Equation 4.4 gives $r_{\text{eff}} = \overline{r} = 0.77$. If the user desires to reproduce a blending synergistic case, then the effective recovery is calculated using $w < 1$, and the r_{eff} is greater than $\overline{r}$. For example, using $w = 0.5$, $w = 0.25$ or $w = 0.125$ results in $r_{\text{eff}} = 0.82$, $r_{\text{eff}} = 0.86$, and $r_{\text{eff}} = 0.88$, respectively. On the opposite side, if the desire is to reproduce an antagonistic case, the user should input a w value greater than 1.0. The greater the value w, the more influence the low value has on the effective property. In the example, for $w = 2.0$, $w = 4.0$ or $w = 8.0$ results in $r_{\text{eff}} = 0.70$, $r_{\text{eff}} = 0.65$ and $r_{\text{eff}} = 0.63$, respectively. Figure 32 exemplifies a case where the dispersion of the metallurgical recovery values in the X-axis is symmetrical about the average. This case (case I) is representative of situations where two or more mining faces are mined simultaneously and blended with similar proportions.

For sensitivity analysis purposes, let us now consider a second case in which the dispersion is not symmetrical. A low-value outlier is mixed with other high-value components. This may reproduce situations where waste is misclassified and sent to the plant together with ore, or where a tiny portion of the mine behaves badly when processed whereas the major part of the mine has good recovery. For case II, consider the components' recovery values are 0.40, 0.81, 0.82, 0.83, 0.86, and 0.90, such that the linear average is yet 0.77. Figure 33 shows how the effective recovery value could be estimated by varying the power w for case II. Note that, the lesser the power w, the little the difference in the effective property value between cases I and II. For example, using $w = 0.5$ yields an

effective recovery of 0.82 in case I, and 0.83 in case II; using $w = 8.0$ yields an effective recovery of 0.63 in case I, and 0.44 in case II. That is, the low-value outlier has a big impact on the mixture for high w values (antagonistic blending behavior), but not so much for the synergistic blending behavior.

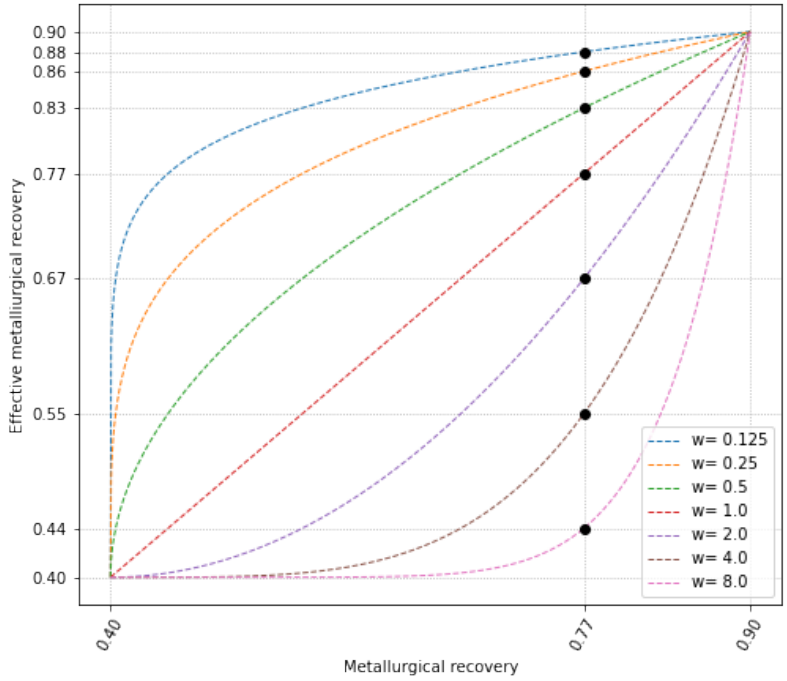

Figure 33 – Effective metallurgical recovery values in function of the w value. Case II.

The reasoning is valid in the opposite way when a high-value outlier is mixed with other low-value components. For case III, consider the components' recovery values are 0.63, 0.73, 0.74, 0.76, 0.77, and 0.99, such that the linear average is yet 0.77 (Figure 34). The high-value outlier impacts the mixture for synergistic blending behavior. It is now the antagonistic blending behaviors that are not influenced by the outlier.

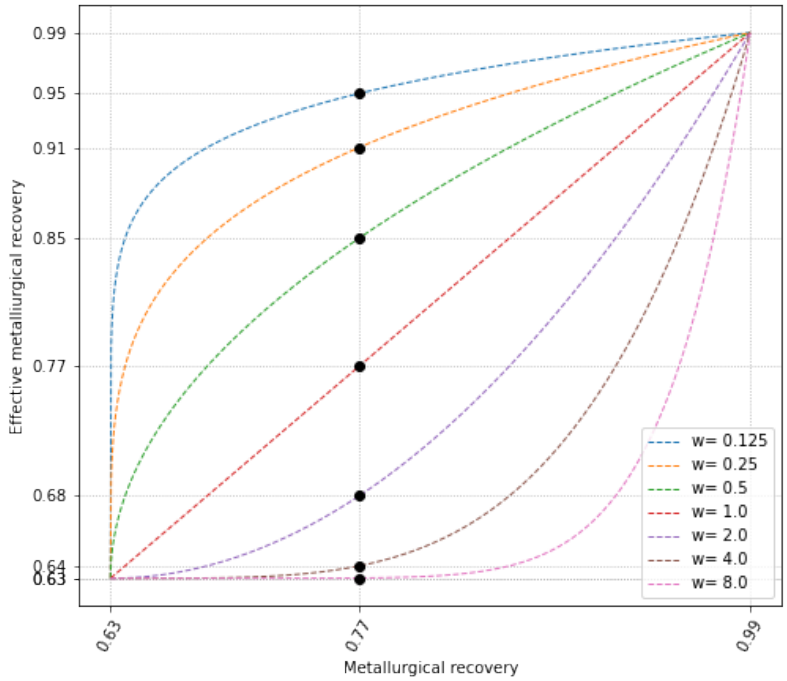

Figure 34 – Effective metallurgical recovery values in function of the w value. Case III.

4.7 Discussion

Models for estimating the blended BWI usually takes as input the proportion of each component in the mixture and their individual BWI values to estimate a regression function. Based on this idea, we propose a model that estimates the blended metallurgical recovery using each component's metallurgical recovery estimated values. It is important to highlight that the metallurgical recovery estimation of a mining block should consider its geological characteristics and the expected mill parameters, which would act on it when processed. Therefore, primary variables are implicitly embedded in the estimation. The proposed model only adjusts the estimation of a block to the estimated value of a feed volume, which considers both blending and scaling nonlinearity.

Some properties of the proposed model are:

- The flexibility of changing the model behavior: from the synergistic ($w < 1$) to the antagonistic ($w > 1$) to the linear model ($w = 1$);
- The capability of the model to tune the influence of the lower and upper component values over the mixture average by progressively increasing or decreasing the factor w;

- The effective property is limited by the lower and upper component values of each mixture;
- When the components of the mixture all have the same value property, then the mixture property is also characterized by that value.

The sensitivity analysis section showed that, in specific cases, a mixture of components that have a symmetrical distribution of values may have the same effective property as an asymmetrical distribution mixture, if both have the same linear average. This happens when the asymmetrical distribution is caused by a low-value outlier and the model is blending synergistic, or the asymmetrical distribution is caused by a high-value outlier and the model is blending antagonistic. In such cases, when the outlier should have an additional impact on the effective property, the user should input a different factor w than the one used when mixtures are formed without outliers.

The exponent w is ideally obtained experimentally through the testing of different proportions of components in a mixture and component values, such that the properties of possible mixtures are characterized. In a less ideal context, where there are no experimental tests, experience and tacit knowledge of the plant engineers are useful in defining the w value.

There is no presumption of faithfully modeling the behavior of ore mixtures or claiming that the proposed model is the best. The author recognizes that this is more indicated to mineral process engineers. The chapter aim is to raise the importance of modeling the nonlinear behavior of blending and scaling such that the model could be used further down in the mine planning phase.

4.8 Summary

Block models are constructed at a scale relevant for mining but not for mineral processing. During the mining and mineral processing stages, blocks are blended, whether intentionally or not. The blended ore properties are often assumed to be the linear weighted average of its components. For nonlinear properties, this assumption is incorrect. Understanding and modeling the nonlinear behavior of a geometallurgical variable is necessary for scaling up and blending, allowing accurate predictions and optimal decisions.

Two usual models to estimate a geometallurgical property are: using the proportion of each component in the mixture and their geometallurgical property values; or through other primary variables of the components of the mixture. The proposed model uses the estimated metallurgical recovery at the block scale as an input to predict the same property but at the feed volume. By doing so, blending and scaling are being considered simultaneously.

The objective of the mathematical model proposed is to provide the user with a tool that estimates nonlinear properties when blending occurs. This model is easy to use, and its flexibility allows a better tuning of each mixture property, given the characteristics of its components. The integration of this tool with mine planning can lead to optimized mine plans.

5 SHORT-TERM MINE PLANNING WITH BLENDING

Mine planning is often based on predictions at the block scale and determines whether it should be extracted or not. In a positive case, decisions should be made regarding when the block is to be mined and its destination, whether plant, stockpile, or waste pile. These decisions are based on several variables' estimated values. Typical variables of interest in a metallic project are ore grade, density, and metallurgical recovery. With the increasing knowledge about geometallurgy, metallurgical recovery and other metallurgical responses are better understood and progressively being considered important to mine planning. As discussed in chapter 4, metallurgical variables often present nonlinear blending and scaling behavior, which impact their prediction at different scales. Estimation of metallurgical recovery at a block scale cannot be achieved as the block will not be processed alone. Therefore, traditional mine planning procedures are performed under biased predictions regarding expected metallurgical recovery. This chapter shows that mine planning decisions should be based on the feed volume scale, that is, the volume of material processed together in the plant. Some authors refer to this as the "processing block" scale. The feed volume is composed of several mining blocks that are blended in the mine and processing operations, and its properties are a (linear or nonlinear) average of the blocks' properties. Different schedules result in different mixtures, named here as *blending units*. This chapter presents a simulated-annealing-based schedule in a short-term mining face optimization problem, with the objective of maximizing the nonlinear metal recovered. The optimized schedule shows improvements in blending synergistic and antagonistic cases when compared to a conventional schedule.

5.1 Problem framework

The problem tackled is the short-term scheduling optimization problem. Consider the usual discretization of a mining face in regularly-shaped parcels, each one with an estimated grade. The term parcel is used as a synonym for block. A 2D representation of a mining face is shown in Figure 35. The parcels have positions along the x-axis (Easting) and the y-axis (Northing), but their coordinates can also be represented by the ix, iy index, starting from left to right and south to north directions.

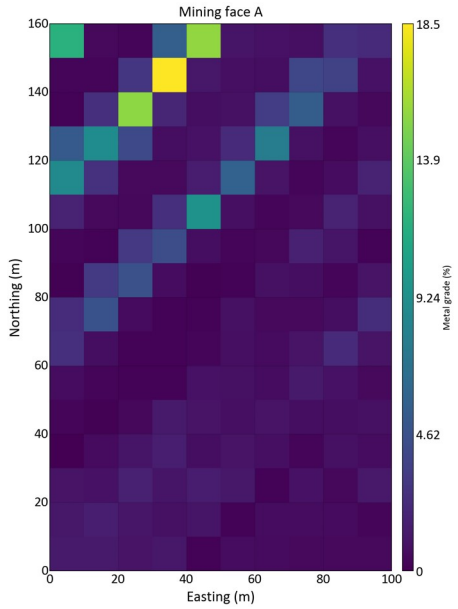

Figure 35 – Mining face with parcel grades.

The mined ore parcels are sent to the processing plant in the order of their extraction. Considering that there is a natural blending during the operations of excavation, haulage, and at the processing plant, the process response is a function of the blended material properties. In this case, metallurgical recovery is the process response of interest. The problem consists of scheduling the parcels in a way that the best mixtures are formed, that is, the global metallurgical recovery is maximized. Global metallurgical recovery refers to the total metal recovered after processing all the parcels. It is, therefore, a global optimization problem. Mixtures are composed of parcels formed according to the time period in which each one is extracted. Each blended mixture is identified by a *blending unit* (b), a discrete variable that reflects the plant feeding order, such that $b = 1, ..., B$, where B is the total number of blending units. Therefore, all parcels assigned to $b = 1$ are to be mined at the first time period and be blended. The blending unit mass is composed of the sum of the masses of its composing parcels, and its effective recovery depends on its composing parcels' recoveries as modeled by the blending model.

Any blending model can be used for estimating the effective recovery. The blending model considered here is based on the model developed in chapter 4. In summary, the blending model calculates the effective recovery of a blending unit (r_{eff}) based on its parcel-components' minimum, maximum, and linear average recovery values (r_{min}, r_{max} and $\overline{r}$, respectively) and on an exponential parameter w of the power-law function. Refer back to Equation 4.4. Then, the estimated value of r_{eff} can be assigned to each parcel that composes that blending unit, substituting the prior recovery values.

The constraints to the scheduling relate to i) operational accessibility to ore parcel and ii) shovel movement. The first constraint is a fixed hard constraint represented by a "free face" precedence, in which to mine a parcel in a (ix, iy) index, the three parcels

below it, that is, the parcels in the indexes $(ix-1, iy-1)$, $(ix, iy-1)$, and $(ix+1, iy-1)$ must have been mined in a previous or equal time period, considering that the direction of mining is from south to north. The shovel movement constraint is a soft constraint, in which the sum of the distances between the parcels composing the same blending unit penalizes the objective function.

Thus, the problem objective function (OF) can be mathematically modeled as:

$$OF : Max \sum_{b=1}^{B} \sum_{p=1}^{P} g_{p,b} m_{p,b} r_{p,b}^{\text{eff}} - PF \sum_{b=1}^{B} \sum_{p=1}^{P-1} d_{p,p+1,b} \tag{5.1}$$

The first term relates to the summation of the quantity of metal recovered in each blending unit, where $g_{p,b}$ is the grade of a parcel p in the blending unit b, $m_{p,b}$ is the parcel mass, and $r_{p,b}^{\text{eff}}$ is the effective recovery of p given its blending unit b. The second term relates to the penalty factor that multiplies the total distance the shovel needs to move to extract the scheduled parcels for each blend unit, where $d_{p,p+1,b}$ is the distance between two consecutive mined parcels p and $p+1$ in the same blending unit b, and PF is a constant penalty factor.

The "free face" precedence is modeled through three equations, all of which should be met:

$$b_{ix,iy} - b_{ix-1,iy-1} \geq 0 \quad \forall b, \forall ix, iy \tag{5.2}$$

$$b_{ix,iy} - b_{ix,iy-1} \geq 0 \quad \forall b, \forall ix, iy \tag{5.3}$$

$$b_{ix,iy} - b_{ix+1,iy-1} \geq 0 \quad \forall b, \forall ix, iy \tag{5.4}$$

where $b_{ix,iy}$ is the blending unit b of the parcel p at the (ix, iy) index and $b_{ix-1,iy-1}$, $b_{ix,iy-1}$, and $b_{ix+1,iy-1}$ are the blending unit b of the parcel p at the $(ix-1, iy-1)$, $(ix, iy-1)$, and $(ix+1, iy-1)$ indexes, respectively. That is, a parcel must have a greater or equal blending unit than the nearest three parcels in the lower iy index. Figure 36 illustrates the hard constraint concept.

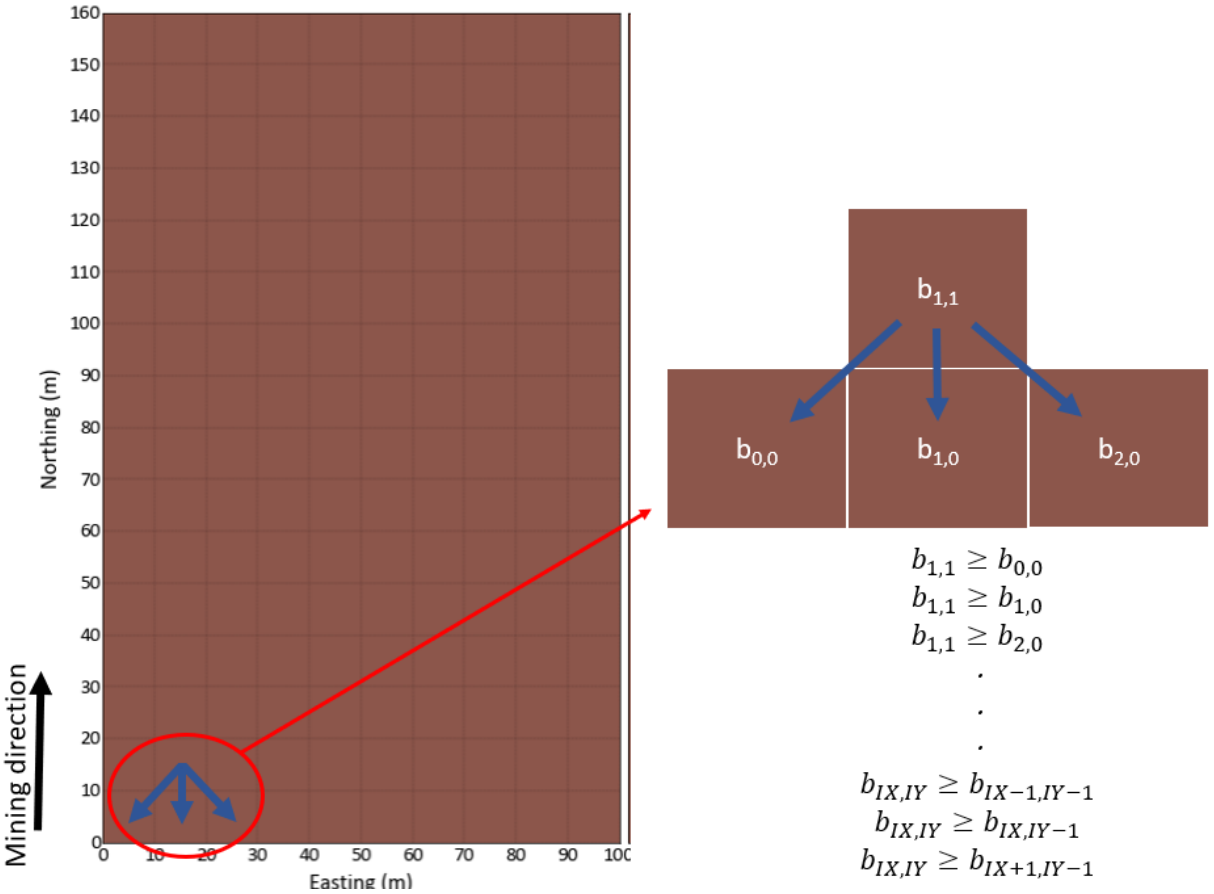

Figure 36 – Illustration of the hard constraint. The blending unit of a parcel at the index (x, y), $b_{x,y}$, must be equal or greater than the blending unit of all the parcels below it, $b_{x-1,y-1}$, $b_{x,y-1}$ and $b_{x+1,y-1}$

Solving this global optimization problem through linear or mixed integer programming is not practical, given the recursive and nonlinear averaging characteristics of the blending of the ores. An iterative procedure appropriate for nonlinear objective functions is necessary. The proposed approach is to use Simulated Annealing.

5.2 Proposed methodology using simulated annealing

Simulated Annealing is a stochastic search metaheuristic for approximating the global optimum of a problem. The idea of the algorithm comes from the annealing process in metallurgy, where a metallic alloy is heated so the molecules can move freely. The cooling process is controlled, allowing the molecules to reorder themselves into a lower energy entropy. As the swapping of the molecules is known to follow the Boltzmann distribution, sometimes molecules swapping positions lead to a higher energy state, but the occurrence of this diminishes as the temperature drops.

In the simulated annealing algorithm, a feasible and simple solution must be given to the system and evaluated through the objective function. This first solution represents

the heating process. The objective function is analogous to the free energy in metallurgy. A mechanism randomly perturbs the current solution, creating a candidate solution, which is evaluated. This reproduces the analogy of the swapping of the molecules in the cooling process. If the candidate solution has lower energy, that is, it is better with respect to the objective function than the current one, then the perturbation is accepted and the candidate solution becomes the current solution. Conversely, if the candidate has greater energy than the current solution, the perturbation may or may not be accepted, according to the probability distribution. This is an iterative process, in which the parameter temperature is set for a high value at the initial solution and decreases gradually. The likelihood of accepting worse solutions starts high because of the high temperature, but decreases with the iterations and the lowering temperature, allowing the algorithm to escape local optima and find the optimum solution. This algorithm is appropriate for nonlinear objective functions given its randomness is part of its perturbation mechanism.

For this short-term scheduling optimization problem, the initial and feasible solution is a default schedule. According to this schedule and how many parcels compose a mixture, parcels are grouped into blending units, which are evaluated through the objective function given by Equation 5.1. The perturbation mechanism is reproduced by swapping two parcels' blending units. The requirements for a successful swapping are *i*) the blending units of the parcels to be swapped are different, and *ii*) the blending unit of a parcel must be smaller or equal to the blending unit of the posterior parcel in the direction of mining. The first requirement prevents the unnecessary situation of swapping two parcels that composes the same blend unit, as this will not change the objective function. The second requirement represents the "free face" precedence, where the prior parcel must be mined before the posterior one. After each perturbation, the objective function of the solution is evaluated and accepted or not according to the acceptance probability distribution (Equation 5.5). The parameter temperature (t) is a function of the initial temperature (T_0) and the iteration number (i) as shown in Equation 5.6. After a large number of iterations, the solution converges to the global optimum.

$$P(accept) = \begin{cases} 1 & , \text{ if } OF_{cand} \geq OF_{curr} \\ e^{\left(\frac{OF_{cand} - OF_{curr}}{t}\right)} & , \text{otherwise} \end{cases} \tag{5.5}$$

$$t = \frac{T_0}{i} \tag{5.6}$$

5.3 Implementation

The current algorithm developed has some flexibilities and requisites. A mining face must be 2D, composed of rectangular-shaped parcels in an (x,y) array. It is allowed to mine one or two mining faces simultaneously. The mining faces do not need to be equal in quantity and (x,y) arrangement of the parcels, and there is no limitation on the number of parcels in each. Parcels in a mining face can be set to have been already mined or set to be prohibited to mine. The user must input the number of parcels making up a blending unit. If considering two mining faces, the ratio of extraction between them is also required. The number of parcels to be mined in each mining face should be a multiple of the proportion of parcels of that face composing a blending unit and the number of blending units in both mining faces must be the same.

5.3.1 Demonstration Example

Consider two 2D mining faces being mined simultaneously. Mining face A has 160 parcels, distributed along the x and y axis in a 10x16 grid. Mining face B is composed of 80 parcels, in a 16x5 grid. Each parcel has an estimated metal grade g_p, metal recovery r_p, and mass m_p. The metal grade and recovery histograms for each mining face are shown in Figure 37. For simplification purposes, mass is considered to be constant for all parcels and equal to one unit of mass; therefore, there are 240 units of ore mass in both mining faces.

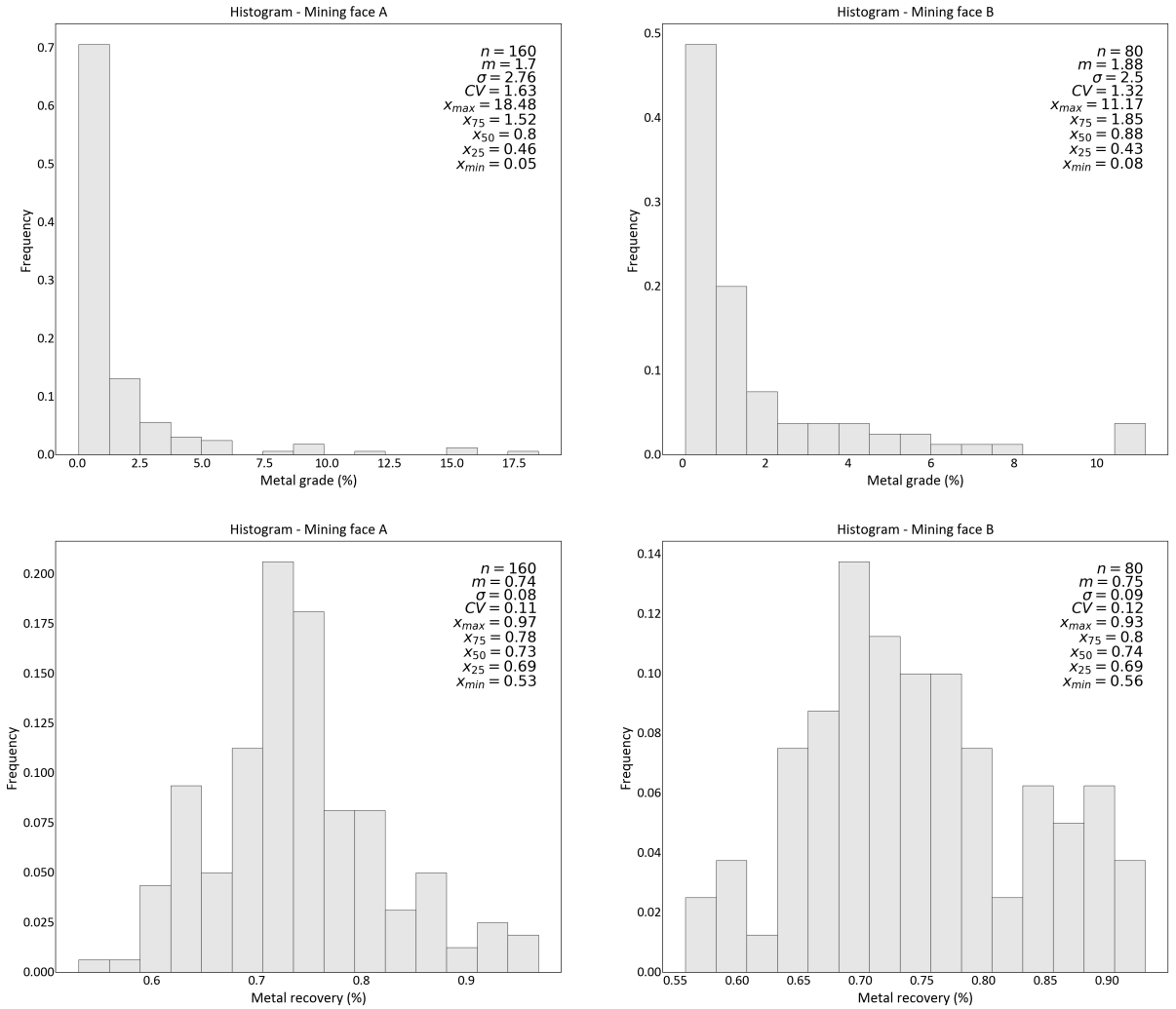

Figure 37 – Metal grade (top) and recovery (bottom) histograms for mining face A (left) and B (right).

Figure 38 shows the parcels' values for total recoverable metal (obtained by multiplying g_p by r_p). Note that the direction of the highest spatial continuity follows the 45-degree azimuth. The sum of these parcels' values is the total metal recovered, which is equal to 3.566 units of mass. This means that, of 240 units of ore mass, 3.566 units are metal and can be recovered. However, this value is based on the recovery of each parcel individually and does not consider the blending effect, which can be synergistic and increase it, or antagonistic and decrease it.

A default schedule was given as the first solution for the simulated annealing algorithm. For both mining faces, the schedule started with the parcel in the left bottom corner and then mined the parcel on its right until there were no more parcels in the first Y row. It advanced to the next parcel on the second Y row, and mined the parcels in the left direction, until all the parcels were mined. This mining direction went on making zigzag until all the parcels were mined. According to the setting of how many parcels composed a mixture, and the rate of mining in each mining face, the parcels were grouped into blending

units. For this example, it was considered that 24 parcels made up a blending unit, and the rate of mining in mining face A was twice the rate of mining face B. Therefore, after mining all the parcels, 10 blending units were formed, each one composed of 16 parcels from mining face A and 8 parcels from mining face B. The default schedule is illustrated in Figure 39.

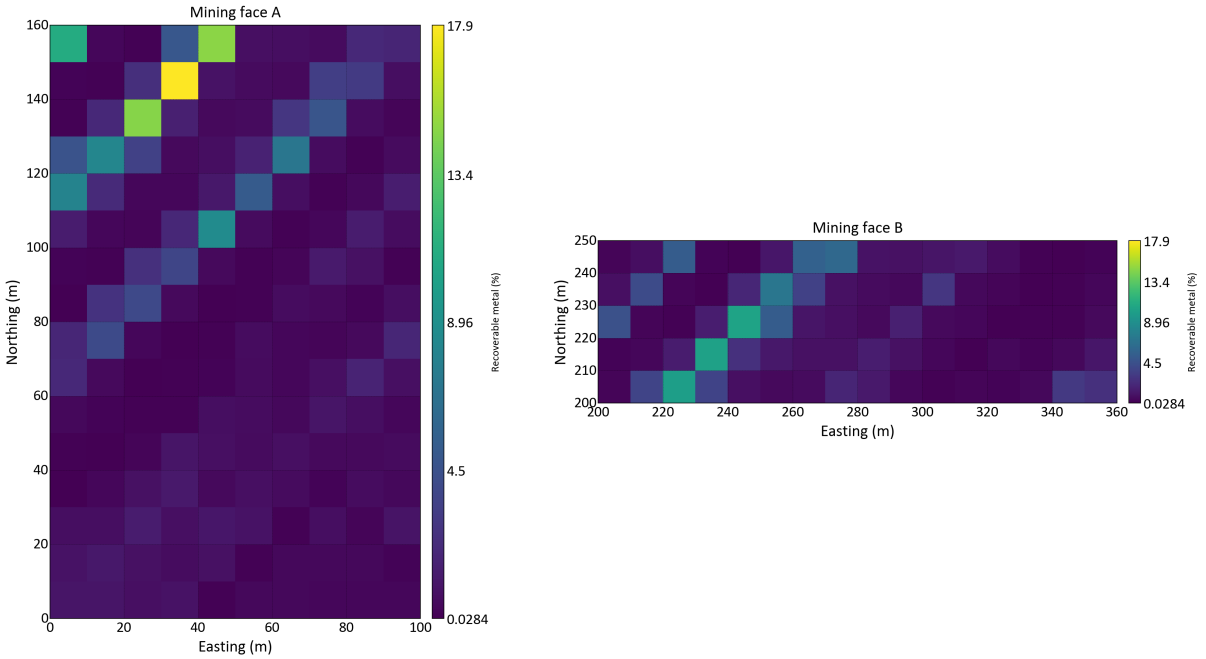

Figure 38 – Mining faces A and B with the total recoverable metal (%).

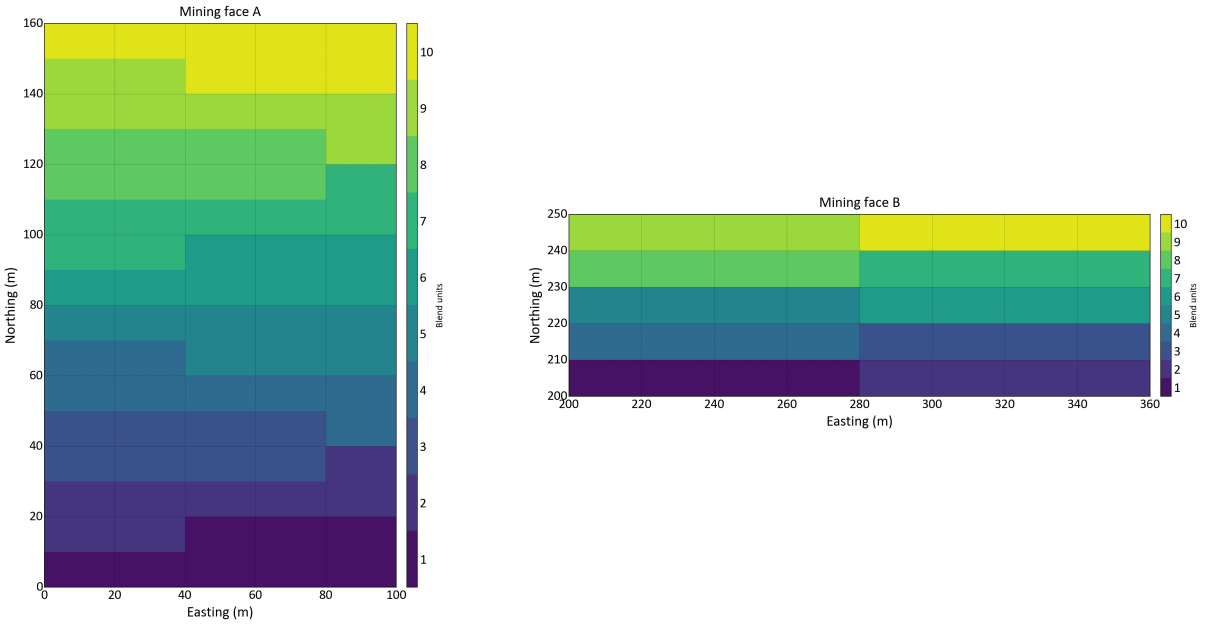

Figure 39 – Default schedule of mining faces A and B and the generated blending units. Blending units go from 1 (dark blue) to 10 (yellow).

5.3.1.1 Synergistic case

Considering that the blending was synergistic, modeled by a power function with $w = 0.8$, the default schedule returned 3.625 mass units of metal recovered; that is, only by considering nonlinear synergistic blending rather than linear neutral blending, the total metal recoverable increased from 3.566 to 3.625. Then, the simulated annealing algorithm was run, resulting in the optimal scheduling seen in Figure 40. Observe that the "free face" constraint was respected. There is a reasonable distance between parcels within the same blending unit in mining face B, which is explained by not considering any penalty factor in the shovel movement constraint. It is clearly visible in mining face A a tendency that parcels composing the same blending unit are displaced along the NW-SE direction, that is, perpendicular to the recoverable metal's major direction of continuity.

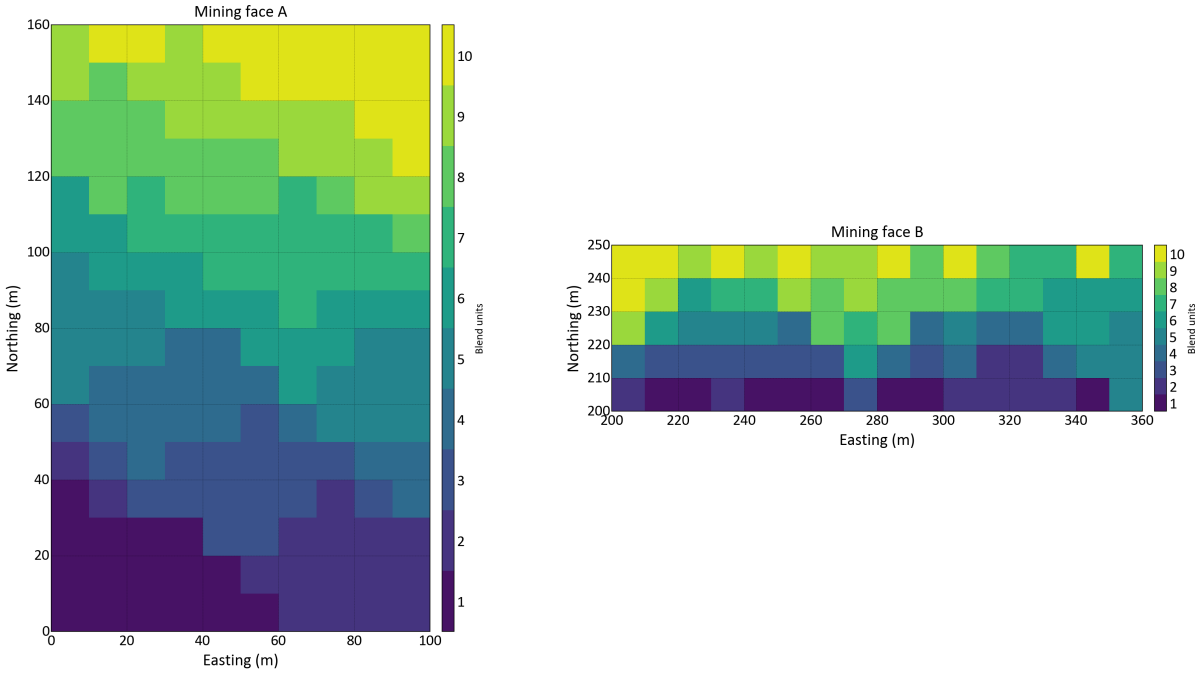

Figure 40 – Optimal scheduling considering the synergistic schedule. Blending units go from 1 (dark blue) to 10 (yellow).

In general, when the blending model is synergistic, the solution converges to grouping the most different parcels together as possible in the same blending unit, such that the heterogeneity of the parcels within the blending unit is high, but heterogeneity between blending units is low. Figure 41 shows several box plots representing the variability in metal recovery within each blending unit, measured from the parcels composing each one; and the variability between the blending units, represented by the line connecting the mean recovery of each blending unit. Note the high variability within blending units represented by the long whisker plot in each box plot.

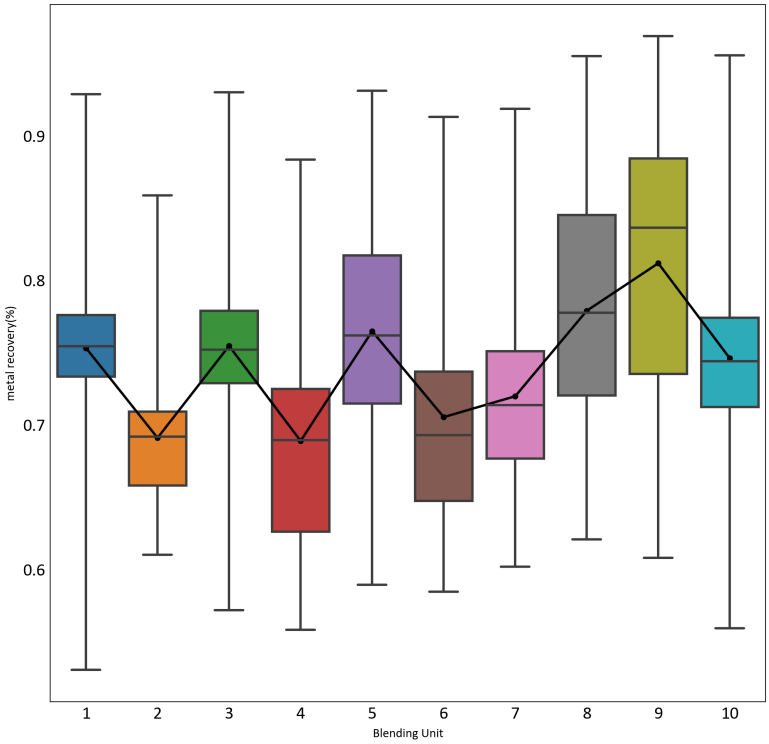

Figure 41 – Variability in metal recovered within blend units and between them - synergistic case.

The optimal schedule returned 3.636 mass units of metal recovered, that is, a 0.32% increase in total metal recovered when compared to the default schedule. This result was achieved after 20,000 iterations. Figure 42 shows the convergence stabilization.

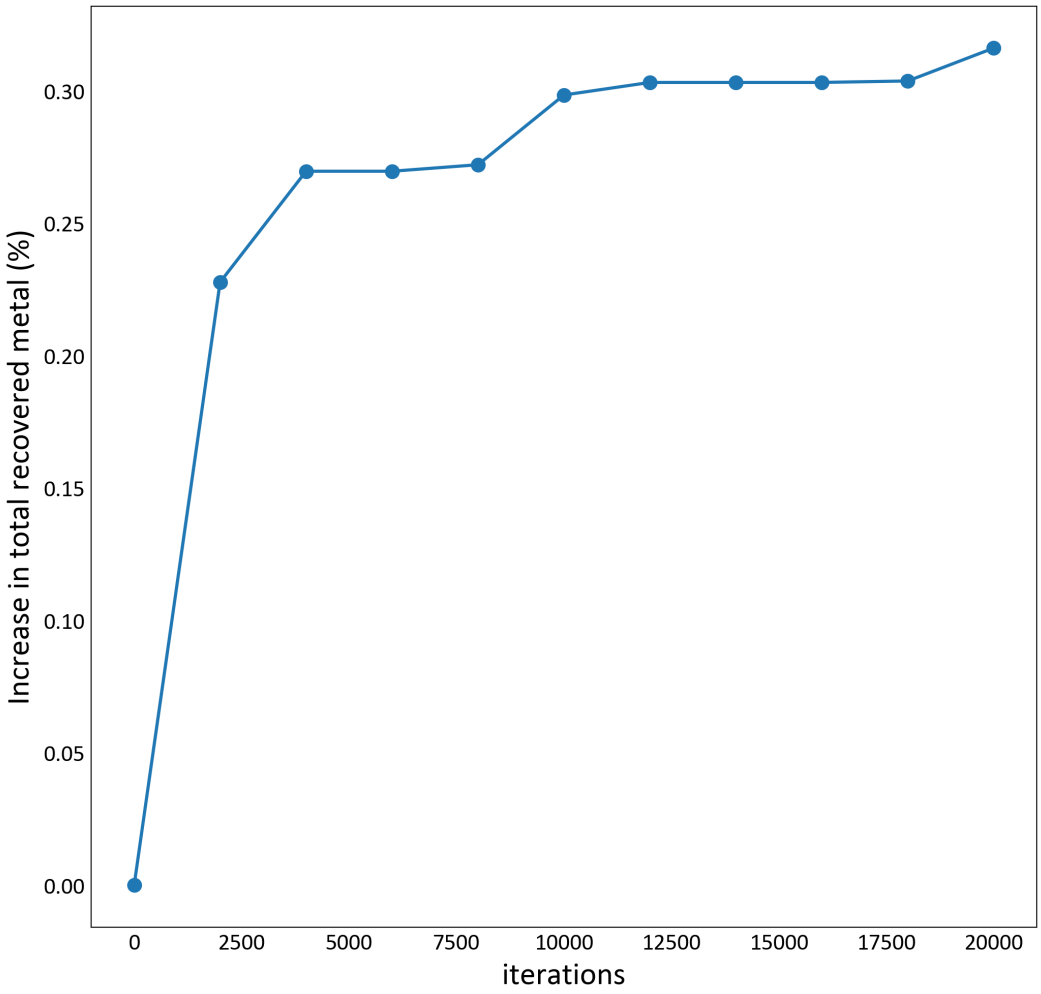

Figure 42 – Iteration convergence - synergistic case.

5.3.1.2 Antagonistic case

Considering that the blending is antagonistic, modeled by a power function with $w = 2.0$, the default schedule returned 3.319 mass units of metal recovered; that is, only by considering nonlinear antagonistic blending, rather than linear neutral blending, the total metal recoverable decreased from 3.566 to 3.319. Figure 43 shows the scheduling for this case. When the blending model is antagonistic, the schedule groups the most similar parcels together as possible in the same blending unit. As a consequence, while the variability within each blending unit is low (short whisker plot in each box plot), the variability among blending units is high (greater difference in the mean recovery for each blending unit) (Figure 44). The optimal schedule returned 3.411 mass units of metal recovered, that is, a 2.77% increase in total metal recovered when compared to the default schedule. This result was achieved after 20,000 iterations but it stabilized after 4,000 iterations (Figure 45).

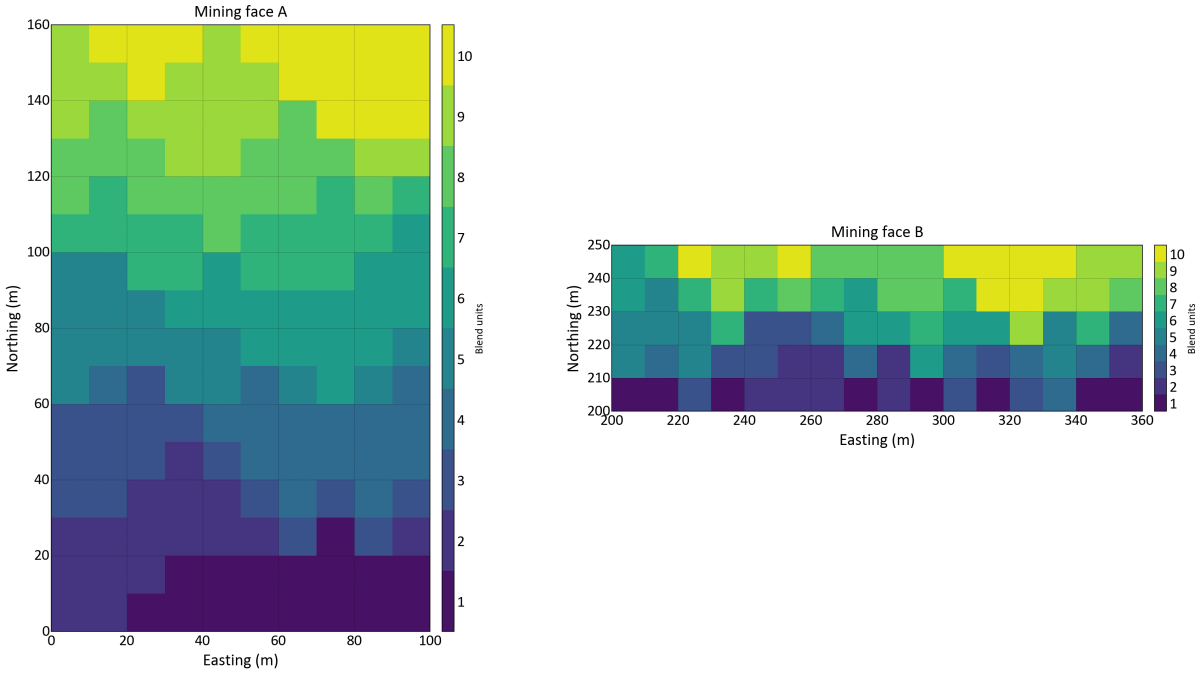

Figure 43 – Optimal scheduling considering the antagonistic schedule. Blending units go from 1 (dark blue) to 10 (yellow).

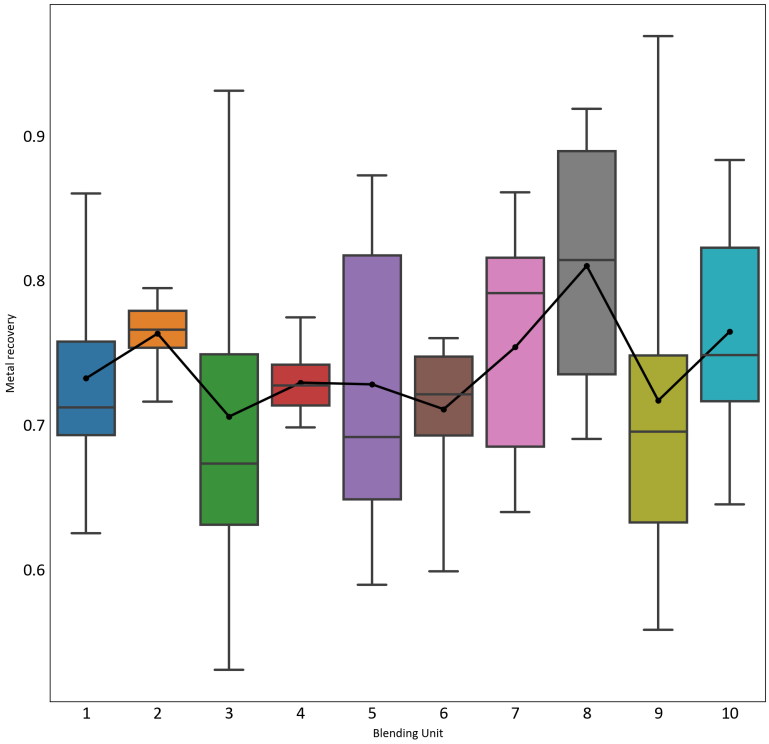

Figure 44 – Variability in recovery within blend units and between them - antagonistic case.

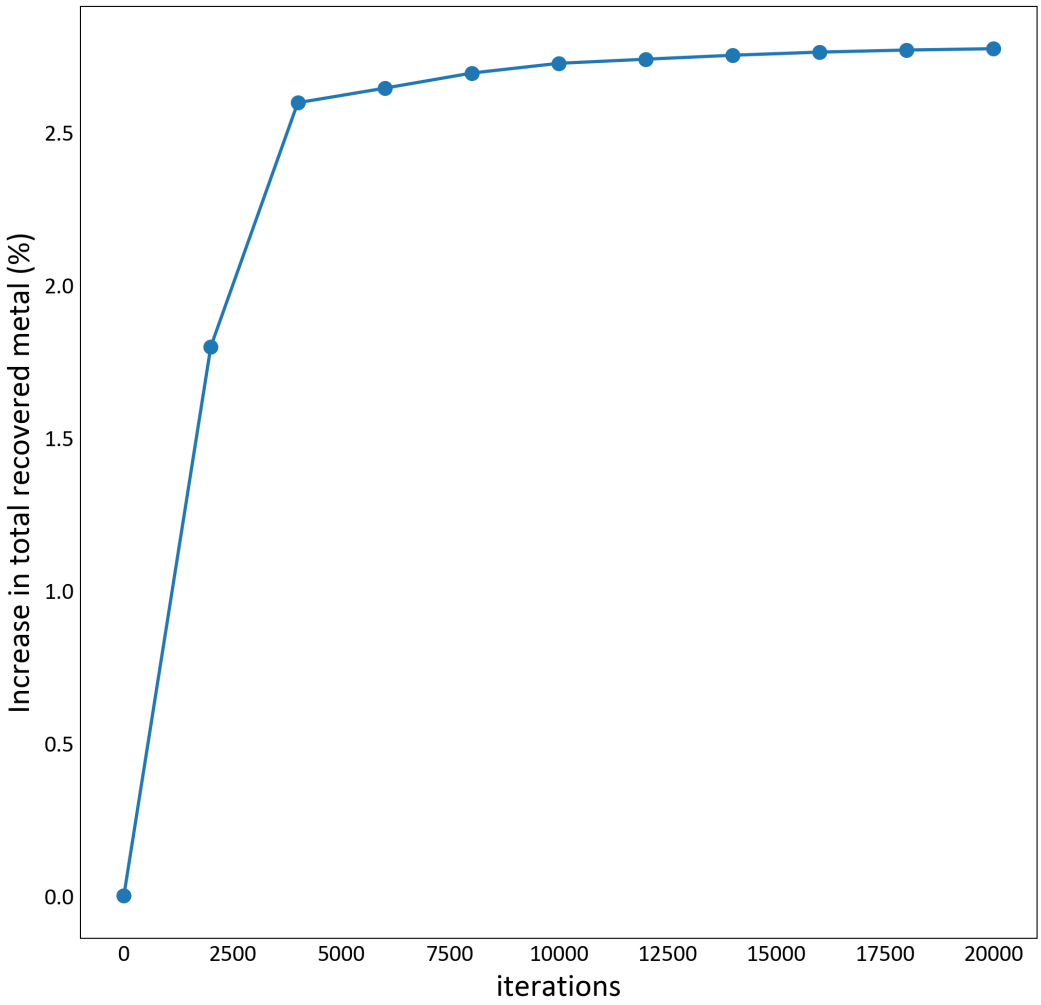

Figure 45 – Iteration convergence - antagonistic case.

5.4 Discussion

The demonstration example showed that the consideration of the blending behavior of the variable affects the expected total metal recovered of any given schedule. The default schedule provided an estimation of metal recovered units of 3.319, 3.566, and 3.625, for considering blending antagonistic, neutral, or synergistic behavior, respectively. Disregarding this behavior leads to a biased expected value. In addition, the consideration of the nonlinear behavior allows the optimization of the schedule. A simulated annealing algorithm was developed to schedule parcels and cluster them into the best blending units possible. When blending is antagonistic, the "best blending unit" concept is related to small variability among the parcels within the blending unit, whereas the concept is the opposite in synergistic blending. This variability is related to the variables that impact the metallurgical response. In this study, the effective metallurgical recovery is a function of each parcel's metallurgical recovery and grade. Therefore, antagonistic blending clusters parcels with similar grade and metallurgical recovery; synergistic blending clusters parcels

with distinct grade and metallurgical recovery.

For the specific case shown in the implementation section, the simulated-annealing optimization provided a schedule with a 2.77% and a 0.32 % increase compared to the default schedule for the antagonistic and synergistic blending, respectively. These values should not be used as a reference, as they should be different according to the blending model, optimization parameters, and data. The blending model used here was developed in chapter 4 with an exponential w. The closer the value of w is to one, that is, a linear model or very close to that, the less is the potential of the schedule to return a high increase in the quantity of metal recovered. The optimization parameter is related to the number of iterations and the temperature set in the simulated annealing. A higher temperature value increases the probability of not getting stuck in local minima. The data parameters are related to the property variability in the data. The greater the variability, the more difference between an optimized and a default schedule. Although the values obtained in the example should not be used as a reference, they prove mathematically that the schedule optimization can do better when nonlinear variables are important to the problem.

A small gain in metallurgical recovery can reflect a large increase in the project's economic value. In the study presented by Campos et al. (2022), an increase of 1.17 percentage points in metal recovery meant an increase of 8% in economic value.

5.5 Summary

In the methodology shown here, the nonlinear variable of interest is assessed at the blending unit scale, rather than considering the property at the individual parcel scale. This acknowledges that parcels are not fed individually to the processing plant, but a material mixture of them, in which the effective property of the mixture influences the result more than any individual parcel property. Most metallurgical variables are nonlinear, so the blended average value is not just a simple linear weighted average. It should be assessed experimentally and represented through a blending behavior model, allowing the optimization of such variables. A simulated annealing heuristic is developed and applied to a small and well-constrained short-term mine planning problem, demonstrating the gain of this proposed approach. Depending on the blending behavior of a variable, the schedule may group parcels that are very similar to one another or group parcels that are very different. The aim is to form mixtures with the best effective property possible. The recovery effective value is only assigned to parcels after the objective function is evaluated.

6 ILLUSTRATION CASE: A REALISTIC DEMONSTRATION

This chapter uses real data to demonstrate how geological and metallurgical properties can be integrated into a spatial geometallurgical model, considering their particular characteristics. Geometallurgical data have specificities related to sampling, scale, change of support, and nonlinearity that are generally not found in geological data. Geological data obtained through exploration or grade-control drilling are often characterized by a large amount of samples spaced in the region of interest. The sample scales are as low as centimeters to a few meters, being considered 'point-scale' samples; regularization of samples and estimations in larger supports are possible through linear upscaling, as geological variables are usually linear. Conversely, geometallurgical data are often characterized by few sparse samples with relatively high cost. The mass of material required for metallurgical test work and the need for sample regularization and estimations in different support makes the whole process troublesome, as metallurgical variables are usually nonlinear.

Given the data and variables differences, EDA and preprocessing must be done before any modeling. Two main methodologies to spatially estimate metallurgical variables are: a modern multivariate geostatistical modeling approach and a machine learning modeling approach. Both of them are shown. The software GSLib (DEUTSCH; JOURNEL, 1997) was used to perform all the geostatistical procedures, while scikit-learn packages were used for machine learning. At last, mine planning considering the blending of nonlinear variables was applied to an estimated spatial model.

6.1 Data introduction

The data analyzed are from a phosphate mine of igneous origin located in Brazil. The mine is located in a carbonatite alkaline dome, consisting of phlogopite, pyroxenite, dunite, phoscorite, and carbonatites. The apatite concentration is related to the weathering mantle developed over these alkaline rocks. The weathering profile is defined, from bottom to top, as follows (RIBEIRO, 2008):

- Fresh rock: composed of phlogopitites, cut by numerous veins of carbonatites;
- Altered rock: in which fresh rock structures are preserved;
- Isalteritic Saprolite: horizon about 25m thick where the texture and structure of the pre-existing rock are preserved;

- Alloteric Saprolite: is due to the evolution of weathering, in which the original structures can no longer be identified;
- Overburden: composed of soil with a high content of Al and Fe, and absence of Ca and Mg.

The apatite mineralized horizon is the isalteritic horizon, in which there is a low MgO and SiO_2 content and a high CaO and P_2O_5 content. The study's database consists of samples from this horizon only.

6.2 Data preprocessing

The data collected from a source, as it is, is known as raw data. Any raw data require preprocessing, which consists of data cleaning, integration, reduction, and transformation procedures aiming to adjust the data so that they can be used for spatial modeling, prediction, or any other decision-making purpose. It is essential to understand the raw data acquisition processes and their characteristics as they will guide the preprocessing stage. The raw data analysis presented in chapter 3 is recalled here. The raw data consist of 16,095 geometallurgical samples, most of them with sample identification, geological information, chemical assay, and metallurgical variables. Approximately half of the data is obtained from DDH drilling, and the other half is from drilling powder. Sample support ranges between one to 15 meters, but almost 80% is five meters long. Because of accuracy and precision issues, decisions were taken to keep only the DDH data, and those whose support length is 5 m. Four thousand eight hundred sixty-two data complies with both constraints. Some of the variables measured were not considered reliable and/or relevant for this study's purpose. This consideration was supported by understanding the data acquisition and/or statistical analysis.

In chapter 3, there were up to 3 aliquot measurements of metallurgical recovery for each ROM sample. That made it possible to increase the database and analyze the importance of the variable collector dosage. This time, the decision was to only work with one recovery value for each ROM sample since it is impossible to have different values of a variable at the same spatial location for spatial modeling. This chosen value was the one that resulted in the P_2O_5 grade in the concentrate closest to 36%, as this is the aim of the product sold by the company. The cleaned database was subjected to data analysis as part of the modeling process.

6.3 Data analysis

The cleaned database consists of the following information: Easting (X), Northing (Y), Elevation (Z), P_2O_5, Fe_2O_3, Al_2O_3, MgO, SiO_2, CaO, BaO, Nb_2O_5, TiO_2, CaO/P_2O_5 ratio (RCP), Metal recovery and Mass recovery. The term metal recovery is used throughout the text to refer to the recovery of P_2O_5. Not all information is available in all 4.862 samples, such that the data are unequally sampled. Most of the metallurgical recovery information is south or centered located (refer back to Figure 13). The number of missing values in this data can be evaluated in Table 5. Note that the Metal and Mass recovery are undersampled.

Table 5 – Quantity of missing values per variable

Variable	# Missing values
$Al_2O_3\_ROM$	1
SiO_2_ROM	2
BaO_ROM	87
$Nb_2O_5\_ROM$	243
TiO_2_ROM	699
Metal recovery	2761
Mass recovery	2761

Few and widely spaced metallurgical data in the northern region make it impossible to spatially estimate this portion without considerable risk of being inaccurate. Also, the large areal extension determined by the data contributes to increasing the computational complexity involved in the modeling. Constraining the study area to a smaller and more densely sampled region does not prejudice the aim of this chapter, which is to demonstrate how to obtain an estimated geometallurgical spatial model and do mine planning with geometallurgical data. Therefore, the study was constrained within the specific region highlighted in the black square in Figure 46. The region was chosen because it is abundant in samples for all the variables of interest.

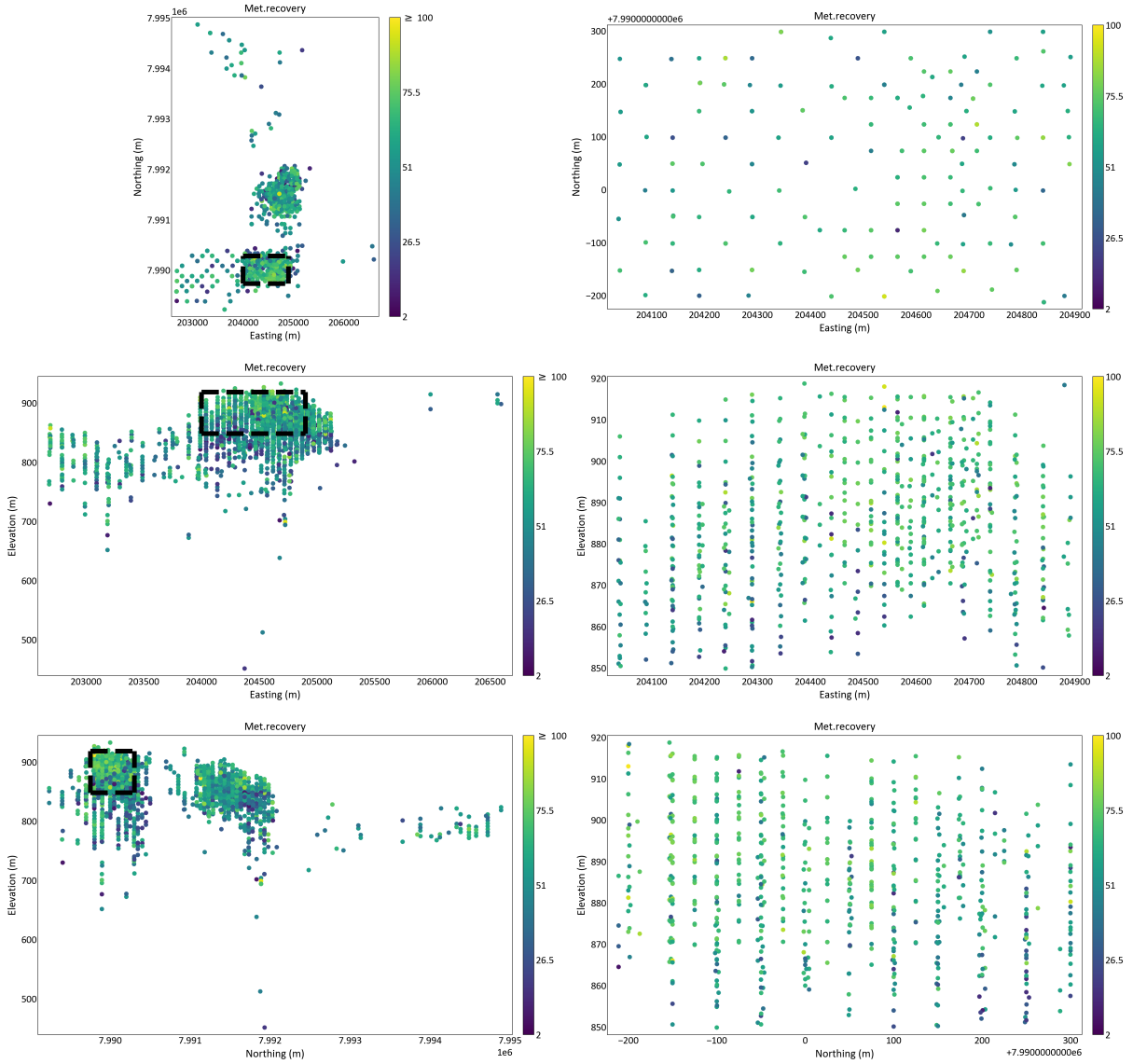

Figure 46 – Constrained region and the samples within it. Left: XY, XZ, and YZ planes crossing the total area sampled and the constrained area of the study highlighted by the black rectangle. Right: XY, XZ, and YZ planes showing only the samples inside the constrained area of study. Colorbar refers to metallurgical recovery.

The constrained region encompasses 717 samples spaced approximately 100 m along the X and Y axis, although there are samples spaced 50 m and 25 m apart also. Along the Z axis, samples are taken every 5 m. The variables Nb_2O_5, Metal, and Mass recovery have some missing values. Figure 47 shows the histograms for each variable. Note that the Nb_2O_5 histogram has spikes, which occur when a large proportion of the data has the same values. This may come from a detection limit or a round-off. A combination of a local average considering the nearest eight data and random despiking is applied to the Nb_2O_5 variable. Failure to break the ties can generate problems when further transforming the original distribution to normal score values, which is required for simulation purposes.

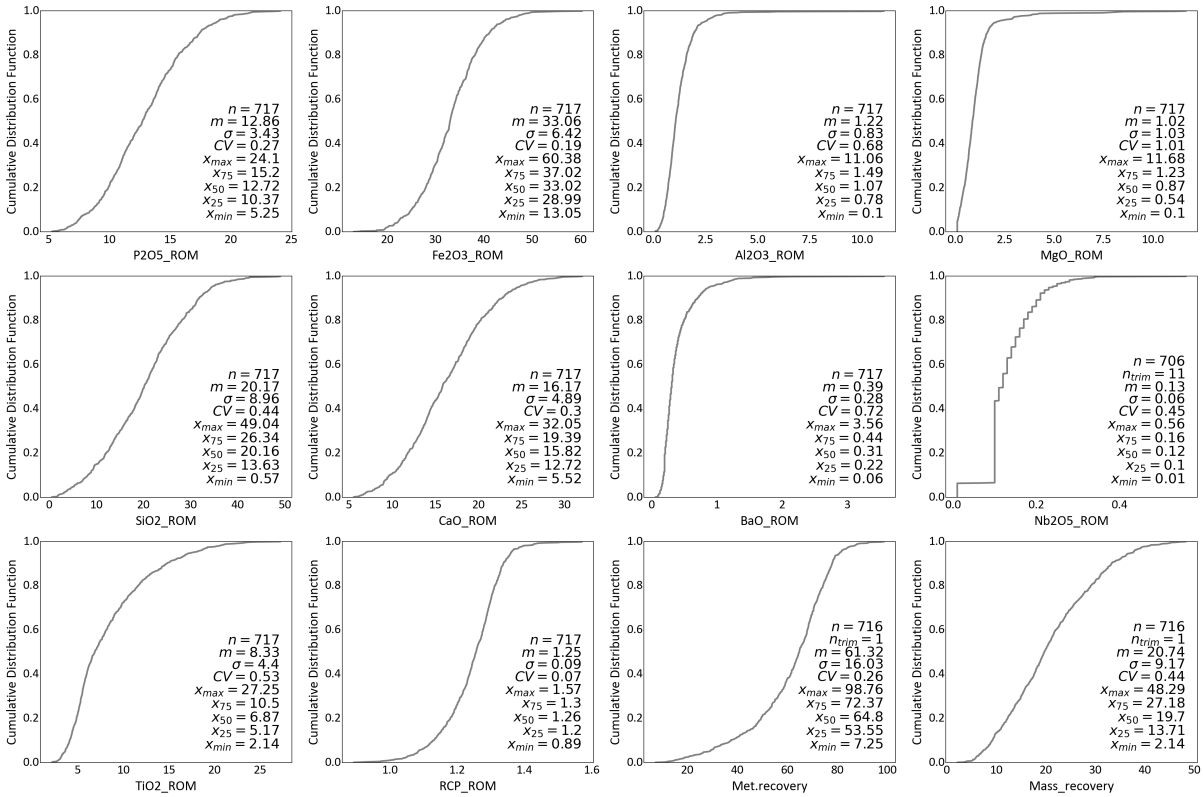

Figure 47 – Histograms for each variable.

After despiking, the linear correlations between the variables are evaluated (Figure 48). There are strong (0.7 or greater) positive correlations between P_2O_5 and CaO, P_2O_5 and Mass recovery, and CaO and Mass recovery. There are no strong negative correlations. Bivariate relationships depicted in Figure 48 are similar to those established in Figure 14, which means that the relationships within the constrained region are approximately the same as in the whole sampled area. Figure 49 displays the scatter-plot between each pair of variables, along with the number of data, the Pearson, and the Spearman correlation. This plot is interesting for understanding nonlinear complexities between variables. While Pearson refers to linear correlation, Spearman refers to monotonic correlation. Almost all the plots show approximate numbers for the two correlations. The most significant differences were found between $Al_2O_3 - MgO$ and $Al_2O_3 - TiO_2$ correlations. In $Al_2O_3 - MgO$, there is an intermediate Pearson correlation but a null Spearman correlation. In $Al_2O_3 - TiO_2$, the Spearman correlation is greater than the Pearson correlation.

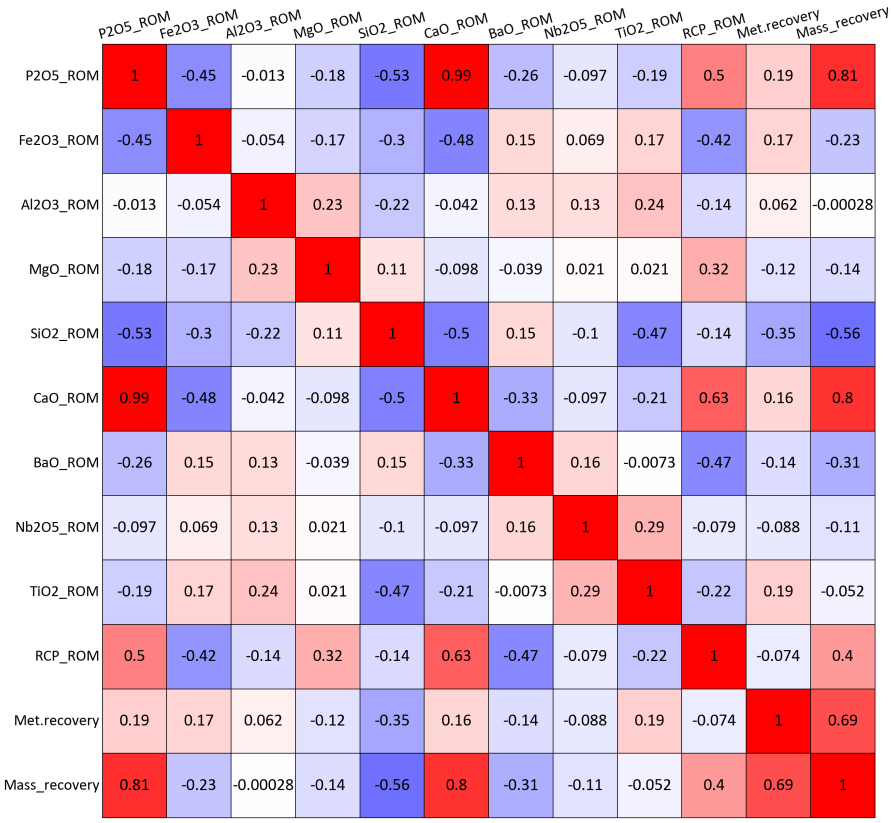

Figure 48 – Linear correlation matrix of the variables.

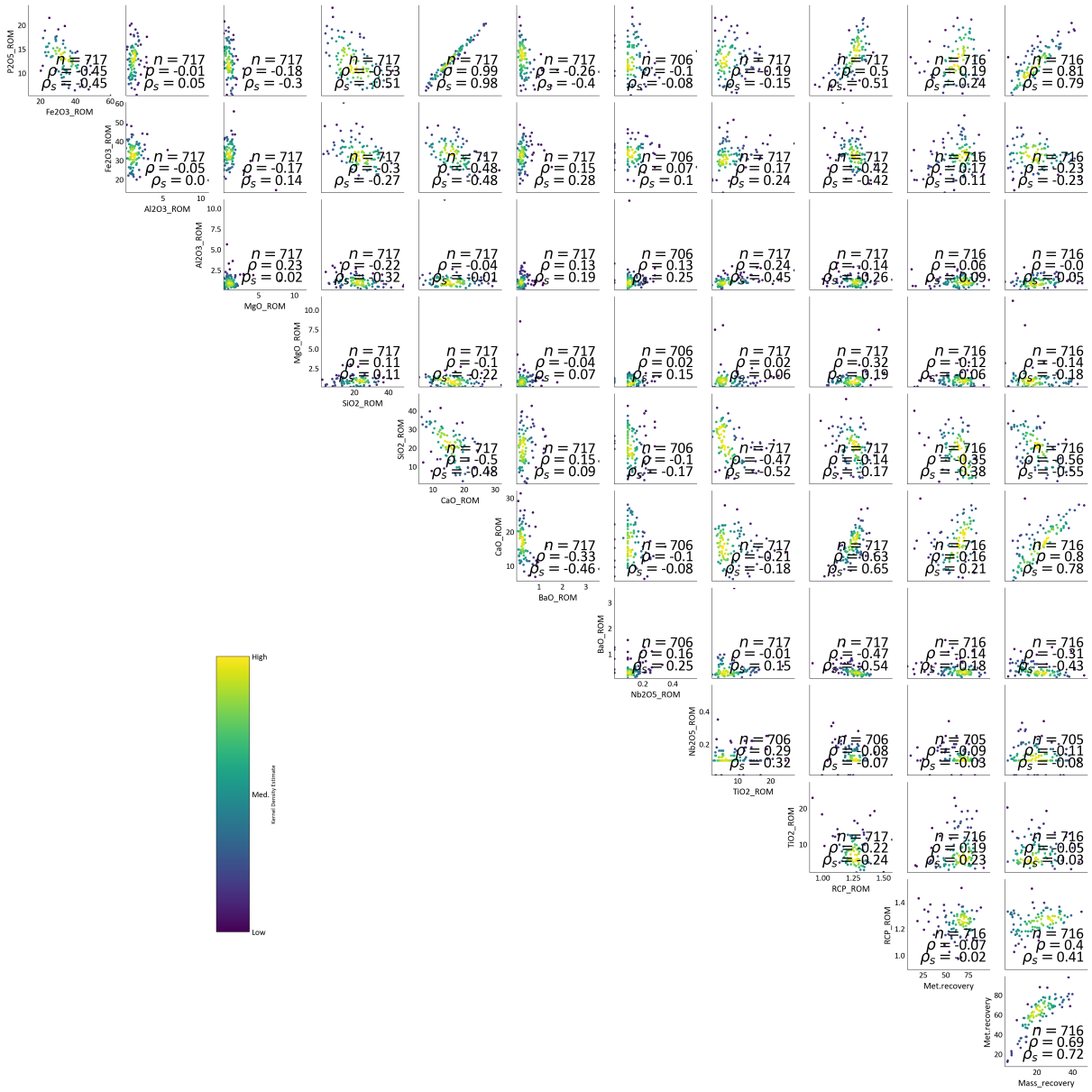

Figure 49 – Scatter-plot of the variables with Pearson and Spearman correlations.

As the data samples are not regularly spaced in the delimited region (Figure 46), declustering was performed using cell declustering (DEUTSCH, 1989). Figure 50 shows a diagnostic plot where the minimum declustered mean corresponds to the cell size of 100 m. This cell size seems reasonable, as this corresponds to the spacing in the sparsely sampled areas. Therefore, this value of cell size was used for cell declustering.

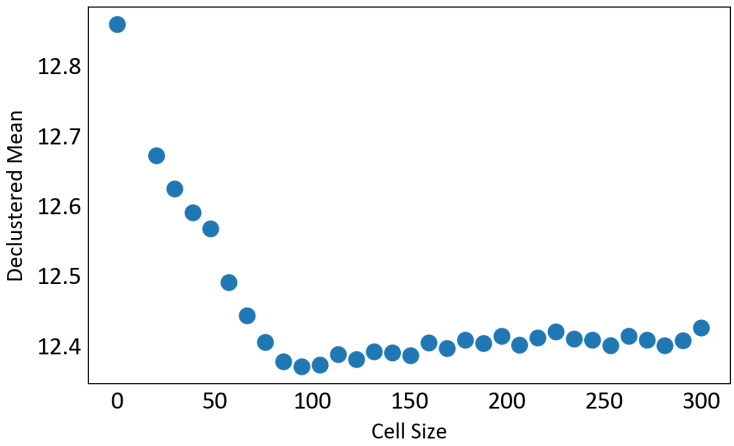

Figure 50 – Declustering diagnostic plot.

6.4 Spatial modelling

There are two main approaches to spatially modeling geometallurgical variables.

The first is the modern geostatistical approach, where each variable is decorrelated from each other, simulated, and then back-transformed to original units. This approach is applied to both linear and nonlinear variables and requires enough spatial sampling of the variables such that each variogram can be inferred. Unlike kriging, the simulation does not take averages, and its use is theoretically correct when working with nonlinear variables. If predictions are necessary in larger support, upscaling is deferred to the last moment possible. This is the only step where the consideration of linearity is assumed.

The second approach is to work with machine learning models. These models learn the relationship between the less sampled variables (often the metallurgical ones) and the more sampled (often the geological variables) through the homotopic samples. Geological variables are spatially estimated in a grid through geostatistics and the machine learning model is applied, providing the estimates of the metallurgical variables at the same grid locations. As the metallurgical variables are expected to be nonlinear, it is reasonable to use a nonlinear regression model. For this study, both approaches were performed to highlight their differences.

6.5 Modern geostatistical approach

The workflow for this approach is illustrated in Figure 51. The modern geostatistical approach for multivariate modeling is to decorrelate the variables such that simulation can be done for each variable independently. We need homotopic data to decorrelate with PPMT. Rather than using just the samples that possess reading for all the variables, data imputation was the alternative chosen. Multiple Imputation uses the incomplete dataset to

generate complete data realizations, such that each imputed data realization is used for a simulation realization in subsequent analysis. The first step was to normal score all twelve variables. For imputation, it is required the definition of a Mixture Model. The mixture model chosen was a Gaussian Mixture Model, obtained with the Expectation-Maximization (EM) Algorithm and 14 fitted components from the normal scored data. This number of fitted components was chosen based on the Likelihood Ratio Test (LRT) (GOMES et al., 2022), where increasing the number of Gaussian components did not significantly improve the likelihood estimate (Figure 52). The number of iterations for the EM algorithm was set to 500.

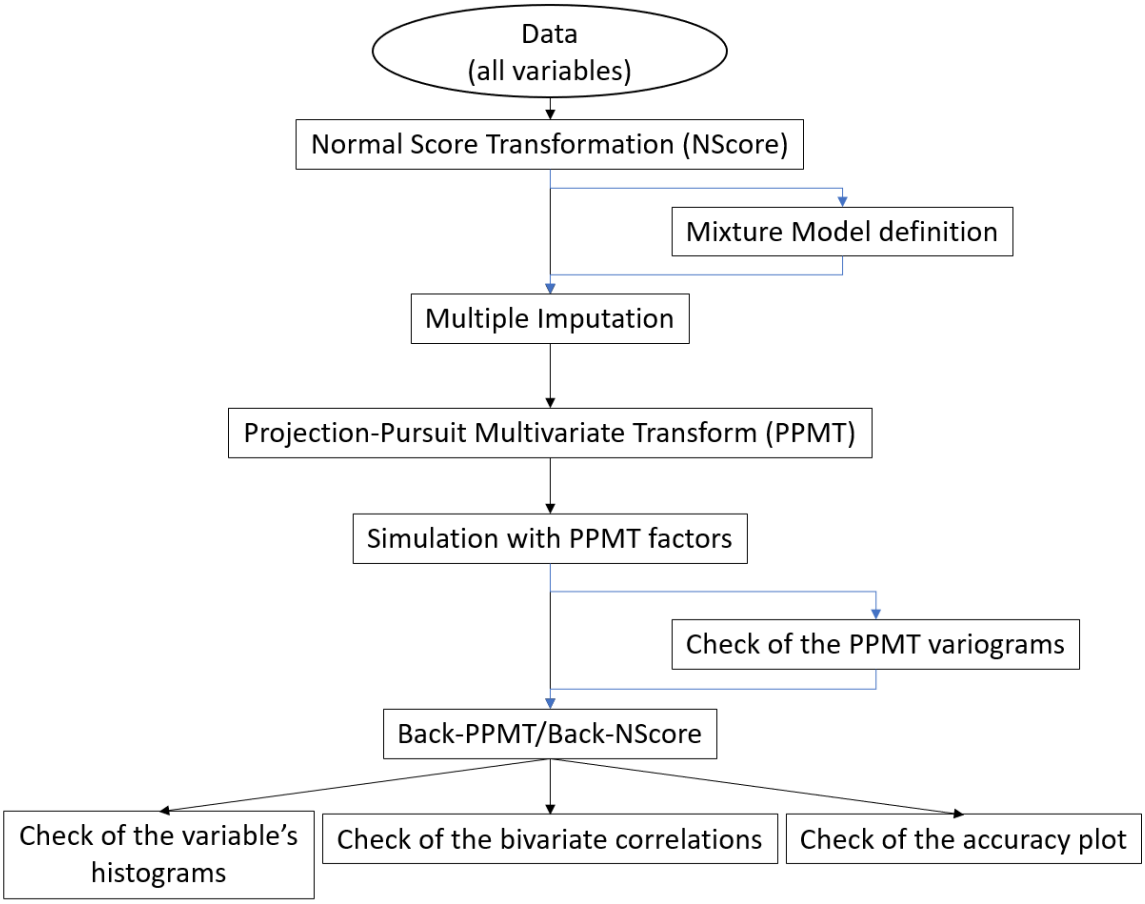

Figure 51 – Applied workflow for the modern geostatistical approach.

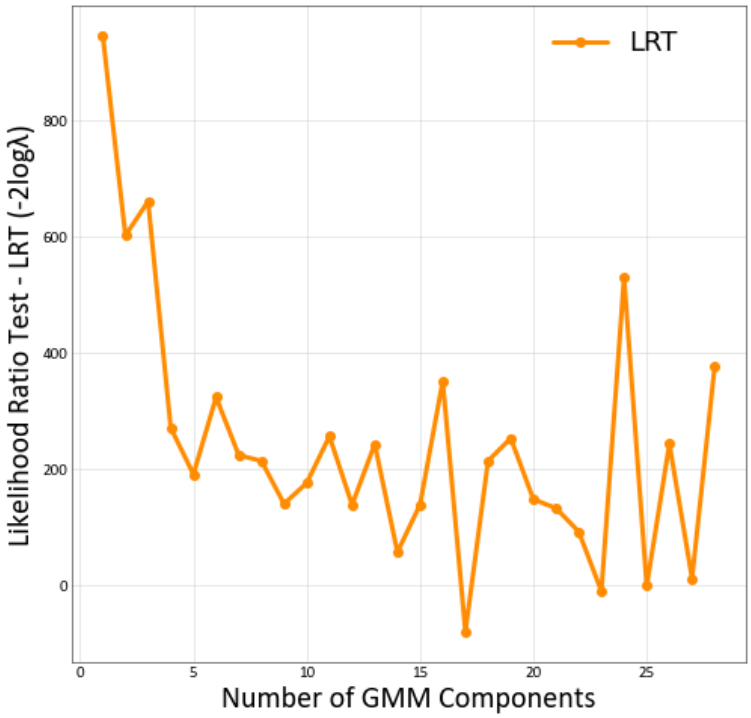

Figure 52 – Estimation of the GMM number of components based on the LRT.

Besides the mixture model, imputation also requires the normal score variograms and configurations regarding search radii and maximum previously simulated nodes to be used. The parameters used are shown in Table 6.

Table 6 – Imputation parameters

Parameter	# Value
Data realizations	20
maximum data/previously simulated nodes	50
maximum search radii (hmax,hmin,vert)	500, 500, 50

With each of the twenty data realizations, PPMT was performed to decorrelate the variables, and Sequential Gaussian Simulation was done for each PPMT factor individually. Each simulated realization was done with each data realization, one by one. Table 7 shows the simulation parameters.

Table 7 – Simulation parameters

Parameter	# Value
Simulation realizations	20
maximum data/previously simulated nodes	50
maximum search radii (hmax,hmin,vert)	500, 500, 50

Checking the simulation was done by comparing the variogram reproduction of the simulations and of each PPMT factor (Figure 53). PPMT back-transformation returned the

variables' realizations to their original values. Figure 54 shows the histogram reproduction between declustered original data (in red) and back-transformed realizations (in grey).

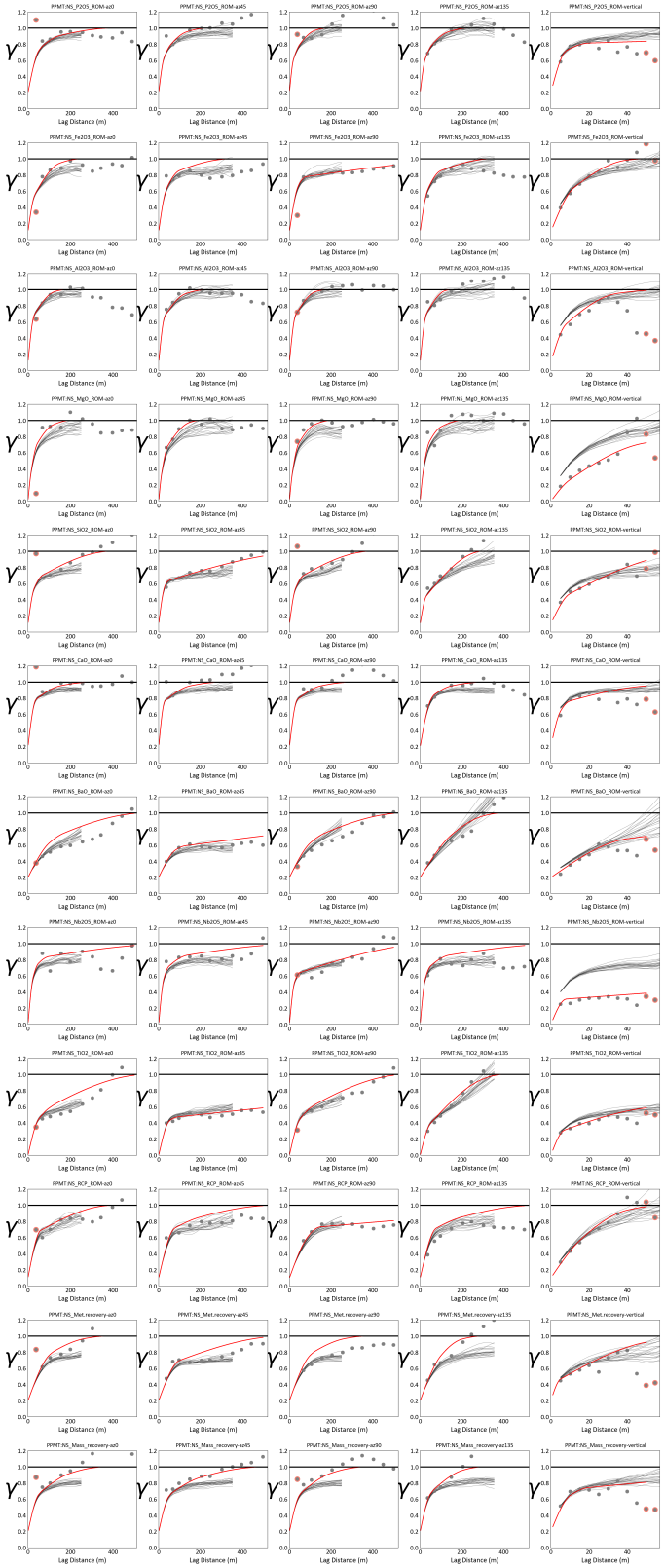

Figure 53 – Variogram reproduction for each PPMT factor. In red is the variogram model. In grey are the variograms of the realizations. Each row is a PPMT factor. From top to bottom: PPMT P_2O_5, PPMT Fe_2O_3, PPMT Al_2O_3, PPMT MgO, PPMT SiO_2, PPMT CaO, PPMT BaO, PPMT Nb_2O_5, PPMT TiO_2, PPMT CaO/P_2O_5 ratio (RCP), PPMT Metal recovery and PPMT Mass recovery. Columns represent the direction of the variogram. From left to right (azimuth/dip): 0°/0°, 45°/0°, 90°/0°, 135°/0°, and downhole direction (0°/90°)

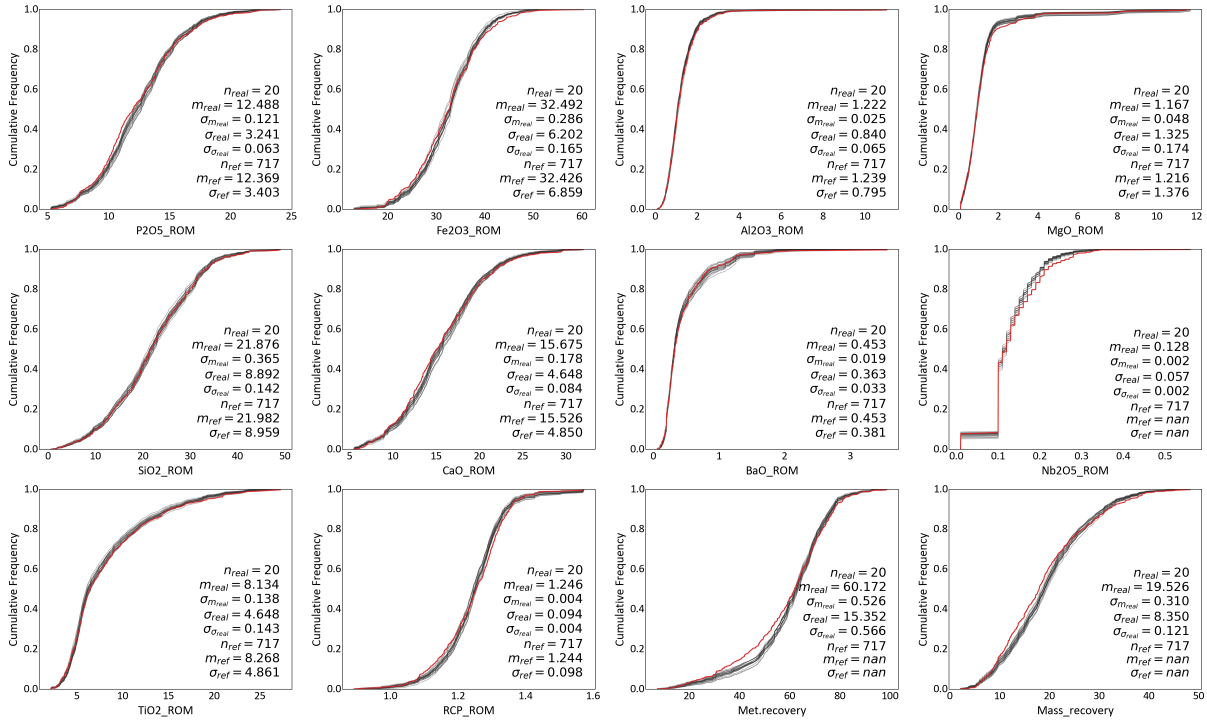

Figure 54 – Histogram reproduction in original units for each variable. In red is the histogram of the data. In grey are the histograms of the realizations.

Another check was performed comparing the bivariate relationship of the simulation results with the relationship of the samples. The relationships shown in Figure 55 adhere to those in Figure 48.

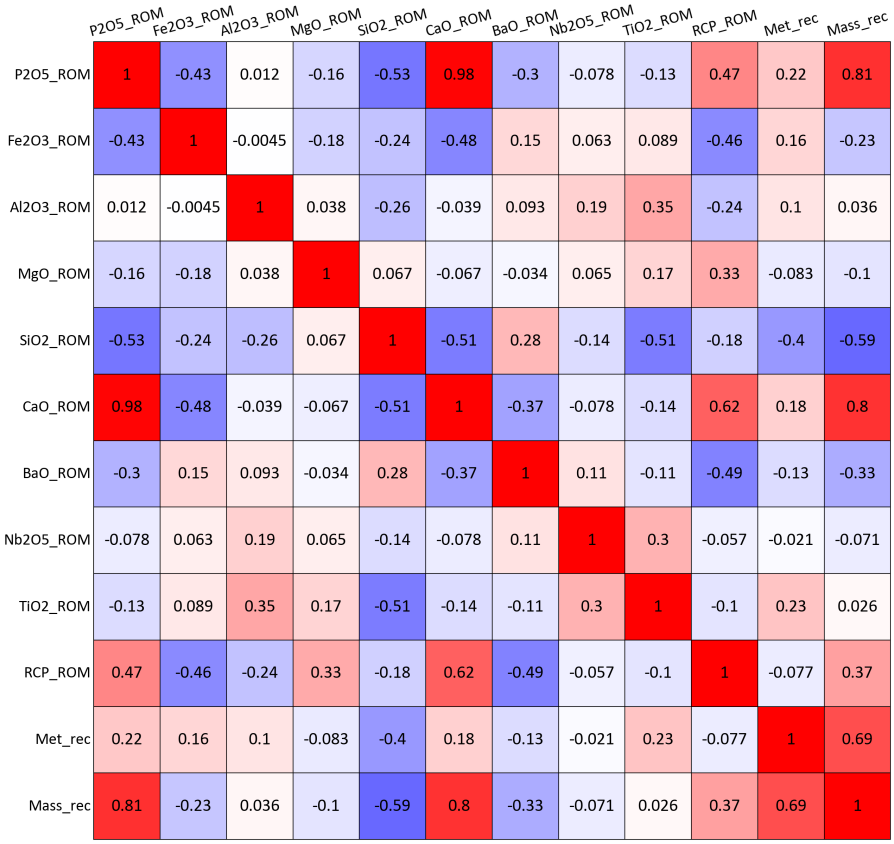

Figure 55 – Correlation of variables after simulation.

For illustration purposes, Figure 56 and Figure 57 show three slices (XY, XZ, and YZ) of the first realization of P_2O_5 and metal recovery, respectively, in original units.

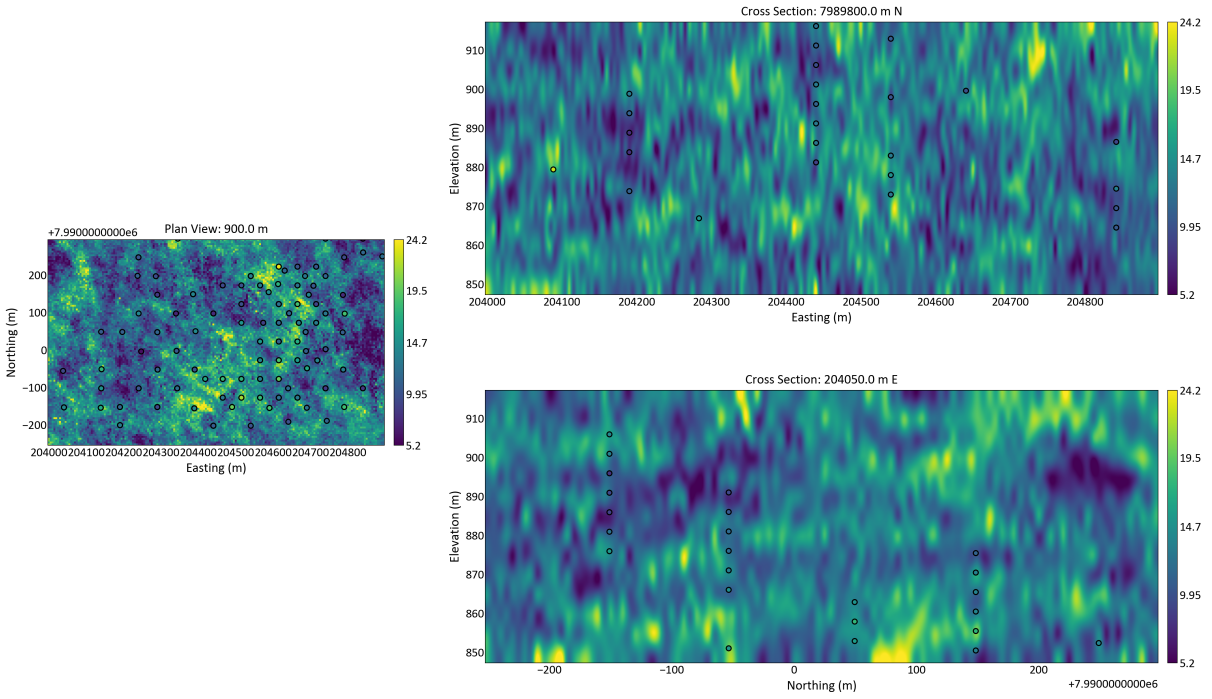

Figure 56 – One realization of P_2O_5 variable.

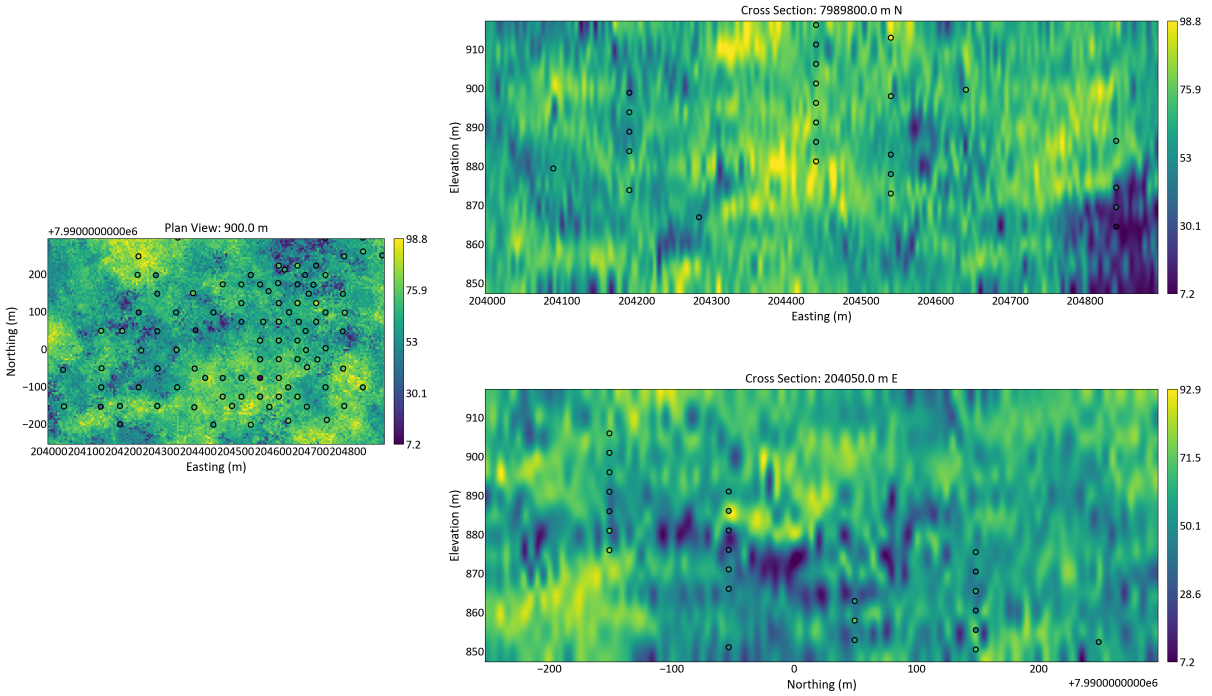

Figure 57 – One realization of metal recovery variable.

Note that histogram and variogram reproductions are good. The bivariate relationships in simulation do honor those in the data. One other option for validating a simulation is through the accuracy plot. The accuracy plot needs the data to be split into train and test sets. In this case, the data were randomly split into 70% (train), and 30% (test), and all the variogram and simulation parameters used were the same as the ones obtained with all the data. The accuracy plot in Figure 58 shows that the simulation was both accurate and precise.

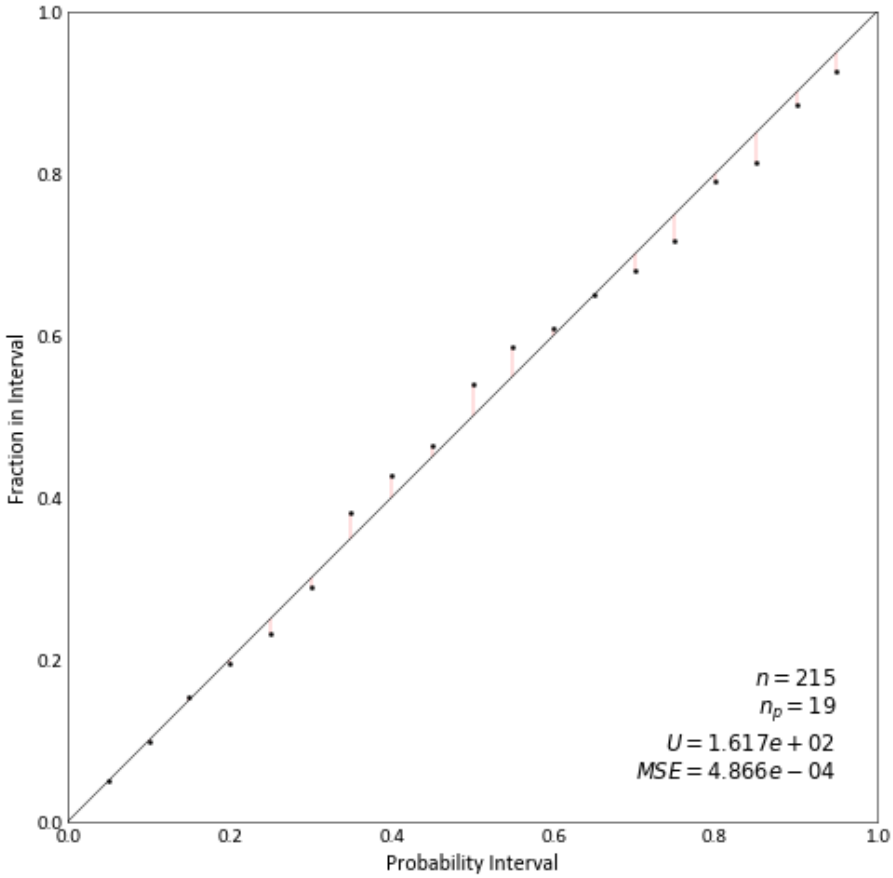

Figure 58 – Accuracy plot for metal recovery variable.

6.6 Machine learning approach

The machine learning approach consists of two parallel streams. The first stream is to spatially estimate only the geological variables. The procedure for this estimation can be the modern geostatistical approach mentioned previously. The second stream models a machine-learning regression between geological and metallurgical variables based on the data. The regression model is then applied to the spatial estimates of the geological variables obtained through the first stream to get estimates of the metallurgical variables at the same locations. The workflow of this approach is illustrated in Figure 59.

As the first stream has already been explained in the previous section, let us explain the second stream. The data need to be homotopic. However, the use of data imputation is not justified. The samples containing information on all the variables were used, which is 705 data, more than 98% of all the data. All the homotopic data were used to obtain a machine-learning model that uses the geological variables as features to predict the dependent metallurgical variables.

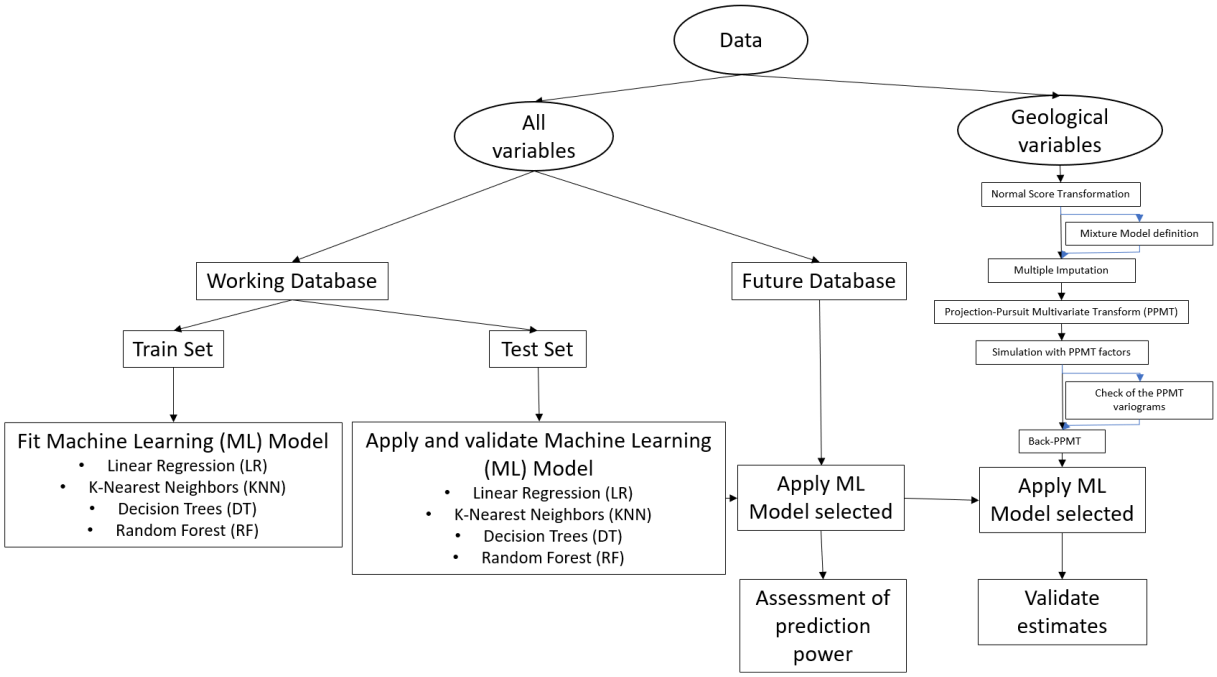

Figure 59 – Applied workflow for the machine learning approach.

To assess the accuracy of the model, the database was randomly divided into working (80%) and future (20%) datasets. The future set mimics data obtained in the future and is used to analyze the future prediction performance of the model. The working dataset is used for the modeling and is further split into ten consecutive folds, such that each fold is used once as a testing/validation set, which is used to analyze the performance of the prediction, while the nine remaining folds form the training set, used to train the model for the prediction

The objective was to simultaneously predict metal and mass recovery, both nonlinear variables. Four multiple outputs regressors were tested: LR, KNN, DT, and RF. KNN regressor requires the data to be standardized so that the features with higher values do not dominate the learning process. The 'StadardScaler' method on Scikit Learn was used. All the other regressors used do not require the standardization of the variables since they are not sensitive to the magnitude of variables.

The testing set was used to identify the best regressor. The scatter-plots between the predicted and the true values for each ML model - LR, KNN, DT, and RF - are shown in Figure 60, Figure 61, Figure 62, and Figure 63, respectively. RF regressor yielded the greatest Pearson correlations, 0.45 and 0.84 for metal recovery and mass recovery, respectively, and also resulted in the greater R^2 mean: 0.44.

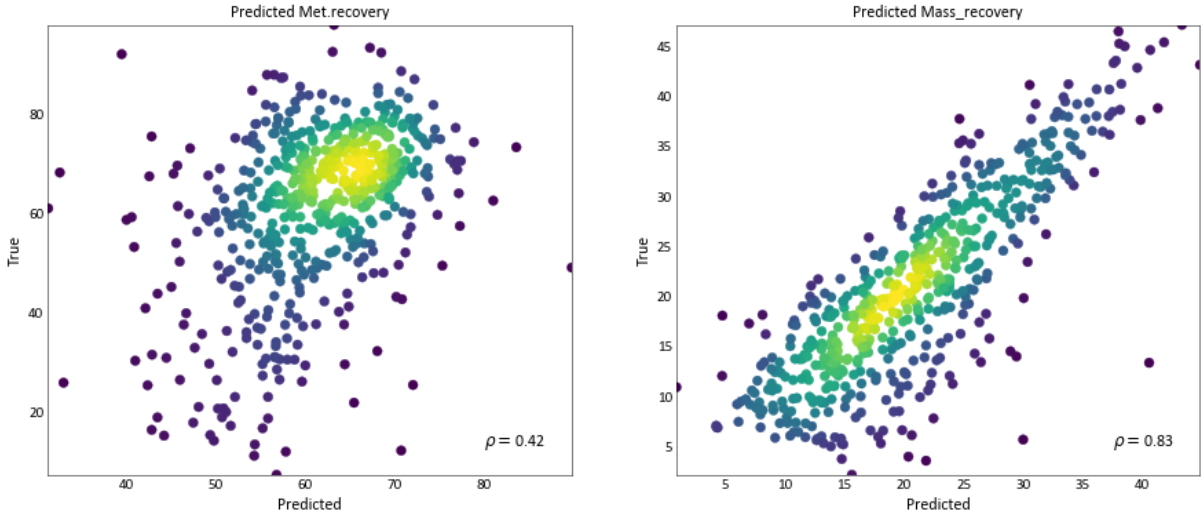

Figure 60 – Scatter-plot of LR-predicted and true values in the working database

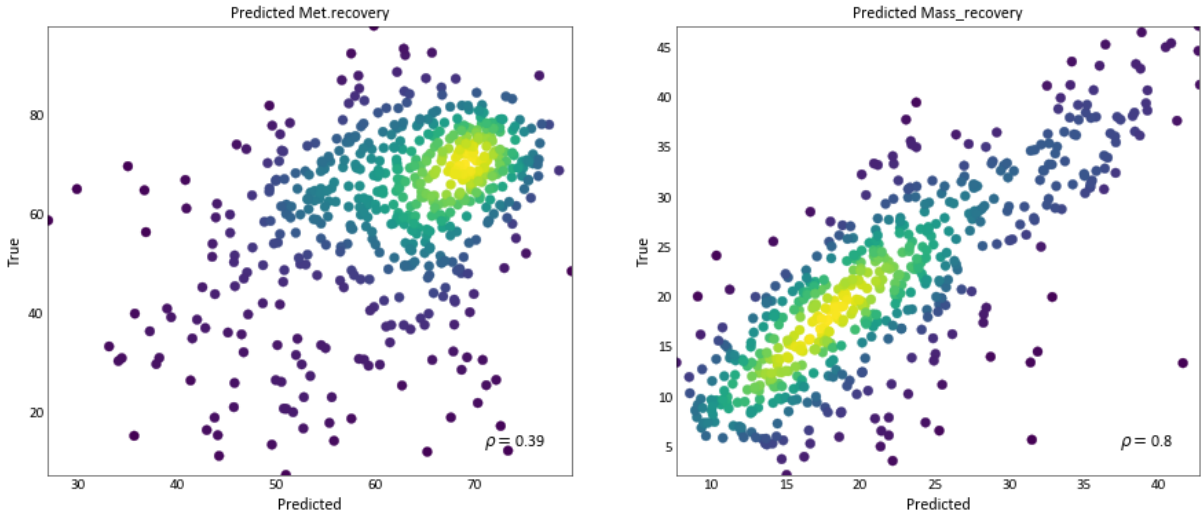

Figure 61 – Scatter-plot of KNN-predicted and true values in the working database

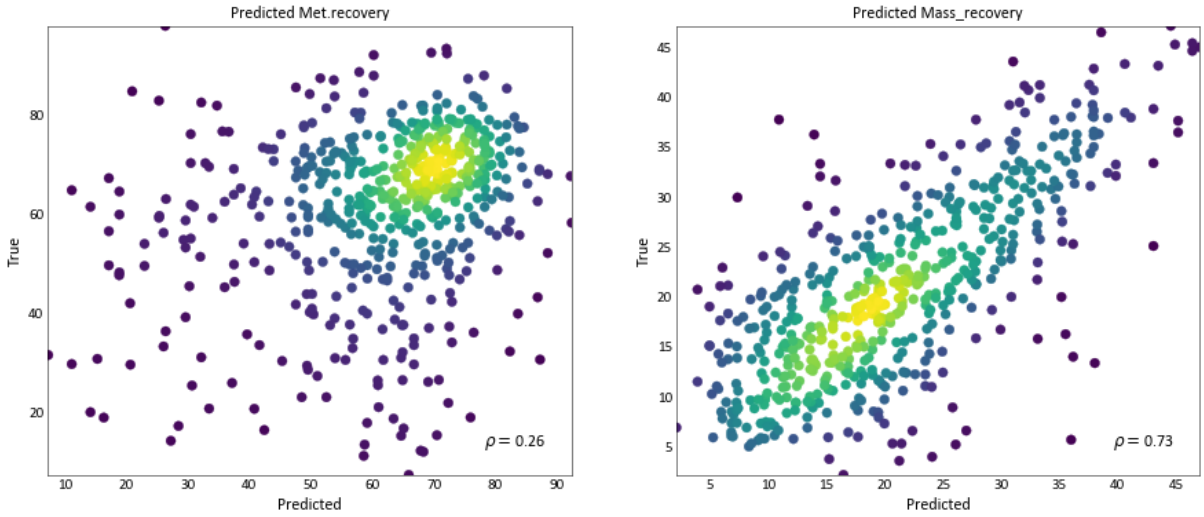

Figure 62 – Scatter-plot of DT-predicted and true values in the working database

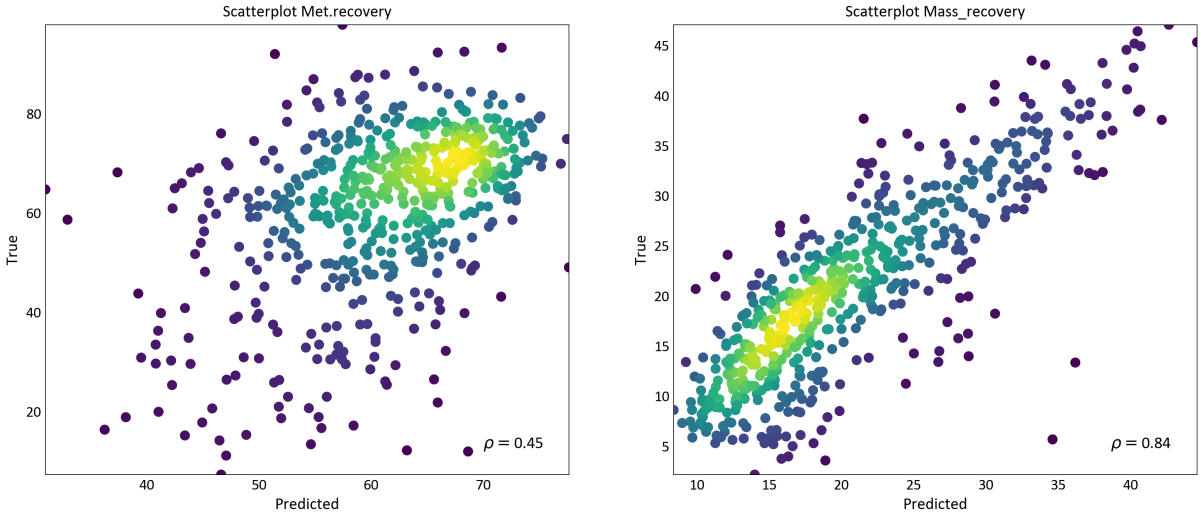

Figure 63 – Scatter-plot of RF-predicted and true values in the working database

RF was the only model applied in the future set. In this case, the Pearson correlations were 0.44 and 0.85 (Figure 64). The proximity between the values in the working test dataset and the future dataset is indicative that the model is neither over nor under-fitted.

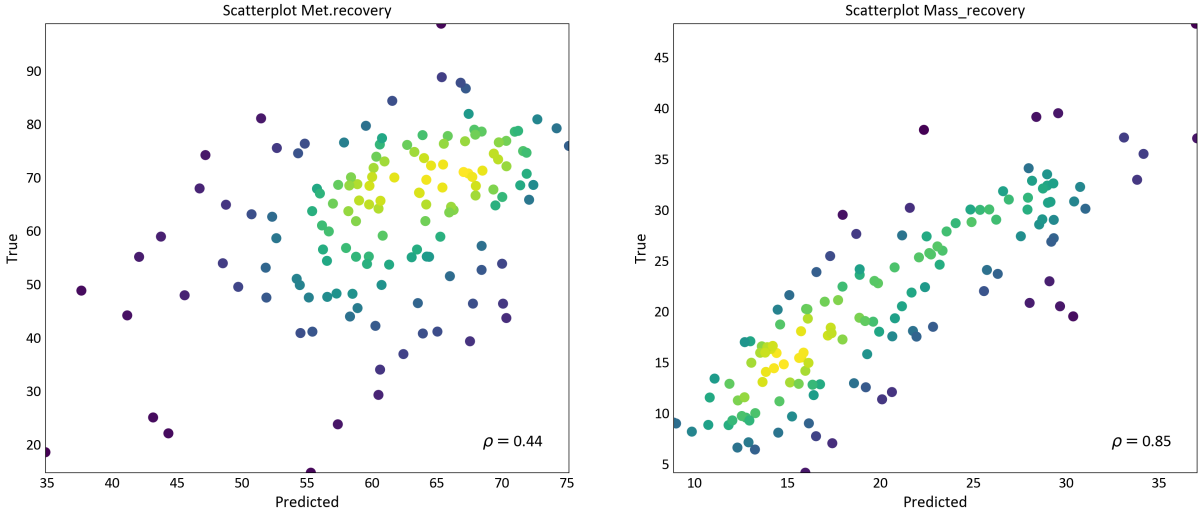

Figure 64 – Scatter-plot of RF-predicted and true values in the future database

It makes sense that RF was the better model because of its robustness and applicability to nonlinear variables. RF gives a list of the most important variables for the prediction (Table 8). As one can see, P_2O_5 is the first one, given the high correlation with mass recovery. CaO is redundant with P_2O_5 and therefore does not gain too much weight. A technique of grid search was used to tune the hyperparameters of RF better. Still, it did not significantly increase the results, as it returned a predicted-true Pearson correlation for the metallurgical and mass recovery of 0.45 and 0.85, respectively.

Table 8 – Variable importance

Variable	**Importance**
P_2O_5	0.24
Fe_2O_3	0.11
SiO_2	0.11
TiO_2	0.10
CaO	0.09
Nb_2O_5	0.08
RCP	0.08
BaO	0.07
MgO	0.06
Al_2O_3	0.05

Of all regressors, RF was the best one. However, the R^2 and the predicted-true Pearson correlation for the metal recovery are still low. That is because the predictor's variables are not very explicative of the metal recovery response, as discussed in chapter 3. Considering the variable 'Collector' as an input feature would probably increase the prediction power of the model. As this variable is related to process input, its spatial estimation is not straightforward and, therefore, was not chosen as a predictor of recovery.

The RF model was applied to the geological variables' twenty realizations to predict metallurgical and mass recovery. The spatial estimation for the metal recovery variable on the first realization of the geological variables is shown in XY, XZ, and YZ slices in Figure 57.

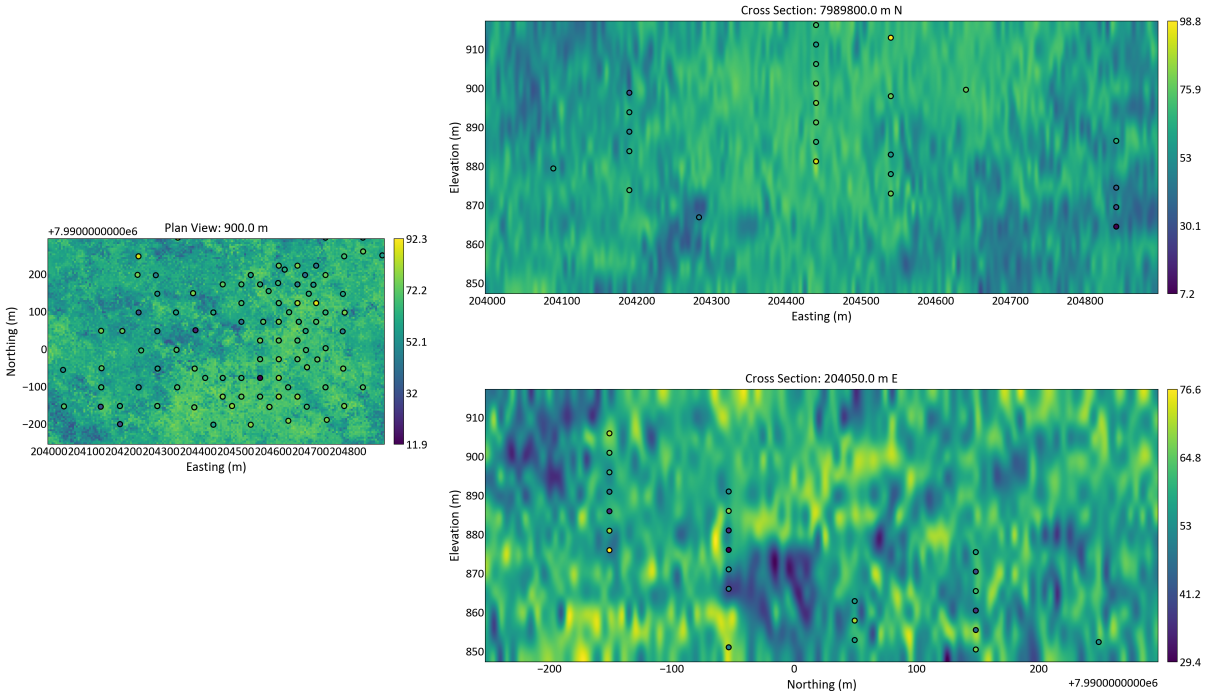

Figure 65 – RF prediction for metal recovery variable. Left: XY slice. Right: XZ slice (above) and YZ slice (below)

6.7 Comparison between geostatistical and machine learning approaches

By comparing the spatial estimates for the metal recovery from the modern geostatistical approach (Figure 57) and the ML approach (Figure 65), it is clear that the latter provided a smoother spatial model. This is also shown in Figure 66 by comparing the distributions of the metallurgical data in red, the distributions of the twenty realizations of the metallurgical variables from the modern geostatistical approach in grey, and the distributions of the twenty realizations of the metallurgical variables from the machine learning approach in blue.

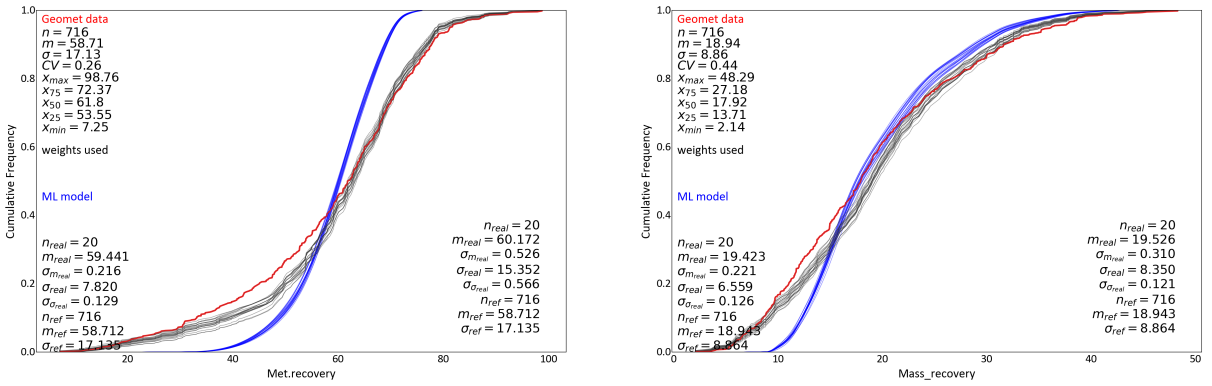

Figure 66 – Metal and mass recovery histogram reproduction. Data histogram in red. Simulated realizations in grey. RF realizations in blue.

Least squares regression models cannot reproduce the extremes of the variable predicted, just like kriging. Figure 67 compares the histograms of the true data against the predicted values for each machine learning model applied to the working database (true data in grey, RF model in red, DT model in yellow, LR model in blue, KNN model in green). The DT model is the only model that reproduces the data variability. The mass recovery histogram seems to be more reproduced by the machine learning models than the metal recovery histogram. The stronger correlations between the geological variables and the mass recovery explain this. The weaker the correlations between features and the variable predicted, the smoother the prediction is.

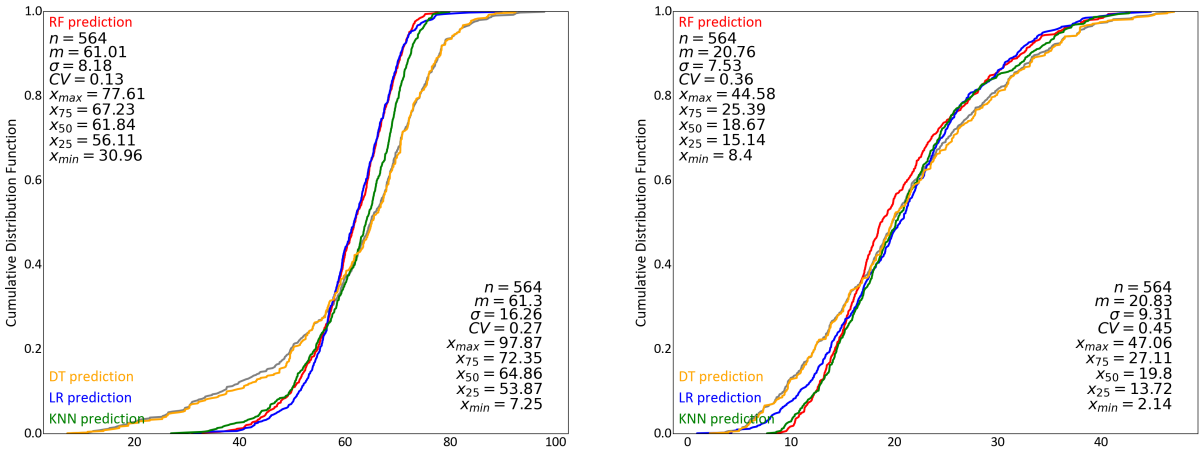

Figure 67 – Metal (left) and mass (right) recovery histogram reproduction of the true data for each machine learning model. In grey is the histogram of the true data in the working database. In red is the RF-model histogram. DT-model histogram in yellow, LR-model histogram in blue, and KNN-model histogram in green.

In summary, the approach to spatially model metallurgical variables depends on the data availability and the study's objective. In the case of few spatial data, such that variograms of the variables are impossible to infer, the machine learning approach is applicable. It is desirable to have features with high correlations with the predicted variable. Otherwise, the consequence is smoothed predictions with underestimated variability. In case there is enough data for variogram inference, the modeling of each variable independently and simultaneously can be done using a multivariate technique such as the combination of PPMT and simulation. The histogram variability is reproduced. The probabilistic model provides a reliable measure of uncertainty.

6.8 Short-term ore scheduling and blending

The use of multiple simulation realizations in mine planning is a topic of great discussion in research and a challenge faced in the mining industry. The optimization of a decision should ideally be done using multiple realizations simultaneously. However, this

consideration would go beyond the scope of this thesis, which is to demonstrate how to make better conventional-deterministic mine planning considering metallurgical variables.

The assessment of a better decision value is only realistic through a process that simulates reality. In reality, we sample a truth, which is unknown, and make decisions based on the small knowledge we have from the sampling. By random chance, a better decision could lead to a worse outcome in reality, but in expected value, a better decision should lead to a better outcome.

Short-term scheduling is often performed after grade-control (GC) sampling. We simulated a GC drilling in a small region of the already constrained area to mimic a mining face that will be mined soon (Figure 68). GC drilling was at 20 x 20 x 5m and only the geological variables are measured. Estimation was performed for all the variables simultaneously, following the same decorrelation procedure explained previously. For this study purpose, the first realization of the simulation is considered to be the unknown truth.

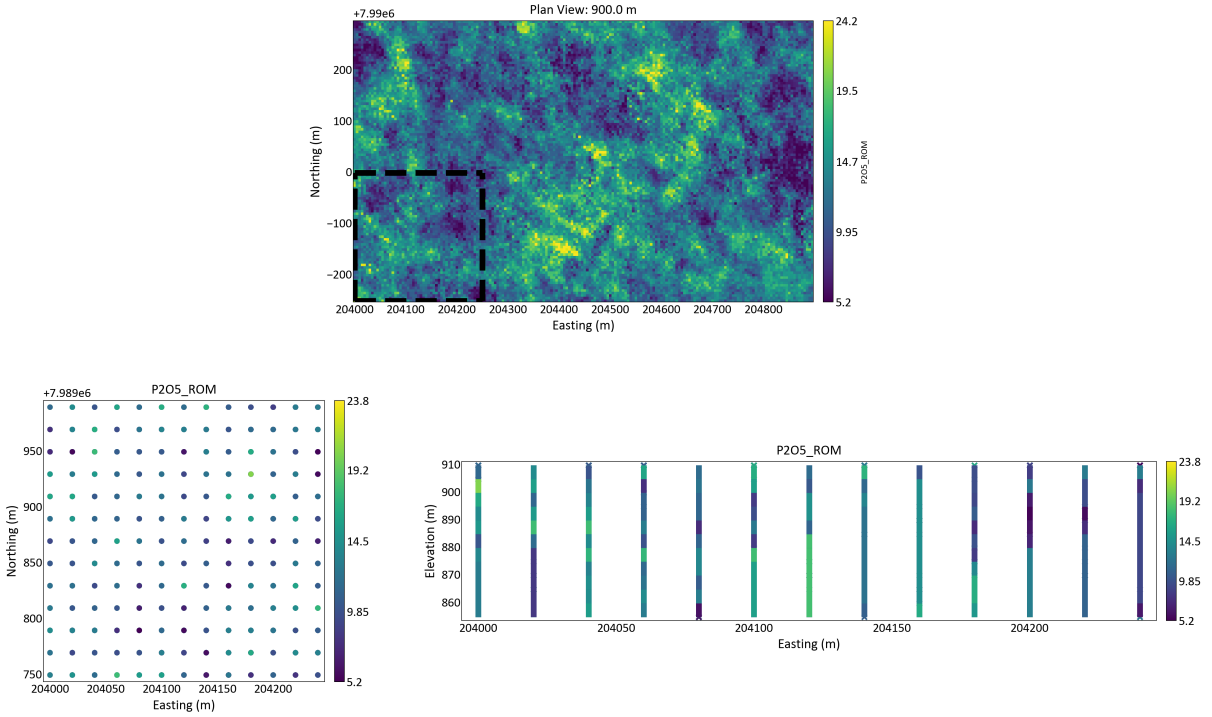

Figure 68 – Delimitation of a GC drilling area. At the top: mining face area for GC drilling with the unknown truth. At the bottom: GC drilling spacing on XY and XZ slices. The color bar refers to P_2O_5.

The geological variables are kriged in a 5 x 5 x 5 m grid, considered to be the parcel's volume. Since the parcel and the data have similar support, the kriged values of the geological variables can be used as predictors in the machine learning model for the recovery variables estimations at the same grid. Figure 69 shows the kriged estimation of P_2O_5 on the left and the RF estimation of metal recovery on the right.

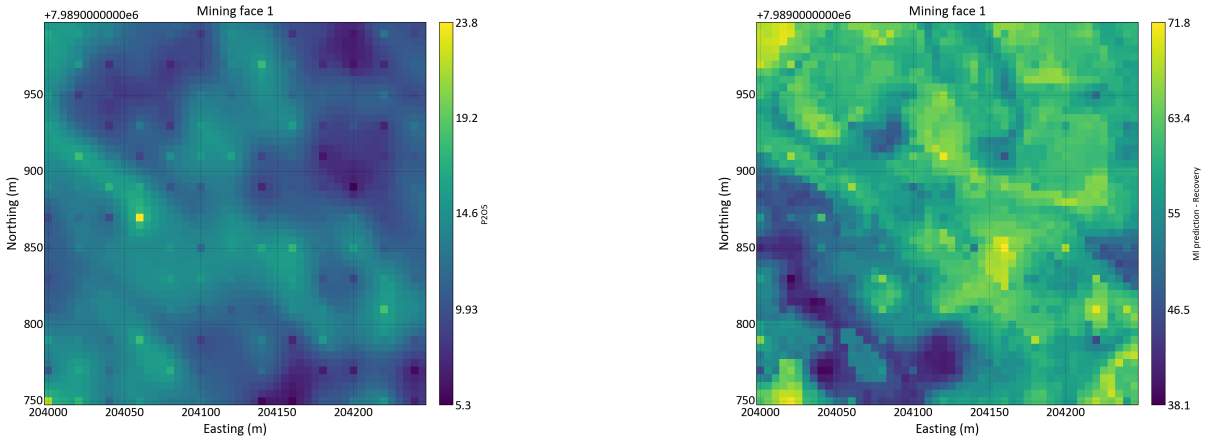

Figure 69 – Kriged P_2O_5 grade (left) and RF-estimated metal recovery (right).

With all the geological and metallurgical variables estimations, this model is now used to support the scheduling. An optimization schedule based on Simulated Annealing developed and explained in chapter 5 is applied to the model. This schedule considers how ore parcels are blended during mining and processing operations and how this process affects the mixture properties. In the real operation, the ore is sent to 110,000 t homogenization piles, before feeding the plant. Therefore, the capacity of the pile is the tonnage of the mixture. Using the estimated grid volume and a mean ore density of 1.8 t/m^3, approximately 500 parcels are blended in a pile. The short-term mining face mass is equivalent to five piles. Regarding blending, it is assumed that the blending of ores with different recoveries is beneficial, such that the blending behavior can be reasonably modeled by a power-law function described by a w factor of 0.8 (refer back to chapter 4).

A default schedule is performed on the mining face. The default schedule mining occurs from south to north in a zigzag, from left to the right, right to left, and so on. Each parcel, according to the period of its extraction, is assigned to a pile/blend unit through an indicator number. Parcels designated to pile one are mined before those set to pile 2, which are mined before those assigned to pile 3, and so on. Figure 70 shows on the left how each parcel would be categorized in each of the five piles. The optimization algorithm yields another schedule (Figure 70, right).

Based on the estimated model, the increase in metal recovered in the optimized scenario is 0.04%. Two main reasons justify the little difference. The first is related to the optimization being supported by a smoothed kriged/RF estimated model of the truth. If the truth and its real variability could be known, applying the optimal-defined schedule increases metal recovered by 0.1%. This value could be smaller or even negative as the variability of the truth could be enough to make the optimal schedule wrong. Applying the optimization algorithm to simulated realizations, which have more variability than any estimated model, would result in more significant differences between the optimal and the default schedule. The second reason for the low difference is related to the use of the

homogenization pile. The pile diminishes the impact of optimal parcel scheduling, as many of them are mixed in huge piles. In a situation where the mine does not use homogenization piles, the mixtures of parcels would be formed by mining and processing operations in one shift, for example. Considering the mass of material fed to a plant in a shift is 6,000 t, twenty-five parcels would be blended. Running the optimization on that same kriged/RF estimated model, but using blending units of 25 parcels, the optimized result is 0.58% better than the default schedule. Without a homogenization pile, the scheduling of the parcels is more relevant. This shows that this methodology can be additionally used to evaluate the need for homogenization piles better.

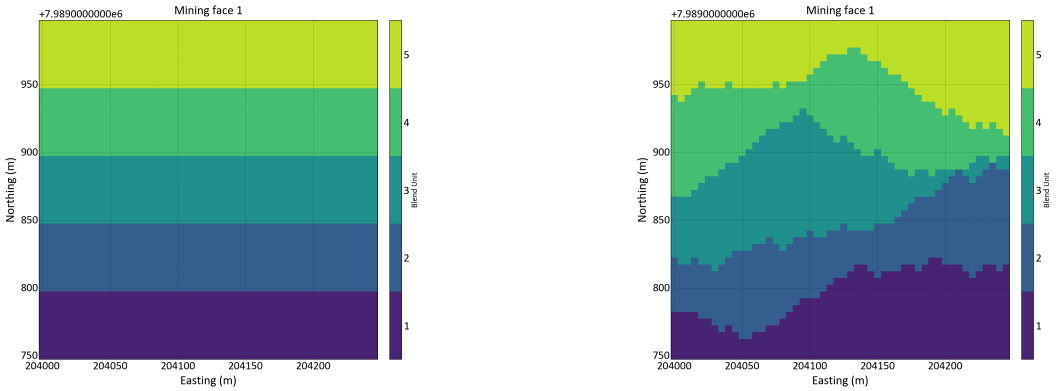

Figure 70 – Scheduling of the parcels in the mining face. Left: default schedule. Right: Optimal schedule

6.9 Summary

Rock and metallurgical properties should be spatially modeled and used in mine planning. One of the main issues with metallurgical variables is nonlinearity, which prevents using kriging or any other linear estimate. Simulation is an alternative as long as there are enough samples for variogram inference. For multivariate simulation, Multiple Imputation and decorrelation may be necessary. The product of simulation is N equiprobable models that have the same statistical features as the sample data used to generate them. If mine planning works only with one model, and since kriging is not an option, nonlinear machine learning techniques combined with simulation are the solution. Good regression techniques naturally smooth the prediction.

Mine planning can take advantage of the spatial geometallurgical model when scheduling the ore parcels. By recognizing and understanding how ores are naturally blended during mine and process operations, mine scheduling can be done to optimize the formation of the ore mixtures globally (maximizing metal recovery, minimizing BWI, maximizing profit, etc).

For the application example, even after some data cleaning and preprocessing,

enough data allow the spatial modeling of all the variables by multivariate simulation, which is the best approach indicated. However, as for the time this thesis is written, mine planning is based on only one deterministic model. In that case, the best approach is to krige the linear variables and estimate the nonlinear ones by machine learning regressions. After having one model with estimates for all variables, a simulated-annealing-based algorithm was applied to the model to provide an optimum mine scheduling regarding the total metal recovered. The increase in comparison to a default schedule was 0.04%. This value is insignificant because the spatial model is smoothed and the mine uses homogenization piles to blend the ore. In case there was no pile, the optimal schedule could result in an increase of 0.58% in comparison to a default schedule. If the spatial model had more variability and depending on how beneficial blending is, the increased value would be even greater.

7 CONCLUSIONS AND FUTURE WORK

This thesis aimed to investigate how nonadditive geometallurgical variables must be estimated in the block model and used in mine planning. This thesis' workflow included understanding geometallurgical data and variables, possible solutions for spatial modeling, and using a nonlinear blending model along with spatial estimation to proceed with mine planning. Recall the objectives presented in chapter 1:

1. Understand particularities related to geometallurgical data and variables;
2. Review different spatial modeling approaches for geometallurgical variables;
3. Demonstrate that the current practice of estimating individual and independent values of a geometallurgical variable for each block is conceptually incorrect;
4. Propose a blending model that can be used to estimate process responses for the blending unit volume effectively;
5. Propose a methodology for estimating the geometallurgical variables in each block that considers the blending of the blocks;
6. Develop a production schedule that identifies the best combinations of blocks to form each blending unit.

The first objective was addressed in chapter 3 and the main topics and conclusions are provided in section 7.1. The second objective was accomplished in chapter 2, with applications shown in chapter 6. The main points and conclusion related to geometallurgical spatial modeling are reviewed in section 7.2. The third and fourth objectives were addressed in chapter 4, whereas the fifth and sixth objectives were met in chapter 5. The conclusion of these objectives is provided in section 7.3.

7.1 Geometallurgical data and variables

This thesis highlighted the importance of understanding the specificities related to geometallurgical data and variables. While some geometallurgical variables are intrinsic rock properties (primary variables), others are a response to a specific process. A metallurgical variable is a response variable to a processing operation. In that sense, metallurgical recovery is the response of the ore to the concentration, whilst BWI is the ore's response to ball mill grinding. Response variables often present characteristics that are unusual to primary variables. They usually average nonlinearly, respect defined constraints, and

they have multivariate complex relationships. Challenges of geometallurgical modeling are related to the complexities in the variables and also in the data. Missing data, heterotopic and sparse sampling, and differences in the data support are common characteristics of a geometallurgical database that must be analyzed before any decision on spatial modeling. This type of analysis is often carried out during Exploratory Data Analysis. At this stage, one also understands the univariate distributions of each important variable and their multivariate relationships. Preprocessing is a stage done along with EDA, which is responsible for extracting the features from the raw data, selecting the important ones, and cleaning the database. Important features are the target variables for spatial modeling and their highly-correlated variables. Redundant features may be dropped for convenience; they demand more computational power, and they can decrease prediction performance. Errors and missing values are treated in the cleaning phase, by correcting or deleting the data.

A real mine bench test and plant databases were compared with EDA analysis in Chapter 3. In a bench test, there is more control over the tests, the inputs, the outputs, and the whole process. One can understand the impacts on the output caused by variations in input. The analysis showed that the metallurgical recovery has just one reasonable correlation with the variable collector. Conversely, mass recovery has high correlations with P_2O_5, CaO, and intermediate correlations with SiO_2 and collector. A Random Forest regressor was applied to predict these two target variables. The high correlations with the primary variables collaborate to an accurate and precise prediction of mass recovery. The prediction of metallurgical recovery is accurate but not precise, because of the inexistence of high correlations. Nevertheless, Random Forest still performs fairly.

In a plant, the process dynamic is complex. There may be more than one stream of material feed, each with different characteristics; the processing conditions (e.g., air flow rate, agitation) can change; sampling a continuous feed and matching it to the correspondent concentrate is complicated. In addition, in this specific case, the material is homogenized in piles before feeding the plant, resulting in material feed with low variability. All of those reasons contribute to the poor understanding of the impacts of the input on the output. The consequence is that the data collected in the plant do not show high bivariate correlations. Any regressor performs poorly when input variables do not explain the target variables. This problem is amplified when the variable collector, shown by the bench test data as the most important predictor variable to the metallurgical response, is not measured in the plant. The result is that it is challenging to predict the results in the plant with precision.

This obstacle should not prevent us from using geometallurgical data to perform spatial estimations of metallurgical response and using these estimations in mine planning. Bench tests are well-controlled procedures and provide reliable data. Reliable data combined

with the right spatial modeling technique results in accurate models. These models can be used to enhance mine planning.

7.2 Geometallurgical spatial modeling

The combination of variables and data complexities turns geometallurgical spatial modeling bewildering. It is good practice to avoid kriging or any other linear estimation technique as they would result in biased estimations. The amount of bias, however, may be small enough not to compromise the objective of the estimation. This may be the case if the variable presents a "small degree of nonlinearity".

At the time of this thesis, two methodologies stood out for the spatial modeling of nonlinear variables. One well-established approach is to use modern multivariate modeling. In this approach, techniques such as Normal Score Transformation, Multiple Imputation, and the Projection Pursuit Multivariate Transformation are required steps to decorrelate all the multivariate relationships and turn them into multiGaussian factors. The multiGaussian factors can be independently simulated in all nodes of the grid. Then, back transformations return each factor to the original variable. The second approach to geometallurgical modeling applies machine learning to predict the target variables. Modern multivariate modeling is still applied in this approach, but only for the geological variables. The geological estimates in all nodes of the grid were used as features to predict the metallurgical variables using a Random Forest regressor. The latter was trained and tested with the samples that contained information on all (geological and metallurgical) variables.

Both approaches were applied in chapter 6 in an illustration case with real data. The comparison of the two methods showed that while the modern multivariate modeling approach reproduced the uni and bi-variate relationships and the spatial continuity of all the variables, the prediction by machine learning was smooth and did not reproduce the statistics of the response variables. By comparing the reproduction of the metallurgical and mass recovery histograms, it is clear that the latter was fairly reproduced, given some high correlations with the features. However, the metallurgical recovery histogram was poorly reproduced, given the absence of high correlations. The conclusion is that: the workflow selection depends on the objective of the modeling, the spacing of the samples, and the explanatory power of the geological variables over the metallurgical ones. If the aim consists in obtaining a single estimated model, then the machine learning approach is applicable when there are reasonable correlations between features and target variables. Suppose the objective consists in having multiple equal-probable models, and there are enough samples that variogram modeling is possible for the metallurgical variables. In that case, the modern multivariate approach is a good option. The machine learning method can be applied with multiple realizations of the geological variables, but it may

not reproduce the variability of the response variables.

7.3 Mine planning with nonlinear blending

Planning a mine using multivariate spatial models is the ultimate goal of a geometallurgical program. The plan will not just consider one geological variable but all the geological, metallurgical, and other variables that impact the project's value. However, mine planning is usually supported by estimations in a block model, which is convenient for mineral resource evaluation but is not for predicting plant processing performance. The volume of material that goes into a plant (the feed volume) is greater than the volume of a block. The feed volume properties depend on the blending and upscaling behavior of the blocks. If the blending and upscaling behaviors are linear, no problem arises with this traditional procedure of estimating block properties. However, if the blending and upscaling are nonlinear, as is often the case with metallurgical variables, this standard procedure provides biased results. The correct approach is to estimate the feed volume properties through nonlinear blending and scaling models. These behaviors are explained in chapter 4, along with a proposal of a simple, flexible, and easy-to-use mathematical blending model. The purpose of this proposal is not to provide an accurate blending model. This can only be accomplished by processing engineers with several testing of different blends of the ore. However, we needed a blending model as input to mine planning to show how the blending behavior can change the mine plan.

A short-term mine planning considering a nonlinear blending behavior was shown in chapter 5. The usual approach of optimizing mine scheduling based on the individual block properties cannot be applied because the properties of a block depend on the feed volume that it will compose (the blending unit). Therefore, it is a recursive problem. The proposed solution is to optimize through simulated annealing, where several possibilities of blending units are tried and the algorithm keeps the best solution. The algorithm groups heterogeneous blocks in the same blending unit when blending is synergistic. When blending is antagonist, the algorithm groups homogeneous blocks in the same blending unit. For a small demonstration study consisting of 160 blocks, four thousand iterations were enough to reach convergence and increase the recovered metal. For the specified synergistic case, there was a 0.32% increase. For the specified antagonistic case, the increase was 2.77%. These numbers should not be evaluated quantitatively, as it is a consequence of a particular example. The purpose is to demonstrate that we can plan better considering the nonlinear blending of metallurgical variables. This small increase in metallurgical recovery can result in significant raise in the project's value.

The simulated annealing algorithm was applied to the multivariate spatial models in chapter 7. When simulating the mine operation, where the ore is homogenized in piles,

the optimization did not increase the result much. However, when simulating a scenario without piles, the algorithm significantly increased the result. The conclusion is that this algorithm can provide the best plan considering nonlinear blending and can also be used to evaluate the need for homogenization piles.

7.4 Future Work

Some topics of future work related to this thesis are:

- A better understanding of the data obtained in the processing plant and how they relate to bench-test data through an upscaling law. Ore reconciliation problems are intrinsically linked to the difficulty in sampling and analyzing all the complexities in a plant;
- A well-defined evaluation of the circumstances under which a nonlinear variable can be kriged without harming the estimation;
- The development of a model that predicts the effective metal recovery from multivariate functions, related to chemical, lithological, and mineralogical variables; and its use as an input to the proposed scheduling algorithm;
- The application of the proposed methodology of scheduling blocks based on blending units to long-term mine planning. The impacts may be seen in the life-of-mine and the project's economic value. Blocks considered waste could be blended with ore blocks in the case of synergistic blending. In the case of antagonistic blending, different processing routes could be planned for different types of ore.
- Evaluation of the trade-off between using homogenization piles or using the proposed scheduling algorithm to take advantage of the natural blending. Homogenization piles have considerable costs that could be avoided by scheduling blocks considering the natural mixture that occurs during the mining and processing operations. The question is whether this natural blending is enough to meet the plant's specifications for the material feed.
- The improvement of this study by considering ore feeding and ore mixtures in a continuous flow and not in batches. This study used the simplification that the plant feed can be discretized in defined feed volumes, when the most realistic would be to consider that the plant feed changes gradually, being better represented through a continuous flow.

7.5 Final comment

Recall the thesis statement: *A nonlinear geometallurgical variable value of an individual block depends on the set of blocks that are blended with it (blending unit) when processed. It is possible to model the nonlinear blending behavior of a variable and use it to optimize mine scheduling when nonadditive geometallurgical variables are of interest.*

This thesis showed that estimating the value of variables to an individual block can introduce bias if the blending and upscaling behaviors are nonlinear and disregarded. The nonlinear blending behavior must be inferred or modeled experimentally and used to estimate the effective properties of the blended mixture of blocks. As the individual block's value depends on the mixture, the scheduling of the blocks can be optimized, leading to better results.

REFERENCES

ADELI, A.; DOWD, P.; EMERY, X.; XU, C. Using cokriging to predict metal recovery accounting for non-additivity and preferential sampling designs. *Minerals Engineering*, Elsevier, v. 170, n. 106923, 2021. Cited 3 times in pages 16, 17, and 21.

AGGARWAL, C. C. *Data mining: the textbook*. New York: Springer, 2015. v. 1. Cited in page 36.

BARNETT, R. M. *CCG Solutions - Multivariate modeling for resources and geometallurgy*. 2016. Retrieved from: http://www.ccgalberta.com/solutions. Cited 7 times in pages 16, 17, 20, 32, 33, 34, and 35.

BARNETT, R. M.; DEUTSCH, C. V. Imputation of geologic data. *Centre for Computational Geostatistics (CCG) Annual Report*, v. 15 (102), 2013. Cited in page 31.

BARNETT, R. M.; DEUTSCH, C. V. Guide to multivariate modeling with the ppmt. *Centre for Computational Geostatistics (CCG) Guidebook Series*, v. 20, 2015. Cited in page 46.

BARNETT, R. M.; MANCHUK, J. G.; DEUTSCH, C. V. Projection pursuit multivariate transform. *Mathematical Geosciences*, Springer, v. 46, n. 3, p. 337–359, 2014. Cited in page 33.

BLOM, M.; PEARCE, A. R.; STUCKEY, P. J. Short-term planning for open pit mines: a review. *International Journal of Mining, Reclamation and Environment*, Taylor & Francis, v. 33, n. 5, p. 318–339, 2019. Cited 2 times in pages 41 and 42.

BOISVERT, J. B.; ROSSI, M. E.; EHRIG, K.; DEUTSCH, C. V. Geometallurgical modeling at Olympic dam mine, South Australia. *Mathematical Geosciences*, Springer, v. 45, n. 8, p. 901–925, 2013. Cited 3 times in pages 16, 17, and 19.

BYE, A. Case studies demonstrating value from geometallurgy initiatives. In: *The first AusIMM International Geometallurgy Conference*. Brisbane, Australia: Australasian Institute of Mining and Metallurgy, 2011. p. 9–30. Cited 2 times in pages 17 and 19.

CAMPOS, L. J. F.; SILVA, P. H.; MAZZINGHY, D. B.; TAVARES, L. M.; CAMPOS, P. H. A.; GALéRY, R. O índice de trabalho de bond para moagem de bolas (bwi) é uma váriavel aditiva? In: *XXVIII Encontro Nacional de Tratamento de Minérios e Metalurgia Extrativa*. Belo Horizonte, Brasil: Universidade Federal de Minas Gerais, 2019. Cited 2 times in pages 68 and 72.

CAMPOS, P. H. A.; COSTA, J. F. C. L.; KOPPE, V. C.; BASSANI, M. A. A. Geometallurgy-oriented mine scheduling considering volume support and non-additivity. *Mining Technology*, Taylor & Francis, v. 131, n. 1, p. 1–11, 2022. Cited 3 times in pages 72, 73, and 96.

CARRASCO, P.; CHILÈS, J.-P.; SÉGURET, S. A. Additivity, metallurgical recovery, and grade. In: *Proceedings of the 8th International Geostatistics Congress*. Santiago, Chile: FCFM, Gecamin, 2008. p. on–CD. Cited 6 times in pages 15, 16, 18, 19, 45, and 48.

CASTILLO, M. F. D.; DIMITRAKOPOULOS, R. A multivariate destination policy for geometallurgical variables in mineral value chains using coalition-formation clustering. *Resources Policy*, Elsevier, v. 50, p. 322–332, 2016. Cited 3 times in pages 17, 71, and 75.

CHILES, J.-P.; DELFINER, P. *Geostatistics: modeling spatial uncertainty*. New York: John Wiley & Sons, 2009. Cited in page 29.

CORNAH, A. Assessment of the impact of non-additivity in the estimation of iron ore attributes. In: *Iron Ore Conference*. Perth, Australia: Australasian Institute of Mining and Metallurgy, 2013. p. 129–136. Cited 3 times in pages 19, 45, and 48.

COWARD, S.; VANN, J.; DUNHAM, S.; STEWART, M. The primary-response framework for geometallurgical variables. In: *Seventh International Mining Geology Conference*. Perth, Australia: Australasian Institute of Mining and Metallurgy, 2009. p. 109–113. Cited 7 times in pages 15, 16, 18, 23, 45, 47, and 48.

DAVID, D. The importance of geometallurgical analysis in plant study, design and operational phases. In: *Proceedings Ninth Mill Operators' Conference*. Fremantle, Australia: Australasian Institute of Mining and Metallurgy, 2007. p. 241–248. Cited in page 18.

DEUTSCH, C.; ZANON, S.; NGUYEN, H. Power-law averaging for inference of effective permeability. In: *Canadian International Petroleum Conference*. Calgary, Canada: [s.n.], 2002. Cited in page 76.

DEUTSCH, C. V. Declus: a fortran 77 program for determining optimum spatial declustering weights. *Computers & Geosciences*, Elsevier, v. 15, n. 3, p. 325–332, 1989. Cited 2 times in pages 26 and 103.

DEUTSCH, C. V. Geostatistical modelling of geometallurgical variables. *Centre for Computational Geostatistics (CCG) Annual Report*, v. 15 (310), 2013. Cited 2 times in pages 39 and 40.

DEUTSCH, C. V. Cell declustering parameter selection. *J. L. Deutsch (Ed.), Geostatistics Lessons*, 2015. Retrieved from: https://geostatisticslessons.com/lessons/celldeclustering. Cited in page 26.

DEUTSCH, C. V. *Geostatistics with Nonlinear Variables*. 2020. Retrieved from: https://resourcemodelingsolutions.com/geostatistics-with-nonlinear-variables. Cited 2 times in pages 68 and 69.

DEUTSCH, C. V. *Course Notes: Citation in Applied Geostatistics*. 2021. Cited in page 25.

DEUTSCH, C. V.; JOURNEL, A. G. *GSLIB: Geostatistical Software Library and Users Guide*. 2. ed. New York: Oxford University Press, 1997. Cited 2 times in pages 31 and 97.

DEUTSCH, J. *Multivariate spatial modeling of metallurgical rock properties*. Edmonton, Canada: Ph.D. thesis, University of Alberta, 2015. Cited 6 times in pages 17, 20, 23, 28, 48, and 67.

DOMINY, S. C.; OCONNOR, L.; GLASS, H. J.; PUREVGEREL, S.; XIE, Y. Towards representative metallurgical sampling and gold recovery testwork programmes. *Minerals*, MDPI, v. 8, n. 5, 2018. Cited 5 times in pages 15, 16, 20, 23, and 48.

DOMINY, S. C.; OCONNOR, L.; PUREVGEREL, S. Importance of representative metallurgical sampling and testwork programmes to reduce project riska gold case study. *Mining Technology: Transactions of the Institute of Mining and Metallurgy*, Taylor and Francis Ltd., v. 128, p. 230–245, 2019. Cited in page 48.

DOWD, P.; XU, C.; COWARD, S. Strategic mine planning and design: some challenges and strategies for addressing them. *Mining Technology*, Taylor & Francis, v. 125, n. 1, p. 22–34, 2016. Cited 3 times in pages 16, 20, and 67.

DUNHAM, S.; VANN, J. Geometallurgy, geostatistics and project value - does your block model tell you what you need to know? In: *Project Evaluation Conference*. Melbourne, Australia: Australasian Institute of Mining and Metallurgy, 2007. p. 189–196. Cited 5 times in pages 16, 18, 23, 48, and 75.

GARRIDO, M.; SEPÚLVEDA, E.; ORTIZ, J.; TOWNLEY, B. Simulation of synthetic exploration and geometallurgical database of porphyry copper deposits for educational purposes. *Natural Resources Research*, Springer, v. 29, n. 6, p. 3527–3545, 2020. Cited in page 17.

GOMES, C. C.; BOISVERT, J. B.; DEUTSCH, C. V. Gaussian mixture models. *J. L. Deutsch (Ed.), Geostatistics Lessons*, 2022. Retrieved from: https://geostatisticslessons.com/lessons/gmm. Cited in page 105.

GOOVAERTS, P. *Geostatistics for natural resources evaluation*. New York: Oxford University Press, 1997. Cited in page 28.

HASTIE, T.; TIBSHIRANI, R.; FRIEDMAN, J. H.; FRIEDMAN, J. H. *The elements of statistical learning: data mining, inference, and prediction*. 2. ed. New York: Springer, 2009. Cited 2 times in pages 37 and 38.

HOFFIMANN, J.; AUGUSTO, J.; RESENDE, L.; MATHIAS, M.; MAZZINGHY, D.; BIANCHETTI, M.; MENDES, M.; SOUZA, T.; ANDRADE, V.; DOMINGUES, T.; SILVA, W.; SILVA, R.; COUTO, D.; FONSECA, E.; GONçALVES, K. Modeling geospatial uncertainty of geometallurgical variables with bayesian models and hilbert–kriging. *Mathematical Geosciences*, Springer, v. 54, n. 7, p. 1227–1253, 2022. Cited in page 21.

HOGBEN, L. *Handbook of Linear Algebra*. 2. ed. New York: Chapman and Hall/CRC, 2013. Cited in page 45.

HUSTRULID, W. A.; KUCHTA, M.; MARTIN, R. K. *Open pit mine planning and design*. 3. ed. New York: CRC Press, 2013. v. 1 - Fundamentals. Cited 2 times in pages 15 and 41.

IACO, S. D.; HRISTOPULOS, D. T.; LIN, G. Geostatistics and machine learning. *Mathematical Geosciences*, Springer, v. 54, n. 3, p. 459–465, 2022. Cited in page 35.

ISAAKS, E.; SRIVASTAVA, R. *An introduction to applied geostatistics*. New York: Oxford University Press, 1989. Cited in page 44.

JAMES, G.; WITTEN, D.; HASTIE, T.; TIBSHIRANI, R. *An introduction to statistical learning*. New York: Springer, 2013. Cited 3 times in pages 36, 37, and 38.

JOURNEL, A.; HUIJBREGTS, C. *Mining Geostatistics*. London: Academic Press, 1978. Cited 3 times in pages 25, 26, and 44.

KOZHEVNIKOV, E.; TURBAKOV, M.; RIABOKON, E.; POPLYGIN, V. Effect of effective pressure on the permeability of rocks based on well testing results. *Energies*, MDPI, v. 14, n. 8, 2021. Cited in page 76.

KUHN, M.; JOHNSON, K. et al. *Applied predictive modeling*. New York: Springer, 2013. Cited in page 36.

KUMAR, A.; DIMITRAKOPOULOS, R. Application of simultaneous stochastic optimization with geometallurgical decisions at a copper-gold mining complex. *Mining Technology*, Taylor & Francis, v. 128, n. 2, p. 88–105, 2019. Cited in page 17.

LAMBERT, W. B.; BRICKEY, A.; NEWMAN, A. M.; EUREK, K. Open-pit block-sequencing formulations: a tutorial. *Interfaces*, Informs, v. 44, n. 2, p. 127–142, 2014. Cited in page 42.

LEUANGTHONG, O.; DEUTSCH, C. V. Stepwise conditional transformation for simulation of multiple variables. *Mathematical Geology*, v. 35, n. 2, p. 155–173, 2003. Cited in page 33.

LISHCHUK, V. *Geometallurgical programs–critical evaluation of applied methods and techniques*. Luleå, Sweden, 2016. Licentiate Thesis: Luleå University of Technology. Cited 2 times in pages 17 and 20.

LISHCHUK, V.; KOCH, P.-H.; GHORBANI, Y.; BUTCHER, A. R. Towards integrated geometallurgical approach: Critical review of current practices and future trends. *Minerals Engineering*, v. 145, n. 106072, 2020. Cited 3 times in pages 16, 21, and 47.

LIU, B.; ZHANG, D.; GAO, X. A method of ore blending based on the quality of beneficiation and its application in a concentrator. *Applied Sciences*, MDPI, v. 11, n. 11, 2021. Cited in page 15.

MORALES, N.; SEGUEL, S.; CÁCERES, A.; JÉLVEZ, E.; ALARCÓN, M. Incorporation of geometallurgical attributes and geological uncertainty into long-term open-pit mine planning. *Minerals*, MDPI, v. 9, n. 2, 2019. Cited in page 17.

NAVARRA, A.; MONTIEL, L.; DIMITRAKOPOULOS, R. Stochastic strategic planning of open-pit mines with ore selectivity recourse. *International Journal of Mining, Reclamation and Environment*, Taylor & Francis, v. 32, n. 1, p. 1–17, 2018. Cited in page 17.

NEWMAN, A. M.; RUBIO, E.; CARO, R.; WEINTRAUB, A.; EUREK, K. A review of operations research in mine planning. *Interfaces*, Informs, v. 40, n. 3, p. 222–245, 2010. Cited in page 42.

NEWTON, M.; GRAHAM, J. Spatial modelling and optimisation of geometallurgical indices. In: *Proceedings of the Second AusIMM International Geometallurgy Conference*. Brisbane, Australia: Australasian Institute of Mining and Metallurgy, 2011. p. 247–261. Cited 4 times in pages 19, 71, 72, and 75.

NIQUINI, F. *Predição simultânea de produtos e rejeitos em plantas de processamento de zinco e ouro a partir das características do minério*. Porto Alegre, Brasil: Ph.D. thesis, Universidade Federal do Rio Grande do Sul, 2020. Cited in page 21.

OSANLOO, M.; GHOLAMNEJAD, J.; KARIMI, B. Long-term open pit mine production planning: a review of models and algorithms. *International Journal of Mining, Reclamation and Environment*, Taylor & Francis, v. 22, n. 1, p. 3–35, 2008. Cited 2 times in pages 41 and 42.

PERONI, R. *Análise da sensibilidade do seqüenciamento de lavra em função da incerteza do modelo geológico*. Porto Alegre, Brasil: Ph.D. thesis, Universidade Federal do Rio Grande do Sul, 2002. Cited in page 16.

RIBEIRO, C. C. *Geologia, geometalurgia, controles e gênese dos depósitos de fósforo, terras raras e titânio do complexo carbonatítico Catalão I, GO*. Brasília, Brasil: Ph.D. thesis, Universidade de Brasília, 2008. Cited in page 97.

ROSSI, M. E.; DEUTSCH, C. V. *Mineral resource estimation*. New York: Springer, 2014. Cited 4 times in pages 17, 29, 31, and 67.

RUBIN, D. B. Inference and missing data. *Biometrika*, Oxford University Press, v. 63, n. 3, p. 581–592, 1976. Cited in page 31.

SCIKITLEARN. *Decision Trees*. 2022. Retrieved from: https://scikit-learn.org/stable/modules/tree.html#regression. Cited in page 37.

SCIKITLEARN. *RandomForest*. 2022. Retrieved from: https://scikit-learn.org/stable/modules/ensemble.html#forest. Cited in page 38.

SEPÚLVEDA, E.; DOWD, P.; XU, C. The optimisation of block caving production scheduling with geometallurgical uncertainty–a multi-objective approach. *Mining Technology*, Taylor & Francis, v. 127, n. 3, p. 131–145, 2018. Cited in page 17.

SILVA, D. S. F.; DEUTSCH, C. V. Multivariate data imputation using gaussian mixture models. *Centre for Computational Geostatistics (CCG) Annual Report*, v. 17 (104), 2015. Cited in page 31.

SINCLAIR, A. J.; BLACKWELL, G. H. *Applied mineral inventory estimation*. Cambridge, UK: Cambridge University Press, 2006. Cited in page 15.

SPLAINE, M.; BROWNER, S.; DOHM, C. The effect of head grade on recovery efficiency in a gold-reduction plant. *Journal of the Southern African Institute of Mining and Metallurgy*, Southern African Institute of Mining and Metallurgy, v. 82, n. 1, p. 6–11, 1982. Cited in page 75.

TAVARES, L. M.; KALLEMBACK, R. D. Grindability of binary ore blends in ball mills. *Minerals Engineering*, Elsevier, v. 41, p. 115–120, 2013. Cited 2 times in pages 68 and 75.

TONDER, E. V.; DEGLON, D.; NAPIER-MUNN, T. The effect of ore blends on the mineral processing of platinum ores. *Minerals Engineering*, Elsevier, v. 23, n. 8, p. 621–626, 2010. Cited 3 times in pages 19, 70, and 72.

VANN, J.; GUIBAL, D. Beyond ordinary kriging–an overview of non-linear estimation. In: *Proceedings of Symposium on Beyond Ordinary Kriging*. Perth, Australia: Geostatistical Association of Australasia, 1998. Cited in page 40.

WALTERS, S. Integrated industry relevant research initiatives to support geometallurgical mapping and modelling. In: *The first AusIMM International Geometallurgy Conference*. Brisbane, Australia: Australasian Institute of Mining and Metallurgy, 2011. p. 273–278. Cited 2 times in pages 16 and 19.

WAMBEKE, T.; ELDER, D.; MILLER, A.; BENNDORF, J.; PEATTIE, R. Real-time reconciliation of a geometallurgical model based on ball mill performance measurementsa pilot study at the tropicana gold mine. *Mining Technology: Transactions of the Institute of Mining and Metallurgy*, Taylor & Francis, v. 127, p. 115–130, 2018. Cited 2 times in pages 17 and 20.

XU, M. Metallurgical testing: Modeling recovery versus ore grade. In: *45thAnnual Canadian Mineral Processors Operators Conference*. Ottawa, Canada: Canadian Institute of Mining, Metallurgy and Petroleum, 2013. p. 181–192. Cited in page 75.

YAN, D.; EATON, R. Breakage properties of ore blends. *Minerals Engineering*, v. 7, p. 185–199, 1994. Cited 2 times in pages 68 and 70.

ZACCHÉ, C. S. *Metodologias de inserção de dados sob mecanismo de falta MNAR para modelagem de teores em depósitos multivariados heterotópicos*. Porto Alegre, Brasil: Ph.D. thesis, Universidade Federal do Rio Grande do Sul, 2018. Cited in page 31.